Structure, Function, and Mechanism of Human MIF and Parasitic Orthologs

Von der Fakultät für Mathematik, Informatik und Naturwissenschaften der RWTH Aachen University zur Erlangung des akademischen Grades eines Doktors der Naturwissenschaften genehmigte Dissertation

vorgelegt von

Diplom-Biologe
Swen Zierow

aus Furtwangen

Berichter: Universitätsprofessor Dr. Jürgen Bernhagen
Universitätsprofessor Dr. Klaus Wolf

Tag der mündlichen Prüfung: 19.12.08

Table of Contents

A. Abbreviations

Abbreviations are also defined where they first appear in the text. For amino acids the three letter code are used.

4-IPP	4-iodo-6-phenylpyrimidine
Å	Ångstrom (1 Å = 10^{-10} m)
ARDS	Acute respiratory distress syndrome
CD74	Major histocompatibility complex, class II invariant chain
CL	Cutaneous leishmaniasis
D-dopachrome	2-carboxy-2,3-dihydroindole-5,6-quinone
DMEM	Dulbecco's modified Eagles's medium
DMSO	Dimethyl sulfoxide
DNA	Deoxyribonucleic acid
DTT	Dithiothreitol
E. coli	Escherichia coli
ELISA	Enzyme-linked immunosorbant assay
ERK	Extracellular signal-regulated kinases
FBS	Fetal bovine serum
HPP	Hydroxyphenylpyruvate
IFN	Interferon
IL	Interleukin
iNOS	Inducible nitric oxide synthase
IPTG	Isopropyl ß-D-thiogalactopyranoside
ISO-1	(S,R)-3-(4-hydroxyphenyl)-4,5-dihydro-5-isoxazole acetic acid methyl ester
Jab1	Jun activation domain binding protein 1
K_d	Dissociation constant
kDa	kilo-Dalton (1 kDa = 1.6605 ◦ 10-21 g)
LmMIF	MIF ortholog from *L. major*
LPS	Lipopolysaccharide

MAD	Multiple Anomalous Dispersion
MAPK	Mitogen activated protein kinase
MIF	Macrophage migration inhibitory factor
NAPQI	N-(4-oxo-1-cyclohexa-2,5-dienylidene)acetamide
NK cells	Natural killer cells
NMR	Nuclear Magnetic Resonance
NO	Nitric oxide
OD	Optical density
OXIM-11	(E)-4-hydroxybenzaldehyde O-cyclohexanecarbonyl-oxime
PAGE	Polyacrylamide gel electrophoresis
PBMC	Peripheral blood mononuclear cells
PbMIF	MIF ortholog from *P. berghei*
PBS	Phosphate-buffered saline
PCR	Polymerase chain reaction
PDB	Protein Data Bank
PEG	Polyethylene glycol
PfMIF	MIF ortholog from *P. falciparum*
PGE_2	Prostaglandin E_2
PMN	Polymorphonuclear neutrophil granulocytes
PMSF	Phenylmethyl-sulfonylfluoride
RMSD	Root mean square deviation
SDS	Sodium dodecyl sulfate
Th cells	T-helper cell
TLR	Toll like receptor
TNF	Tumor necrosis factor
Tris	2-amino-2-hydroxymethylpropane-1,3-diol

B. Acknowledgments

I would like to thank all the people who made it possible to complete this thesis.

My advisor Prof. Jürgen Bernhagen of the Department of Biochemistry and Molecular Cell Biology at the RWTH Aachen University Hospital who made it possible for me to pursue a large part of my thesis at Yale. The excellent training I received during my *Diplomarbeit* prepared me for a successful Ph.D. thesis. I appreciate his support during my thesis.

My advisor Prof. Elias Lolis of the Department of Pharmacology at the Yale University School of Medicine for giving me the opportunity to work in his laboratory. I was fortunate to have Elias as my co-supervisor giving me support and ideas throughout my thesis whenever I needed it, but also allowed me to work out my ideas independently.

Prof. Wolf for reviewing my thesis and accepting the *Co-Referat*; and Prof. Rink for his participation in my committee.

Prof. Rick Bucala of the Department of Internal Medicine at the Yale University School of Medicine for his kind welcome in his lab and for his encouragements and helpful scientific discussions during my work.

All members of the Bernhagen and the Lolis labs, especially Yoonsang Cho and Gregg Crichlow for their patience while teaching me crystallography, James Murphy for his support in NMR spectroscopy and Deepa Rajasekaran for her help in yeast related-assays.

The lab members of Rick Bucala; Lin Leng gave me great support throughout my thesis, Daniela Kamir cloned the Lm1740MIF expression construct and Melanie Merk helped me with the competition binding assays and the confocal microscopy.

Without the constructive advice of Prof. Michael E. Hodsdon of the Department of Laboratory Medicine (Yale University) in NMR-related questions and the provision of instruments, the MIF・CXCR4 interaction studies would not have been possible.

The German Academic Exchange Service for the financial support.

On a more personal note, I would like to thank my fiancée Melanie Merk for the wonderful time we had together and will have in the future.
Last but not least, I thank my parents who always have been there for me and supported me throughout my academic studies and my life.

C. Publications

Parts of this thesis have been published in peer-reviewed international journals.

1. Kamir, D.*****, **Zierow, S.* (* equal contribution)**, Leng, L., Cho, Y., Diaz, Y., Griffith, J., McDonald, C., Merk, M., Mitchell, R. A., Trent, J., Chen, Y., Kwong, Y. K., Xiong, H., Vermeire, J., Cappello, M., McMahon-Pratt, D., Walker, J., Bernhagen, J., Lolis, E., and Bucala, R. (2008) A leishmania ortholog of macrophage migration inhibitory factor modulates host macrophage responses. *J Immunol* 180, 8250-8261

2. Winner, M., Meier, J., **Zierow, S.**, Rendon, B. E., Crichlow, G. V., Riggs, R., Bucala, R., Leng, L., Smith, N., Lolis, E., Trent, J. O., and Mitchell, R. A. (2008) A novel, macrophage migration inhibitory factor suicide substrate inhibits motility and growth of lung cancer cells. *Cancer Res* 68, 7253-7257

3. Merk, M., Baugh, J., **Zierow, S.**, Leng, L., Pal, U., Lee, S., Ebert, A., Mizue, Y., Trent, J., Mitchell, R. A., Nickel, W., Kavathas, P., Bernhagen, J., and Bucala, R. (2008) The Golgi-associated Protein p115 Mediates the Secretion of Macrophage Migration Inhibitory Factor (MIF). *Mol Biol Cell,* (in revision)

1 Introduction

1.1 Parasites and Disease

Millions of people world-wide are affected by diseases caused by parasites. In developing and tropical regions, parasites represent a major cause of death, making parasitic infections one of the world's most important health problems.

Parasitic protozoa are unicellular eukaryotic pathogens that live inside host cells and/or in extracellular fluids. They are responsible for diseases such as malaria, trypanosomiasis, schistosomiasis and leishmaniasis. The parasites initiate a relationship with their host to increase their own chances of survival, proliferation and propagation. An optimal relationship for parasites to their hosts consists of a high prevalence with minimal symptoms of disease to guarantee a lifelong persistence and ample time for the passage to new hosts. However, the vertebrate's immune system mobilizes its immunological arsenal to eliminate the infectious agents. In response, parasites have evolved highly specialized strategies to evade immune destruction and to complete their life cycle (1).

Several host and parasite-specific factors play a role in the persistence of parasites within infected cells and in influencing the clinical manifestations of the disease. Recent observations indicate that parasitic pathogens ensure their survival by a production of immunomodulatory proteins which interact with specific molecular pathways in the host to alter normal protein functions and manipulate the ensuing immune response (2).

1.1.1 Mechanisms of Immune Evasion

There are abundant examples of parasites escaping the effects of adaptive humoral and cellular immunity by producing immunomodulatory proteins. Well documented examples of such immune evasion strategies include filarial nematodes which express the protease inhibitor CPI-2 to inhibit Class II antigen presentation, thereby preventing development of active immunity (3). Another strategy to evade the host immune response is the antigenic variation used by protozoa such as African trypanosomes and malaria parasites. Surface molecules that are important targets of the humoral immune response are encoded in the genome as multicopy, nonallelic gene families that show little or no immunological cross-reactivity. The successive expression of members of these gene families outmaneuvers the host's humoral response (4, 5). One of the most sophisticated mechanisms of immune evasion strategies, the selective activation of specific subsets of T helper cells, is described for *Leishmania major*. It was recently demonstrated that *L. major* actively induces interleukin 10 (IL-10)-producing $CD25^+$ regulatory T cells to prevent complete clearance of the parasite (6). IL-10 has been described extensively as a key immunoregulator during infection as a suppressive or deactivating cytokine (7-10). It has been shown to suppress cytokine production of both T and natural killer (NK) cells and intracellular killing of pathogens. Furthermore, IL-10 inhibits a broad spectrum of activated macrophage/monocyte functions, including NO production, expression of class II MHC, and molecules such as IL-12 and CD80/CD86.

The remarkable diversity of vertebrate immune evasion mechanisms has been reviewed recently by Paul Schmid-Hempel (11), an overview of the manifold immune evasion strategies is given in Figure 1.

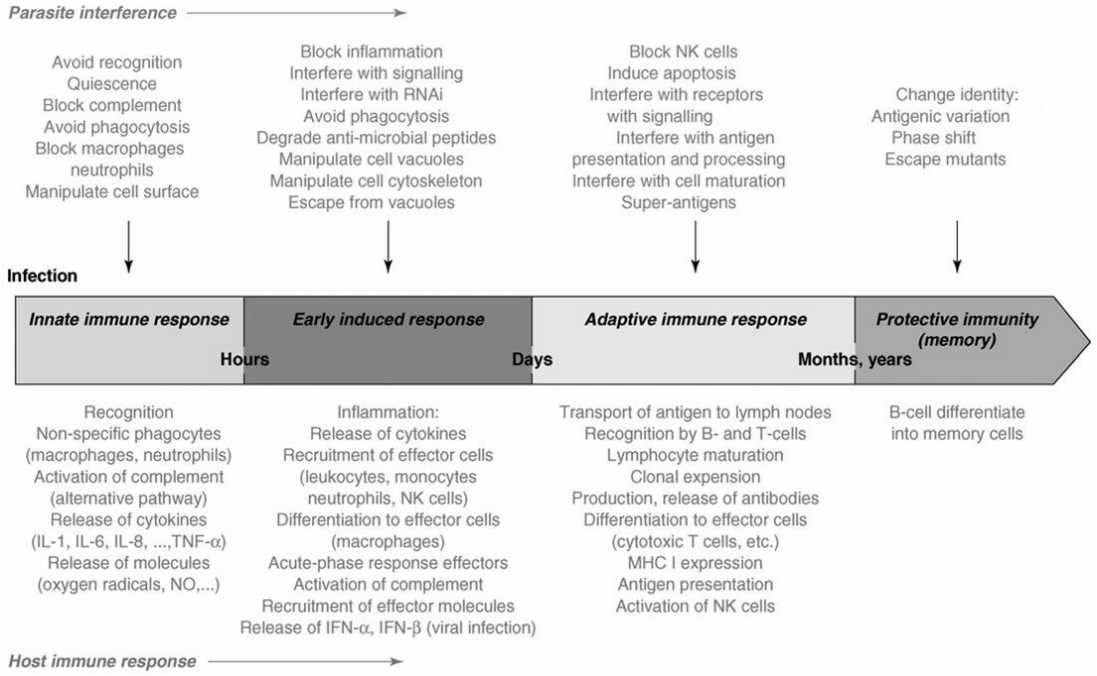

Figure 1. Interference of parasites with the vertebrate immune system. Extending over hours, days and years post-infection, different types of immune evasion strategies are employed. Defense mechanisms of the host are indicated below the arrow and the corresponding interference of the parasites are indicated above the arrow. Figure taken from (11).

1.2 Leishmaniasis

The parasites responsible for the disease leishmaniasis are among the most diverse of human pathogens, both in terms of their geographical distribution and variety of clinical syndromes they produce (12). *Leishmania*, a protozoa of the family *Trypanosomatidae*, currently affects 12 million people in 88 countries (Figure 2*A*). There are an estimated 2 million new infections and 70000 deaths each year (13). It is estimated that over 350 million people are living in regions with a risk of infection (13).

Figure 2. Geographical distribution and clinical signs of leishmaniasis. (*A*) Geographical distribution **(*B*)** A patient from Uganda with visceral leishmaniasis **(*C*)** A patient from Peru with cutaneous leishmaniasis. **(*D*)** A patient from Bolivia with mucosal leishmaniasis. Figure A is taken from (14), figures B-D are from (15).

The clinical manifestations caused by *Leishmania* species are divided into two major categories: cutaneous and visceral leishmaniasis (Figure 2*B-D*). Cutaneous leishmaniasis (CL), the most common form can further be subdivided into localized CL, diffuse CL and mucocutaneous CL. The first sign of infection is typically a small sore where the infected sandfly has bitten the host that develops progressively over a period of 2 to 6 weeks to the typical ulcer that characterizes localized CL (16). This form of cutaneous leishmaniasis can spread from the initial site of infection and develop to diffuse CL, covering the patient's entire body. Mucosal leishmaniasis is the most serious complication and can lead to disfiguring and life-threatening leishmaniasis. It can develop at the same time with localized CL or even 1 – 5 years after the localized ulcer has healed.

While skin sores of cutaneous leishmaniasis will often heal on their own, leaving unpleasant looking scars, visceral leishmaniasis can cause death if not treated. The variety of clinical syndromes is caused due to the variety of Leishmania species and subspecies with more than 20 infect humans, each causing a different spectrum of symptoms (17).

1.2.1 Leishmania Life Cycle

Leishmania is spread through sandflies belonging to the genus *Phlebotomus* in Europe, Africa, Middle East and Asia and through the genus *Lutzomyia* in America (18).

When taking a blood meal, the infected female sandfly injects *Leishmania* promastigotes into the skin. Within the human host, the promastigotes then are ingested rapidly by phagocytes. The first phagocytic cells that infiltrate the site of experimental infection with *L. major* promastigotes are polymorphonuclear neutrophil granulocytes (PMN), followed by a wave of macrophages (19). PMNs phagocytose the parasite but do not kill it; instead they serve as intermediate host cells. The *Leishmania* promastigotes delay the spontaneous apoptosis of the infected PMNs for up to three days and remain inside the PMN without multiplication or transformation (20, 21). After 3 days, the much longer living macrophages arrive at the site of infection and phagocytose the apoptotic PMN infected with the parasite. Here, the promastigotes metamorphose into amastigotes and replicate until the host cell eventually bursts. Released amastigotes then infect other phagocytic cells and continue the cycle. When blood-feeding on an infected host, naïve sandflies become infected with amastigotes. In the stomach of the insect, the amastigotes transform almost immediately into the promastigote form and the cycle continues (Figure 3).

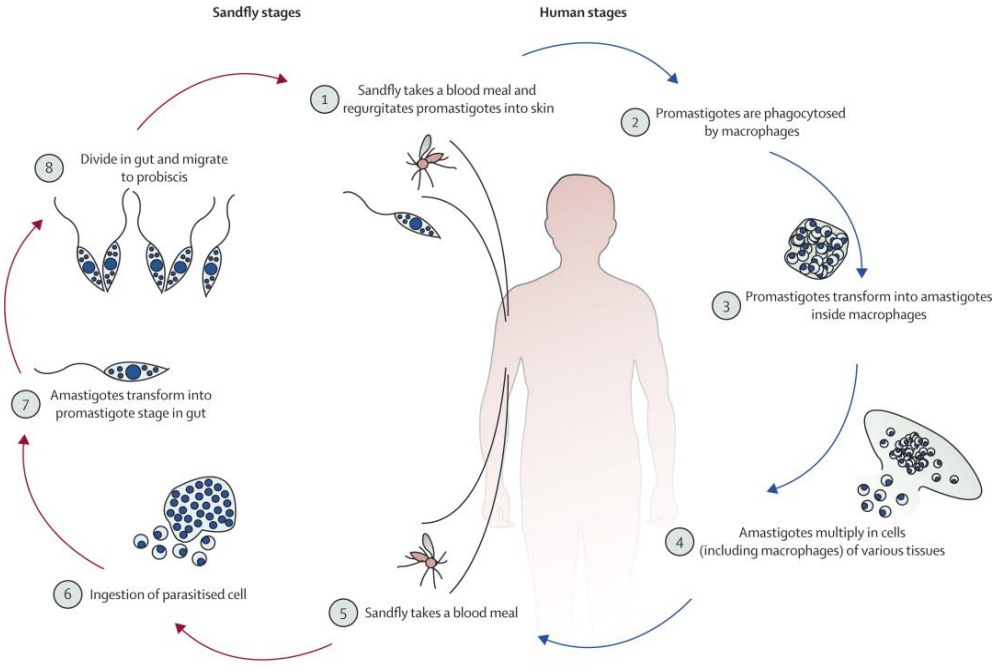

Figure 3. The *Leishmania* Lifecycle. Leishmaniasis is transmitted through the bite of a female sandfly. During their blood meal, infected sandflies inject the infective stage, the so-called promastigote parasite, into the human host [1]. Injected promastigotes are phagocytized by macrophages [2] and transform into the amastigote parasites [3]. These multiply in the infected cells and also affect different tissues, depending on the Leishmania species [4], which causes the corresponding clinical manifestation of the disease. When sandflies take blood meals from an infected host, they take up parasitized macrophages [5, 6]. In the vector fly's midgut, these parasites differentiate into the promastigote form [7], which multiplies and finally migrates to the fly's proboscis [8]. Figure is taken from (14).

1.2.2 Host Defense and Parasite Interactions

Leishmania parasites live exclusively in mononuclear phagocytes, but lack any mechanism to penetrate the membranes of their host cells. After infection, most *Leishmania* promastigotes are rapidly killed in the extracellular tissue environment; their survival depends on the rapid escape from the toxic extracellular milieu via the ingestion by phagocytes. Following infection, a local inflammatory response is initiated leading to an accumulation of leukocytes at the site of parasite delivery (22). The composition of the cells defining this early accumulation appears to be the determinant of the later outcome of the disease as the further steps of immune defense are decided by the specific subset of cytokines released. The balance of these inflammatory responses mediates disease expression

and may result in either symptomless infection, self healing local CL leading to immunity, or chronic leishmaniasis.

While infected macrophages preferentially produce interleukin (IL)-1ß, IL-12 and tumor necrosis factor α (TNF-α), T-helper cell type (Th)-1 cells produce predominantly interferon (IFN)-γ, Th-2 cells produce IL-4, dentritic cells produce IL-12 and natural killer cells produce IFN-γ (23).

Of particular importance for the disease development is whether the released set of cytokines leads to a Th1-dominated immune response, accompanied by cell-mediated immunity (macrophage activation), or to a Th2-dominated immune response which regulates an antibody response.

The control and clearance of *Leishmania* is mainly mediated by the Th1-type immune response. Experimental studies in murine models have established a clear difference between Th2-mediated disease susceptibility and Th1-mediated protection (24). Th1-cells produce IFN-γ, which subsequently induces the production of nitric oxide (NO) in phagocytic cells that harbor *L. major* leading to destruction of the parasite (24-27).

The parasites however actively induce the early secretion of IL-4, thus creating a microenvironment propitious for the development of Th2 cells (28). Further immunomodulating mechanisms include the *Leishmania*-induced inhibition of chemotaxis by neutrophils and monocytes (29). In contrast, a more recent study found a chemotactic factor released from the *Leishmania* parasite in the early phase of infection. This factor has a size between 10 and 50 kDa and was suggested to be responsible for the accumulation of neutrophilic granulocytes following infection (30). The parasite also stimulates the production and release of PGE_2 (31) and promotes its survival inside the macrophage by preventing apoptosis (32). As described later in section 1.5, these mechanisms also are known functions of the cytokine macrophage migration inhibitory factor (MIF).

Additional immune evasion mechanisms proposed for *Leishmania* are listed in Table 1.

Table 1. Immune evasion mechanisms of *Leishmania* spp. Adapted from (Zambrano-Villa *et al*., 2002).

Main strategies of evasion	Result
Inhibition of phagolysosome formation and the proteolytic enzymes from lysosomes	Evades the macrophage proteolytic process
Activation of protein kinase C and scavenging of oxygen intermediates	Inhibits respiratory burst
Prevention of apoptosis of infected macrophages	Extends the survival of the infected macrophage
Inhibition of MHC-protein production, peptide loading and expression of co-stimulatory molecules	Impairs macrophage antigen-presenting function
Induction of PGE_2 and downregulation of TNF-αR	Impairs macrophage function
Inhibition of macrophage and neutrophil chemotaxis	Promotes survival of parasites once established
Shedding of MAC complex and inactivation of some MAC components	Resists complement
Suppression of transcription of the IL-12 gene and induction of IL-10	Blocks the protective Th1 response

Abbreviations: IL-10, interleukin 10; IL-12, interleukin 12; MAC, membrane attack complex; MHC, major histocompatibility complex; PGE2, prostaglandin E2; TNF-αR, tumor necrosis factor α receptor.

1.2.3 Treatment

Cutaneous leishmaniasis is non-fatal and often self-healing; therefore therapy is not routinely indicated for uncomplicated localized CL. However, non-healing, severe and disfiguring lesions are treated to accelerate cure, to reduce scarring and to prevent parasite dissemination. One of the main problems in treating CL is the difficult clinical diagnosis of the broad clinical spectra. The available drugs to treat leishmaniasis can have serious side effects and because of drug-resistant parasites strains (33) and immunosupression in cases of HIV infection, reports of patients non-responsive on drugs are increasing (34).

1.3 Malaria

Malaria is an intracellular infectious disease caused by a protozoan parasite of the genus *Plasmodium*. The single-celled eukaryotes are transmitted by the female *Anopheles* mosquitoes during their blood meal. Four types of the *Plasmodiu*m parasite can infect humans: *Plasmodium falciparum, Plasmodium vivax, Plasmodium ovale,* and *Plasmodium malariae. P. falciparum* is the main cause of severe clinical malaria and death. Approximately 3.2 billion people live in areas at risk of malaria, and in the year 2002, it was estimated that *Plasmodium falciparum* alone caused 300 – 660 million episodes of clinical malaria infections (35), killing approximately 1 – 2 million people, mostly children under the age of 5. (WHO, The Impact of Malaria, a Leading Cause of Death Worldwide). Most clinical events attributable to *P. falciparum* are concentrated in the African region (70%), but the highly populated South East Asia region contributes 25% of the world's clinical attacks in 2002 (35) (Figure 4). People with malaria typically have cycles of chills, fever, and sweating that re-occur every 1 – 3 days. Nausea, vomiting, and diarrhea often go along with the fever and the destruction of red blood cells causes anemia. When the patients survive, recovery is usually complete, but it can also leave some patients with long-term neurological deficits.

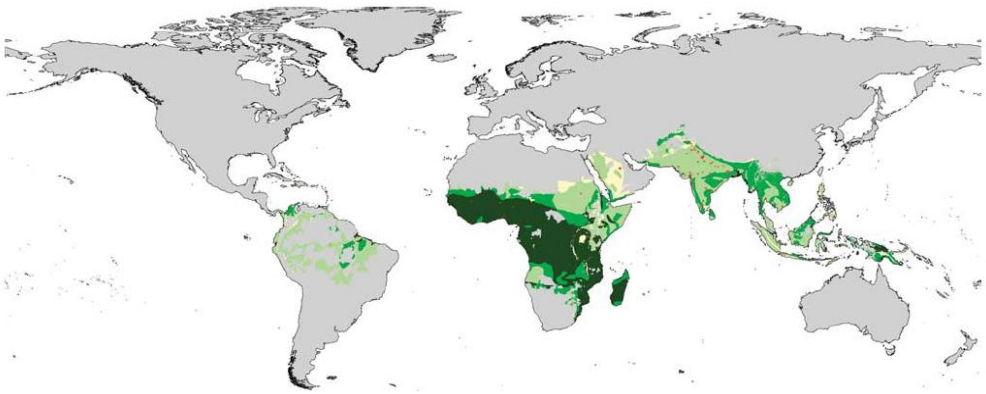

Figure 4. *P. falciparum* endemic distribution. Endemicity classes: light green, hypoendemic (areas in which childhood infection prevalence is less than 10%); medium green, mesoendemic (areas with infection prevalence between 11% and 50%); dark green, hyperendemic and holoendemic (areas with an infection prevalence of 50% or more). Unclassified areas (yellow). Grey areas are a combined mask of areas outside of the transmission limits and areas of population density less than 1 person km^{-2} .Figure and text are from (35).

1.3.1 *Plasmodium* spp. Life Cycle

The life cycle of *Plasmodium* spp. is complex and is divided into several stages. Here, a simplified outline:

Sporozoites injected from the female *Anopheles* mosquito migrate within the human bloodstream to the liver and infect hepatocytes. During the next 9 – 16 days, the liver-stage parasites differentiate and undergo asexual multiplication resulting in tens of thousands of merozoites which eventually burst from the hepatocyte. The merozoites then enter the bloodstream and each potentially invades an erythrocyte, where they undergo another round of multiplication within 48 hours, producing 12 – 16 merozoites within a schizont. The synchronized rupture of the red blood cells full of merozoites induces the typical bouts of fever and chills in the infected individual. The released merozoites invade additional red blood cells and carry on the cycle, progressively breaking down the red cells. Merozoites may also differentiate into gametocytes which do not rupture the erythrocyte. These sexual forms are taken from the bloodstream by a feeding *Anopheles spp.* mosquito and fertilize in the mosquito midgut to form zygotes. The parasites multiply in the mosquito where they develop into sporozoites (36, 37).

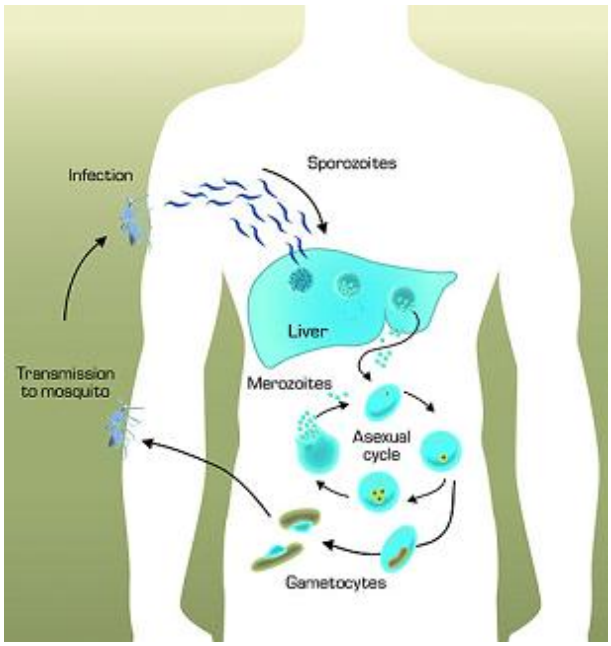

Figure 5. The malaria parasite life cycle. During a blood meal, a malaria-infected female Anopheles mosquito inoculates sporozoites into the human host. Sporozoites infect liver cells and mature into schizonts, which rupture and release merozoites. After the initial replication in the liver the parasites undergo asexual multiplication in the erythrocytes. Merozoites infect red blood cells). The ring stage trophozoites mature into schizonts, which rupture releasing merozoites. Some parasites differentiate into sexual erythrocytic stages (gametocytes) and are ingested by an Anopheles mosquito during a blood meal. The parasites multiply in the mosquito where they develop into sporozoites (image taken from www.learner.org).

1.3.2 Host Defense and Parasite Interaction

During most of its human life cycle the malaria parasite resides within liver and blood cells, and therefore is relatively invisible to the host's immune system. However, mature parasitized red blood cells are cleared by the spleen. To avoid this destruction, maturing parasites in red blood cells express receptor-adhesive proteins on the surface of infected cells mediating adhesion in the vascular beds of organs, a process known as sequestration (38). However, the most notorious survival mechanism of the parasite is its ability to undergo almost unlimited antigenic variation by changing its antigens on the infected erythrocyte surface (39).

The importance of cytokines and their contribution in severe malaria have been studied (37). Malaria parasites modify the production of several cytokines. Protection against malaria may be mediated by TNF-α and IFN-γ and the release of mediators such as NO. Malaria pathogenesis has further been associated with ICAM-1, VCAM-1, E-selectin, MIF, iNOS and uPAR. Further modifications of the immune response induced by *P. falciparum* are a decreased number of circulating T lymphocytes and a marked increase in apoptotic human mononuclear cells (40). An overview of immune evasion mechanisms of *P. falciparum* is shown in Table 2.

Table 2. Immune evasion mechanisms of *P. falciparum*. Adapted from Zambrano-Villa *et al*., 2002.

Main strategies of evasion	**Result**
Antigenic variation and/or polymorphisms	Evades the IR; infected cells are prevented from being swept to the spleen
Induction of blocking antibodies	Blocks the binding of real inhibitory antibodies
Molecular mimicry	Alters immune recognition and might induce autoimmune disease
Anergy of T cells	Immunosuppression
Altered peptide ligand	Alters functions of memory T cells

Abbreviations: IR, immune response

1.4 Macrophage Migration Inhibitory Factor (MIF)

1.4.1 MIF is a Proinflammatory Cytokine

Cytokines are a family of water-soluble signaling proteins with a mass of 8 to 30 kDa that function primarily to effect communication between different cell types. They are important regulators of the innate and adaptive immune response and are often secreted by cells of the immune system in response to pathogens. Released by one activated cell they act through a receptor on their target cell to activate and recruit more immune cells as a way to counter the infectious agent.

Macrophage migration inhibitory factor (MIF) was first described in the late 1950s as a product of activated lymphocytes that inhibits the random movement of cultured macrophages (41, 42). In the following years, MIF production was shown to correlate with general macrophage functions such as adherence and phagocytosis (43-45). The breakthrough for understanding the molecular mechanisms however began only in 1989, when the MIF cDNA was isolated and cloned for the first time (46).

Since then, the knowledge about MIF's role as an important regulator of inflammation and autoimmunity has increased rapidly. In 1993, MIF was identified to be released from pituary cells after stimulation with endotoxins and to potentiate endotoxemia (47). One year later, macrophages were described as an important source of MIF and to release the cytokine after stimulation with proinflammatory stimuli such as bacterial lipopolysaccharide (LPS), TNF-α or IFNγ (48). With the expression and purification of recombinant MIF reported in the same year (49), MIF became available in large quantities to be investigated extensively. Together with genetic knockout studies in mice (50), the availability of recombinant MIF strongly aided in the discovery of MIF's prominent position within the cytokine cascade upstream of TNFα, IL-1ß, IL-2, IL-6, IL-8, IL-12 and IFNγ (51) .

In recent years, MIF has emerged as an important regulator of several autoimmune and inflammatory diseases, including septic shock, atherosclerosis, glomerulonephritis, arthritis and cancer (52). MIF-like proteins also have been reported recently in several parasitic species, including *L. major* with rising evidence that these orthologs play a role in immune evasion of the parasite (53). Consequently, structure-based design of small molecule antagonists targeting MIF is emerging for therapeutic purposes (54).

1.4.2 MIF Receptors

Although MIF was described as one of the first cytokines, the identity of MIF's binding receptors CD74 and CXCR2/4 were not found until very recently (55, 56).

1.4.2.1 CD74 Mediates ERK1/2 Activation

Extracellular signal-regulated kinases (ERKs) act in a signaling cascade that regulates various cellular processes such as proliferation, differentiation, and cell cycle progression in response to a variety of extracellular signals.

CD74, a 31 – 41 kDa Type II transmembrane protein is also known as the cell surface form of the Class II-associated invariant chain (Ii). It has a short N-terminal cytoplasmic tail of 28 amino acids, followed by a single 24-amino acid transmembrane region and, an approximately 150 amino acid lumenal domain (57). It was shown that MIF binds the extracellular domain of CD74 with high affinity ($K_d = 9 \times 10^{-9}$ M) and is required for the MIF-induced secretion of IL-8 (58) and the activation of the ERK1/2- and AKT signaling cascade, the production of prostaglandin E_2 (PGE_2) and cell proliferation (55) in a CD44-dependent manner (59, 60). The MIF-induced activation of ERK1/2 kinases is sustained for a period of at least 24 hours and is dependent upon protein kinase A activity (61).

1.4.2.2 CXCR 2/4 Mediates Cell Migration

MIF acts as a major regulator of inflammatory cell recruitment and atherogenesis. In a recent study these chemokine-like functions of MIF were shown to be mediated through interaction to the chemokine receptors CXCR4 and CXCR2 (56). This study revealed that surface-bound MIF induces arrest of primary human monocytes through CXCR2 and of primary human effector T-cells through CXCR4. Furthermore, CD74 was implicated in CXCR2-mediated MIF-induced arrest.

To test whether MIF directly triggers leukocyte chemotaxis through these receptors, Bernhagen *et al.* compared the promigratory effects of MIF on human blood mononuclear cell-derived monocytes expressing CXCR2 and on CD3+ T lymphocytes expressing CXCR4. MIF induced chemotaxis in both cell types, and, in monocytes, both CXCR2 and CD74 contributed to MIF-triggered chemotaxis.

To assess the physical interactions of MIF with CXCR2 and CXCR4, receptor-binding competition and internalization studies were performed. MIF strongly competed with the cognate CXCR4 and CXCR2 ligands CXCL12 and CXCL8 for receptor binding with nanomolar affinity and elicited internalization of both receptors. The affinity of MIF for CXCR2 (K_d = 1.4 x 10^{-9} M) and CXCR4 (K_d = 19.8 x 10^{-9} M) was comparable to the affinities of the cognate ligands CXCL8 and CXCL12, respectively.

1.4.3 Apoptosis and Cell Proliferation

Mitchell *et al.* showed that both endogenously secreted MIF and exogenously added recombinant MIF stimulate the proliferation of quiescent fibroblasts. This response is associated with the sustained phosphorylation and activation of the classical mitogen activated protein kinases (MAPK), ERK1/2. Activation of ERK leads to the phosphorylation and activation of the cytoplasmic phospholipase A2 ($cPLA_2$) which then induces the release of the proinflammatory and growth-regulating factor

arachidonic acid. Correspondingly, the addition of a neutralizing monoclonal anti-MIF antibody inhibited the proliferative effect (61).

AKT activation promotes a number of cellular responses that are associated with cell division, suppression of apoptosis, inactivation of cell cycle inhibitors, and induction of cyclin and cytokine gene expression (62). The AKT signaling cascade recently was reported to be activated by MIF in a CD74- and CD44-dependent manner with Src and PI3K as upstream signaling components (60, 63, 64). These studies describe that MIF augments NF-κB function and increases expression of Bcl-X_L and Bcl-2, leading to a suppression of apoptosis in several cell types including primary MEFs, fibroblast cell lines and B cells.

In functional screens to isolate genes which bypass p53-mediated growth arrest or apoptosis, MIF was also identified as a negative regulator of p53 activity. Treatment with MIF suppressed p53-dependent transcriptional activity and extended the live span of primary murine fibroblasts and macrophages (65).

1.4.4 Glucocorticoids

Glucocorticoids suppress cell-mediated immunity by inhibiting genes that encode for cytokines. Unlike other cytokines, secretion of MIF is induced rather than inhibited by low concentrations of glucocorticoids. Secreted MIF then was found to override glucocorticoid-induced inhibition of TNF, IL-1, IL6 and IL-8 secretion in LPS-stimulated human monocytes. In a mouse model of endotoxemia, MIF also was demonstrated to override the protective effect of glucocorticoids on LPS-induced lethality (66). Further studies showed that MIF counteracts the glucocorticoid induced suppression of arachidonic acid release (61), inhibition of T-cell proliferation, and IL-2 and IFNγ production (67).

1.4.5 MIF in Disease

MIF has emerged to be an important regulator of several chronic and acute inflammatory diseases including septic shock (68), acute respiratory distress syndrome (ARDS) (69), rheumatoid arthritis (70), arteriosclerosis (71), glomerulonephritis (72), and cancer (73). MIF is released during the immune response by macrophages, activated T-cells and a variety of non-immune cells.

Analysis of the role of MIF during sepsis showed that the administration of recombinant MIF to mice greatly potentiates the effect of LPS alone, leading to decreased survival after challenge. When mice were injected with neutralizing anti-MIF antibodies prior to LPS administration, reduced proinflammatory cytokine production (TNF-α) and a significant reduction in lethality was observed (47). Similarly, *mif*$^{-/-}$ mice have diminished TNF-α levels and resistance to the lethal effects of high doses of the bacterial lipopolysaccharide, or *Staphylococcus aureus* enterotoxin B (50).

MIF also plays a crucial pathological role in the acute respiratory distress syndrome (ARDS), which is a life-threatening disease characterized by diffuse inflammation of lung parenchyma. The common pathogenic event is neutrophilic inflammation of the airspaces, resulting in increased permeability of the alveolar capillary membrane, and destruction of the alveolar airspaces in the lungs. In patients, it was shown that MIF levels are upregulated in the alveolar airspaces (69). As assessed by anti-MIF antibody treatment in a mouse model, the elevated concentration of MIF leads to a increased activity and number of neutrophil granulocytes at the site of inflammation and alveolar inflammation (74).

Recent studies also indicate a role for MIF in atherogenesis. Atherogenesis is characterized by a chronic inflammatory response in the walls of arteries with a continuous immigration and infiltration of activated macrophages and T-cells. The upregulation of MIF during progression of human atherosclerosis was first reported in 2002 (71). Importantly, MIF also is linked to atherosclerosis lesion development (75), and studies

involving *mif* gene-deficient mice or anti-MIF antibodies showed significant reductions in atheroma lesions and in the inflammatory response associated with atherosclerosis development (75, 76).

Numerous reports have linked MIF to cancer. In general, MIF has been described to be highly overexpressed in cancer cells and it has been proposed as a bio-marker of prostate cancer (77) and colorectal carcinoma (78). High levels of MIF also have been observed in the pituitary (79), skin (80), breast (81), brain (82) liver (83) and ovarian (84) tumors. Despite the abundant evidence for the link between MIF and cancer, the molecular mechanisms by which MIF mediates tumorgenesis are largely unknown.

1.4.5.1 MIF in Parasitic Infections

As described in previous chapters, MIF is released primarily by monocytes and macrophages (48). Once released, it modulates the expression and activation of several proinflammatory factors including cytokines, nitric oxide, COX2 and arachidonic acid. MIF prevents the activation-induced apoptosis mediated by the oxidative burst and p53 and thus sustains survival and proinflammatory function of macrophages (85). Interestingly, homologues of MIF have been found in a wide range of parasitic species such as the human parasitic nematodes *Brugia malayi* (86, 87) and *Ancylostoma ceylonicum* (88), in *Plasmodium falciparum* (89) and *Plasmodium berghei* (90), and in the tick species *Amblyomma americanum* (91). The homologues show remarkable similarity in both crystal structure and *in vitro* biological activity.

1.4.5.2 MIF in Malaria

Host MIF Functions

Martiney *et al.* reported that ingestion of *Plasmodium chabaudi*-infected erythrocytes or malarial pigment (hemozoin) induces the release of MIF from macrophages. MIF has been shown to inhibit erythropoiesis *in vitro*

and elevated levels of MIF also were detected in BALB/c mice infected with *P. chabaudi*. Finally, the group demonstrated that serum levels of MIF correlated with disease severity (92). Highly increased MIF levels also were reported in the children and placenta of pregnant woman infected with *P. falciparum* (93). Infection of MIF knockout mice with *P. chabaudi* resulted in less severe anemia, improved erythroid progenitor development, and increased survival compared with wild type controls (94).

Contradictory results were reported recently in a study investigating MIF transcripts in children with acute *P. falciparum* malaria. Circulating MIF levels were significantly lower in children with acute malaria relative to healthy, malaria-exposed children (95). In a follow up study, the group showed that children with prior mild malaria had higher plasma MIF levels than children with an identical number of previous episodes of severe malaria (96). These results suggest that increased basal MIF production may be important in generating immune responses that protects against the development of severe malaria.

Parasite MIF Functions

The MIF ortholog from *P. berghei* (PbMIF) was shown to be expressed in both a mammalian host and a mosquito vector and that, in blood stages, it is secreted into the infected erythrocytes and released upon schizont rupture. Mice infected with PbMIF-knockout parasites had significantly higher numbers of circulating reticulocytes. However, parasites lacking PbMIF were able to complete the entire life cycle and exhibited no evident changes in growth characteristics or virulence features during blood stage infection (90).

The MIF ortholog of *P. falciparum* (PfMIF) also was shown to be expressed during the asexual blood stages of the parasite life cycle (89). Both *Plasmodium* MIF orthologs were characterized *in vitro* and were shown to possess tautomerase and oxidoreductase activities and to inhibit AP-1

activity in human embryonic kidney cells. Monocytes incubated with PfMIF displayed a decreased CD86, Toll like receptor (TLR) 2 and TLR4 expression and showed reduced chemotactic response to monocyte chemotactic protein-1 (MCP-1).

1.4.5.3 MIF in Leishmaniasis

Host MIF Functions

Several *in vitro* and *in vivo* studies have shown that MIF plays a critical role in mediating host resistance to *Leishmania.* Xu *et al.* (97) demonstrated that oral administration of MIF enhances resistance of BALB/c mice to *L. major* and Jüttner *et al.* (98) went on to show that MIF mRNA and protein is up-regulated in lymph nodes of mice during the first week after infection with *L. major* and that MIF-mediated activation of macrophages to kill *Leishmania* is dependent on MIF's ability to promote TNF-α and NO production. A study analyzing the course of cutaneous *L. major* infection in *MIF* gene-deficient mice further revealed that $mif^{-/-}$ mice were susceptible to disease and developed significantly larger lesions and greater parasite burdens than $mif^{+/+}$ mice because of impaired macrophage leishmanicidal activity (99).

Parasite MIF Functions

The genomic analysis of the Leishmania major genome has revealed two genes that exhibit significant sequence identity with the mammalian cytokine, macrophage migration inhibitory factor (100). The first characterization of one of these orthologs, LMF1740 (LmMIF) was part the present work.

1.4.6 The Three-Dimensional Structure of MIF

MIF consists of 114 amino acids and has a molecular weight of 12.5 kDa. The three-dimensional structure of human MIF has been determined independently by three groups in 1996 (101-103) showing MIF to crystallize as a trimer of three identical subunits. Each monomer consists out of a 4 stranded beta-sheet placed above two antiparallel alpha helixes. Two remaining beta-strands are part of intertwining loops and contribute to the stabilization of the trimer by forming interactions with ß-sheets of adjacent subunits (Figure 6).

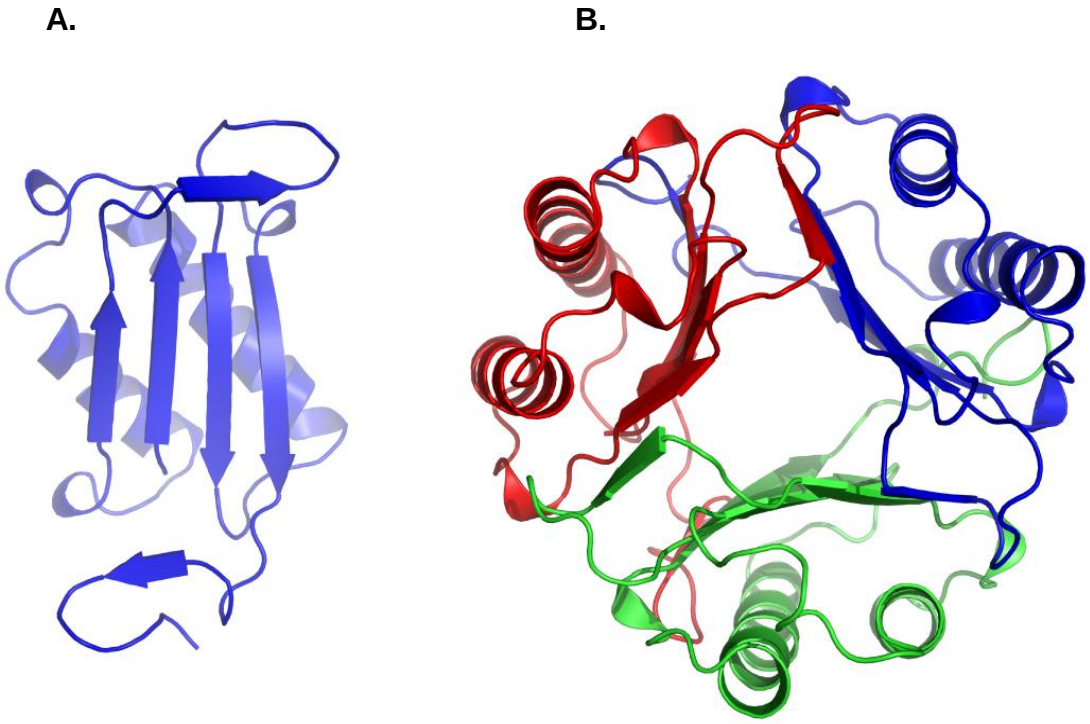

Figure 6. Three dimensional structure of MIF. (***A***) The human monomer and (***B***) trimer drawn from PDB entry 1MIF. The Figure was produced using Pymol (104)

In contrast to the trimer determined by crystallography, studies involving ultracentrifugation, nuclear magnetic resonance (NMR), cross linking and size exclusion chromatography led to the conclusion that monomers, dimers and trimers exist in solution with monomers and dimers representing the major species in physiological concentrations (105-107). A

detailed re-examination of the oligomeric form using sedimentation equilibrium and sedimentation velocity studies indicates an unusually small partial specific volume of MIF and confirmed a strongly associated trimer at the tested concentrations above 10 µg/ml (108). Of note, these concentrations are ~5000 fold higher than MIF-serum levels measured from healthy individuals (109). However, the formation of the trimer is essential for the unexpected enzymatic activity of MIF.

1.4.7 MIF, an Enzyme

MIF exhibits a number of unusual features that distinguish this protein from typical cytokines. For instance, MIF possesses an enzymatic tautomerase/isomerase activity and a thiol-protein oxidoreductase activity.

The tautomerase/isomerase activity is centered on the N-terminal proline that is invariant through all MIF homologs, including orthologs from parasite species like *Leishmania major, Plasmodium falciparum* and *Ancylostoma ceylanicum*.

Physiologically relevant substrates have not yet been identified. However, several substrates have been described to be converted by MIF. The best studied substrates are 2-carboxy-2,3-dihydroindole-5,6-quinone (D-dopachrome), a non-physiological molecule, which is tautomerized to 5,6-dihydroxyindol-2-carboxylic acid (DHICA) and the keto-enol isomerization of both *p*-hydroxyphenylpyruvate (HPP) and phenylpyruvate (110, 111) (Figure 7). The latter two substrates are involved in the metabolism of phenylalanine and tyrosine. High Michaelis constant values suggest, however, that reactions involving these substrates are unlikely to comprise a natural function for MIF (110). The tautomerase/isomerase activity requires the trimerization of MIF, because the active site is formed between subunits of the trimeric human MIF molecule as described for the substrate p-hydroxyphenylpyruvate (112). HPP interacts with Pro1, Lys32, and Ile64 from one subunit and Tyr95 and Asn97 from an adjacent subunit (Figure 7).

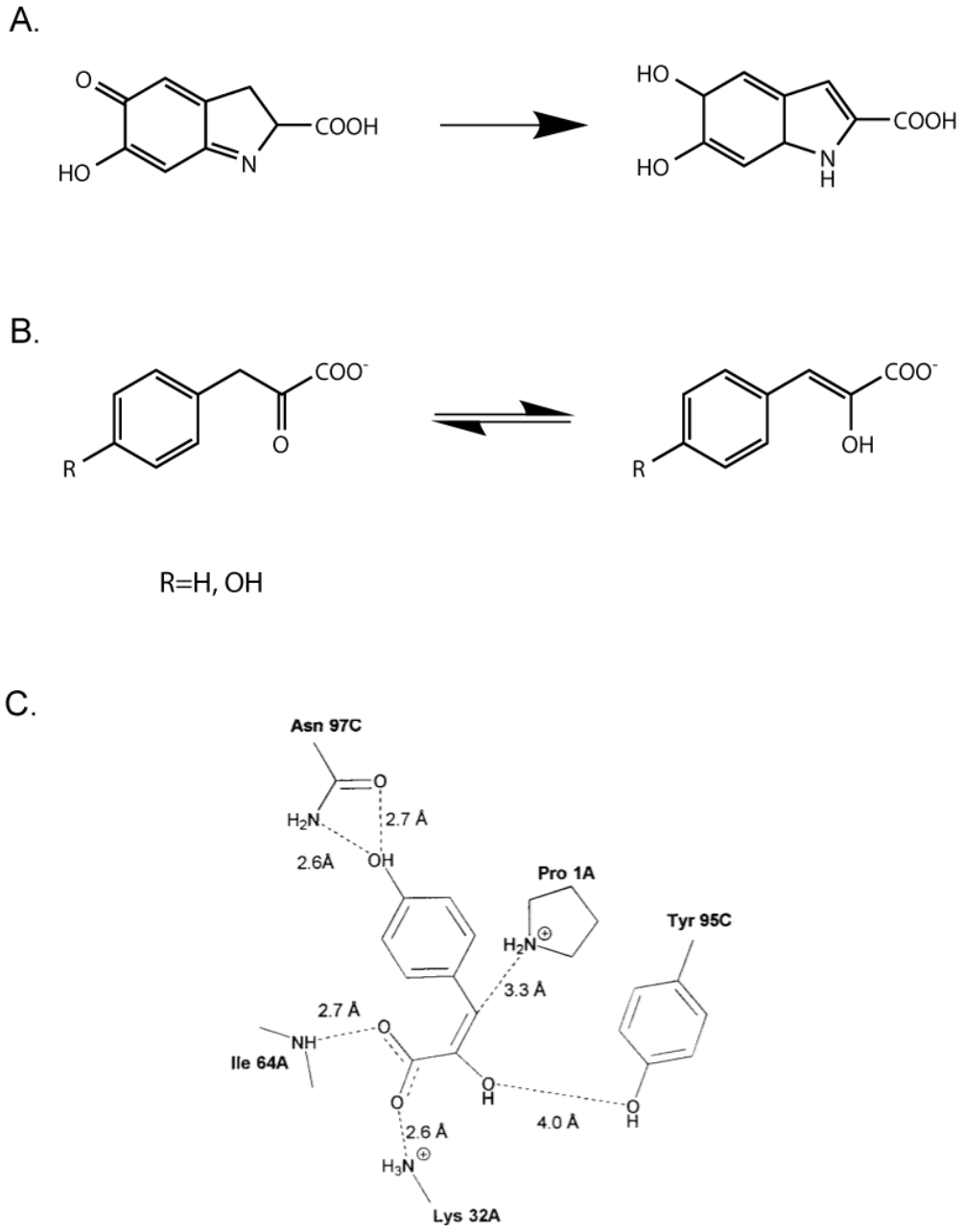

Figure 7. Tautomerase-reaction catalyzed by MIF. (***A***) Scheme of conversion of *D*-dopachrome and (***B***) phenylpyruvate. (***C***) Interactions of MIF with the substrate HPP (112).

The necessary low pKa for the function of Pro1 as the catalytic base in the reaction is given by its position in the hydrophobic cavity formed by these interacting residues. Solution NMR studies determined a pKa value of 5.6

for the nitrogen of Pro1, almost 4 pH units below the expected pKa for a nitrogen in a proline amid (113).

In contrast, the thiol-protein oxidoreductase (TPOR) activity cannot be explained with the static trimeric structure of MIF. The basis of this enzymatic reaction is a CXXC-motif that spans from Cys57 to Cys60 (114). Unlike the tautomerase/isomerase active site, the TPOR activity is buried deep in the interface of two MIF-molecules and can therefore not be active in a trimer. MIF catalyzes the reduction of insulin, 2-hydroxyethyl-disulfide, glutathione, and dihydrolipamide. (114). MIF shares this motif with a variety of enzymes of the TPOR family, including thioredoxin, protein disulfide isomerase and glutaredoxin (115).

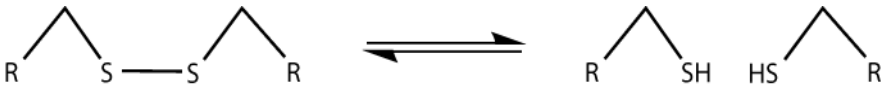

Figure 8. Schematic of oxidoreductase activities.

Both enzymatic activities have been linked to MIF's cytokine function. Amino acids 50-65 of the TPOR site of MIF are important for binding and modulation of the intracellular binding partner Jun activation domain binding protein (Jab1) (116, 117). Mutational studies of Pro-1 of the tautomerase active site showed that the mutant is defective in the neutrophil priming (113) and glucocorticoid counter-regulatory (118) activity of MIF.

1.4.8 Small Molecule Inhibitors of MIF

The observed connection of MIF tautomerase activity and biological function together with the ease of accessibility by enzymatic assays has raised the interest to the design of selective, low molecular weight MIF inhibitors to provide a potentially powerful approach to treat MIF-related diseases. Several small molecule inhibitors of MIF's enzymatic activity

have been developed and inhibitory effects on biological functions of MIF have been identified (Figure 9).

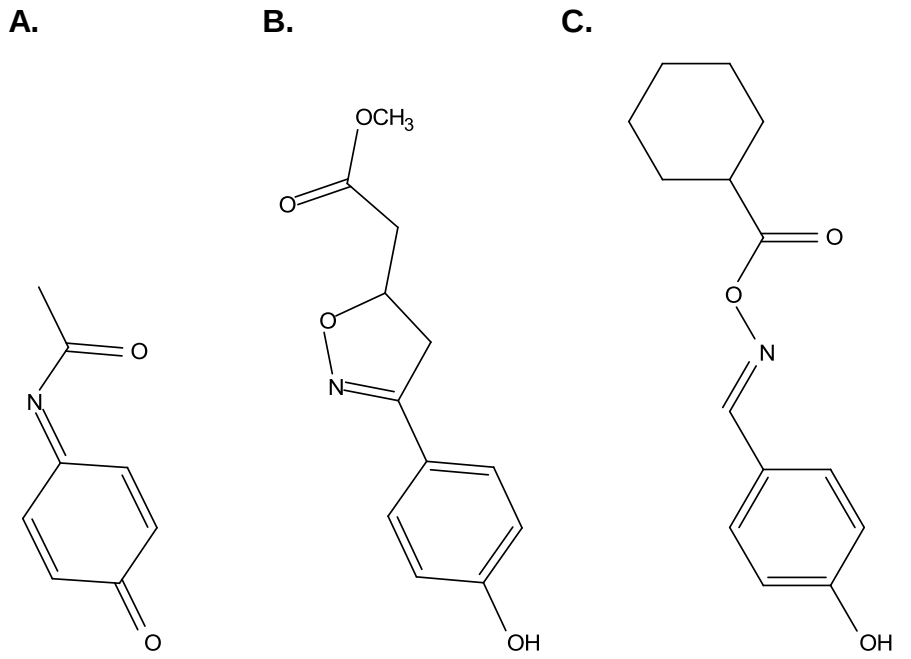

Figure 9. Small molecular MIF inhibitors. (***A***) N-(4-oxo-1-cyclohexa-2,5-dienylidene)-acetamide (NAPQI), (***B***) (S,R)-3-(4-hydroxyphenyl)-4,5-dihydro-5-isoxazole acetic acid methyl ester (ISO-1) and (***C***) (E)- 4-hydroxybenzaldehyde O- cyclohexanecarbonyloxime (OXIM-11).

(S,R)-3-(4-hydroxyphenyl)-4,5-dihydro-5-isoxazole acetic acid methyl ester (ISO-1), a competitive inhibitor of the tautomerase active site was shown to inhibit MIF-mediated glucocorticoid counter-regulatory activity and TNF-α release from cultured macrophages (54, 118). Furthermore, *in vivo* administration of ISO-1 demonstrated a protective effect in a mouse model of endotoxemia (54). Studies involving the inhibitor N-(4-oxo-1-cyclohexa-2,5-dienylidene)acetamide (NAPQI) which forms a covalent adduct between NAPQI and MIF (119) and the competitive inhibitor (E)-4-hydroxybenzaldehyde O-cyclohexanecarbonyloxime (OXIM-11) (120) further support the relationship between MIF's catalytic activity and biological function. Despite these promising effects, universally high IC_{50}s have limited the pharmacologic appeal of further developing existing small molecular MIF inhibitors.

2 Materials and Methods

2.1 Equipment, Consumables and Chemicals

2.1.1 Equipment

Equipment	Manufacturer
Äktapurifier FPLC	GE Healthcare, Piscataway, NJ
Analytical balance AE163	Metller Toledo, Columbus, OH
Beckman Avanti-J-E centrifuge	Beckman, Fullerton, CA
Biofuge pico centrifuge	Heraeus Instruments, Hanau, Germany
CO_2 incubator	VWR Scientific, Bridgeport, NJ
CO_2 incubator	Heraeus Instruments, Hanau, Germany
Confocal microscope LSM510	Zeiss, Thornwood, NY
Electrophoresis power supply	BioRad, Hercules, CA
Eppendorf centrifuge 5415D	Eppendorf, Westbury, NY
FPLC-System	Pharmacia, Uppsala, Sweden
French Pressure Cell Press	SLM Instruments, Rochester, NY
French Pressure Cell Press	Colora, Lorch, Germany
Gen-Cycler PCR	BioRad, Hercules, CA
HisTrap Metal Chelate Affinity Column	GE Healthcare, Piscataway, NJ
HiTrap ion exchange columns	GE Healthcare, Piscataway, NJ
HPLC chromatography system	Waters, Milford, MA
Laminar Flow Hood	Baker Company, Sanford, Me
Light Microscope	Olympus, Center Valley, PA
Microscope Olympus CK40	Olympus Co GmbH, Hamburg, Germany
Mosquito crystallization robot	Molecular Dimensions Ltd, Apopka, FL
pH-meter	Corning, Lowell, MA
Photometer UV-Visible Cary	Varian, Darmstadt, Germany
RAXIS-IV-Image Plate Detector	Rigaku, Tokyo, Japan
SDS-PAGE NuPAGE/XCell SureLock	Invitrogen, Carlsbad, CA
Sorvall RC5cPlus	Thermo Scientific, Waltham, MA
Spectrophotometer Infinite 200	Tecan, Männedorf, Switzerland
Superdex 75 10/300 GL size exclusion column	GE Healthcare, Piscataway, NJ
Superdex 75 16/60 pg size exclusion column	GE Healthcare, Piscataway, NJ
Vacuum concentrator	Bachhofer, Reutlingen, Germany
Western-Blot NuPAGE/XCell II Blot Module	Invitrogen, Carlsbad, CA

2.1.2 Consumables

Consumable	Manufacturer
Amicon-, Microcon-, Centricon-, and Centripep-filter devices	Millipore Corporation, Bedford, MA
Blotting paper	Whatman, Clifton, NJ
C8-SepPak Plus cartridge	Waters, Milford, MA
Cell culture equipment	BD Falcon, Bedford, MA
Cell culture equipment	Greiner Labortechnik, Frickenhausen, Germany
Cell culture insert, 8µm pore size	BD Falcon, Bedford, MA
Cell culture slides	BD Falcon, Bedford, MA
Eppendorf tubes 3810	Eppendorf, Westbury, NY
NuPAGE 12% Bis-Tris-gels	Invitrogen, Carlsbad, CA
Polypropylene tubes	BD Falcon, Bedford, MA
Protein crystallization covers (96 well)	Grace Bio Labs, Bend, OR
PVDF membrane	Millipore Corporation, Bedford, MA
Siliconized glass cover slides	Hampton Research, Aliso Viejo, CA
UV- Half Area Plate, 96 well	Corning, Corning, NY

2.1.3 Multi-Component Systems

Kit	Manufacturer
Biotin Protein Labeling	Roche, Indianapolis, IN
Crystal Screen I	Hampton Research, Aliso Viejo, CA
Crystal Screen II	Hampton Research, Aliso Viejo, CA
PyroGene Recombinant Factor C Endotoxin Detection System	Lonza, Walkersville, MD
QIAprep MiniPrep	Qiagen, Valencia, CA
Qiagen Plasmid Maxi Kit	Qiagen GmbH, Hilden, Germany
SaltRX Crystal Screen	Hampton Research, Aliso Viejo, CA
SlowFade Antifade	Invitrogen, Carlsbad, CA
SuperSignal West Dura	Pierce, Rockford, IL
Wizard I Crystal Screen	Emerald BioSystems, Bainbridge Island, WA
Wizard II Crystal Screen	Emerald BioSystems, Bainbridge Island, WA
Wizard SV Gel and PCR Clean-Up System	Promega, Madison, WI

2.1.4 Chemicals

Chemical	Manufacturer
Acetonitrile	J.T. Baker, Phillipsburg, NJ
Agarose	American Bioanalytical, Natick, MA
Amino acids	Sigma, St. Louis, MO
Ammonium bicarbonate	J.T. Baker, Phillipsburg, NJ
Ampicillin	Sigma, St. Louis, MO
Bacto agar	BD, Franklin Lakes, NJ
Bis-Tris-propane	Sigma, St. Louis, MO
Boric acid	J.T. Baker, Phillipsburg, NJ
Dextrose	J.T. Baker, Phillipsburg, NJ
DMEM	Invitrogen, Carlsbad, CA
DMEM	Gibco, Eggenstein, Germany
DNA ladder	Invitrogen, Carlsbad, CA
Dimethylsufoxide	Sigma, St. Louis, MO
Dopachrome	Sigma, St. Louis, MO
DTT	Sigma, St. Louis, MO
Ethidium bromide	Sigma, Munich, Germany
Fetal bovine serum	HyClone, Logan, UT
Fetal bovine serum	Gibco, Eggenstein, Germany
Glucose	Sigma, St. Louis, MO
Glycerol	Sigma, St. Louis, MO
Glycine	Fluka Chemie AG, Switzerland
Histopaque-1077	Sigma, Munich, Germany
H_2O (HyPure, endotoxin free)	HyClone, Logan, UT
p-hydroy-phenylpyruvat	Sigma, St. Louis, MO
L-3,4-dihydroxypehnylalanine methyl ester	Sigma, St. Louis, MO
Imidazole	Sigma, St. Louis, MO
Kanamycine	Sigma, St. Louis, MO
Luria Broth medium	Invitrogen, Carlsbad, CA
M9 Minimal Salts, 5x	Sigma, St. Louis, MO
Methanol	Fisher scientific, Pittsburgh, PA
ß-Mercaptoethanol	Sigma, St. Louis, MO
Milk powder	BioRad, Hercules, CA
NHS-Fluorescein	Pierce, Rockford, IL
p-nitrophenyl phosphate	Sigma, St. Louis, MO
NuPage LDS sample buffer	Invitrogen, Carlsbad, CA
NuPage SDS running buffer	Invitrogen, Carlsbad, CA
NuPage transfer buffer	Invitrogen, Carlsbad, CA
Penicillin/Streptomycin	Gibco, Eggenstein, Germany
Phosphate buffered saline, 10x	Sigma, St. Louis, MO
PIC-complete EDTA free	Roche, Indianapolis, IN
RPMI 1640	Gibco, Eggenstein, Germany
Sodium acetate	J.T. Baker, Phillipsburg, NJ

Sodium chloride	J.T. Baker, Phillipsburg, NJ
Sodium citrate	Invitrogen, Carlsbad, CA
Sodium hydroxide	J.T. Baker, Phillipsburg, NJ
Sodiumdodecylsulfate	Sigma, St. Louis, MO
Sodium m-periodate	Sigma, St. Louis, MO
Streptavidin-HRP	Promega, Madison, WI
Superblock buffer	Pierce, Rockford, IL
Texas Red-X phalloidin	Invitrogen, Carlsbad, CA
Tris	American Bioanalytical, Natick, MA
Tween-20	Sigma, St. Louis, MO
Urea	American Bioanalytical, Natick, MA

2.2 Bacteria, Yeast, and Mammalian Cells

2.2.1 Bacteria

Strain	**Genotype**	**Origin**
E.coli BL21(DE3)	F- ompT hsdSB (rB-mB-) gal dcm rne131 (DE3)	Invitorgen, Carlsbad, CA
E.coli DH5a	F- mcrA Δ(mrr-hsdRMS-mcrBC)φ80lacZ ΔM15 ΔlacX74 recA1 araD139 Δ(araleu)7697 galU galK rpsL (StrR) endA1 nupG	Invitrogen, Carlsbad, CA
E.coli M15 [pREP4]	(Nal^{s} Str^{s} rif^{s} lacI^{-} ara^{-} gal^{-} mtI^{-}F recA^{-} uvr^{+})	Qiagen, Valencia, CA

2.2.2 Yeast Cells

Strain	**Genotype**	**Origin**
AH109	MATa, trp1-901, leu2-3, 112, ura3-52, his3-200, gal4Δ, gal80Δ, LYS2::GAL1UAS-GAL1TATA-HIS3, GAL2UAS-GAL2TATA-ADE2,URA3::MEL1UAS-EL1TATA-lacZ, MEL1	Clontech Laboratories, Palo Alto, CA

2.2.3 Mammalian Cells

Description	Characterization	Reference
RAW 264.7	Macrophage; Abelson murine leukemia virus-transformed	ATCC

2.3 Plasmids and Primers

2.3.1 Plasmids

Plasmid	Insert	Description	Resistance	Reference
pET22b	PfMIF-HIS	Bacterial expression	Amp	This work
pET11b	MIF		Amp	Lolis Lab
pCRT7-NT-TOPO	PfMIF		Amp	Bucala Lab
pCRT7-NT-TOPO	LmMIF		Amp	Bucala Lab
pQE-30-uA	HIS-CD74		Amp	Lolis Lab
pET22b	p115-HIS			Bucala Lab
pGBKT7	LmMIF	Yeast two-hybrid	Kan	This work
pGBKT7	hMIF		Kan	This work
pGADT7	LmMIF		Amp	This work
pGADT7	hMIF		Amp	This work

pGADT7 and pGBKT7 positive and negative control plasmids are from Clontech Laboratories, Palo Alto, CA.

2.3.2 Primers

hMIF-yeast-fw	5'-GGAATTCCATATGCGATGTTCATCGTAAACACC-3'
hMIF-yeast-rv	5'-CGGGATCCTTAGGCGAAGGTGGAGTTGT-3'
LmMIF-yeast-fw	5'-GGAATTCCATATGCCGGTCATTCAAACGTTTG-3'
Lm-yeast-rv	5'-CGGGATCCTTAGAAGTTTGTGCCATTCCAG-3'
PfMIF-fw	5'-CGCTAGACATATGCCGTGCTGCGAAGTG-3'
PfMIF-rv	5'-CCGCTCGAGGCCAAACAGGCTGCCGCATTTG-3'

2.4 Media, Buffer and Solutions

2.4.1 Media for Bacterial Culture

LB-media			Trypton	10 g
			Yeast extract	5 g
			NaCl	10 g
			H_2O	ad 1 L
		For plates	Bacto agar	10 g
		For selection	Ampicilin or kanamycin	50 mg
10x M9 media			Na_2HPO_4	60 g
			KH_2PO_4	30 g
			NH_4Cl	10 g
			NaCl	5 g
			H_2O	ad 1 L

2.4.2 Yeast Media

YPD			1% Bacto yeast extract	10 g
			2% Bacto peptone	20 g
			2% Dextrose	20 g
			2% Bacto agar	20 g
			H_2O	add 1000 ml
SD minium media	2xAgar	- autoclave - warm to 70°C	4% Bacto agar in 25mM HEPES, pH 6.8	250 ml
	Nutrient mix	- sterile filtrate - warm to 70°C	10x YNB (67g/l)	50 ml
			10x Glucose (200g/l)	50 ml
			Amino acids	As needed for selection
			H_2O	add 250 ml
		Mix 2x agar and nutrient mix		

2.4.3 Cell Culture Media

Media for PBMCs	Dulbecco's RPMI	
	Penicillin	100 µg/ml
	Streptavidin	100 µg/ml
	L-glutamine	2 mM
Media for RAW 264.7	DMEM	
	Penicillin	100 µg/ml
	Streptavidin	100 µg/ml
	L-glutamine	2 mM

2.4.4 Buffers and Solutions

If not indicated otherwise, all buffers and solutions were prepared in reagent grade water (ddH_2O)

2.4.4.1 General Buffers

PBS, pH 7.4	NaCl	137	mM
	KCL	2.7	mM
	KH_2PO_4	1.5	mM
	Na_2HPO_4	8.1	mM
TAE-buffer (50x)	Tris-HCl, pH 8,5	2	M
	Acetic acid	1	M
	EDTA	100	mM
TBS	Tris, pH 7.4	20	mM
	NaCl	150	mM
TBST	TBS		
	Tween-20	0.05	%
Coomassie staining	Coomassie Brilliant Blue R-250	0.25	%
	Methanol	40	%
	Glacial acidic acid	10	%

2.4.4.2 Tautomerase Assay

Dopachrome assay		
Preparation of dopachrome*		
L-3,4 dihydroxyphenylalanine methyl ester	4	mM
Sodium m-periodate	8	mM
Working mixture		
Potassium phosphate buffer, pH 7.4	40	mM
L-dopachrome	750	µM
Hydroxyphenylpyruvate assay		
Preparation of p-hydroxyphenylpyruvate (5 mM)**		
18 mg of the crystalline free acid (enol)	18	mg
0.05 M acetate,pH 6	20	ml
Working mixture		
Boric acid, pH 6.2	424	mM
p-hydroxyphenylpyruvate	750	µM

* Mix and incubate at RT for 5 min, then put on ice.
** store at RT for 24 hours to tautomerize. It is then in the keto form and can be stored at 4°C for two weeks.

2.4.4.3 FPLC, HPLC and Refolding Buffers

Protein	**Column**	**Buffer**		
LmMIF	Q-Sepharose	Binding-buffer		
		Bis-Tris-propane, pH.6.8	30	mM
		NaCl	20	mM
		Elution-bufferI (salt gradient)		
		Bis-Tris-propane, pH.6.8	30	mM
		NaCl	400	mM
		Elution-buffer II (pH gradient)		
		Citric buffer, pH 5.5	20	mM
		NaCl	20	mM
PfMIF	Q-Sepharose	Binding-buffer I (pH gradient)		
		Tris-HCL, pH.8.5	20	mM
		NaCl	10	mM
		Elution-buffer I (pH gradient)		
		Bis-Tris-propane, pH.6.3	20	mM
		NaCl	10	mM

PfMIF	Q-Sepharose	Binding-buffer II (salt gradient)		
		Tris-HCL, pH.8.0	20	mM
		NaCl	10	mM
		Elution-buffer II (salt gradient)		
		Tris-HCL, pH.8.0	20	mM
		NaCl	500	mM
PfMIF-HIS and $p115^{728-962}$-HIS	HisTrap-Nickel Affinity	Binding buffer		
		Tris-HCl, pH 8	50	mM
		NaCl	200	mM
		Imidazole	20	mM
		ß-mercaptoethanol	10	mM
		Glycerol	10	%
		Elution buffer		
		Tris-HCl, pH 8	50	mM
		NaCl	200	mM
		Imidazole	400	mM
		ß-mercaptoethanol	10	mM
		Glycerol	10	%
$CD74^{73-232}$		Lysis buffer (French Press)		
		Tris-HCl, pH 8.0	20	mM
		NaCl	150	mM
		Imidazole	10	mM
		Homogenization/Binding buffer		
		Imidazole, pH 9.0	10	mM
		Urea	8	M
		NaCl	150	mM
		Elution buffer		
		Imidazole, pH 9.0	500	mM
		Urea	8	M
		NaCl	150	mM
		Refolding buffer		
		Tris-HCl, pH 8.0	10	mM
		NaCl	150	mM
human MIF	DEAE/Q-Sepharose	Loading/Elution buffer		
		Tris-HCL, pH.7.4	20	mM
		NaCl	20	mM

2.5 Cell Culture Techniques

Cells were cultured by routine protocols at 37°C in a humidified atmosphere with 5% CO_2. When cells where > 80% confluent, adherent cells were detached from culture flask using Trypsin/EDTA, washed twice with PBS, and replated at 1:4 dilution.

2.5.1 Isolation of PBMCs

Blood was collected in a heparinized syringe and slowly layered on top of 7 ml of Histopaque-1077 in a 15 ml colonial centrifuge tube. Following centrifugation at 400 x g for exactly 30 min at RT, the upper plasma layer to within 0.5 cm to the mononuclear cells containing opaque interface was carefully removed and discarded. PBMCs were transferred into a new 15 ml conical tube, washed 3 times with PBS and resuspended in RPMI to $1x10^6$ cells/ml.

2.5.2 Chemotaxis Studies

Aliquots of PBMCs were placed in the upper chamber of a 24-well cell culture insert with 8 μm pore size (Falcon). In the lower chamber, MIF or LmMIF was placed following a 30 min pre-incubation with test compounds. Test compounds included the MIF inhibitors ISO-1 and 4-IPP or an N-terminal peptide of CXCR4 ($CXCR4^{1-27}$). After incubation for 3 hours at 37°C, 5% CO_2 transmigrated cells were methanol fixed, stained with Giemsa and counted under light microscopy.

2.5.3 Cellular Uptake Studies

Fluorescein labeling of LmMIF and MIF was performed with N-hydroxysuccinimide (NHS)-fluorescein as described by manufacturer. For uptake studies, murine RAW264.7 macrophages cultured on glass cover

slides were incubated with fluo-MIF or fluo-LmMIF (1.5 µM) for 30 min at 37°C. Cells were washed three times with PBS, three times with 50mM glycine/PBS, and then fixed for 20 min at 37°C with 3.7% formaldehyde/0.1% Triton-X/PBS solution. Actin staining was visualized with Texas Red-X phalloidin.

2.6 Methods in Molecular Genetics/Biology

2.6.1 Transformation of Bacteria

Plasmid DNA was added to 50 µl of competent cells and incubated on ice for 30 min. The mixture was transferred to a water bath at 42°C for 45 sec and than placed on ice for 2 min. Subsequently, 400 µl LB medium were added and the cells were incubated at 37°C for one hour. This period allows the bacteria to recover and to begin to express antibiotic resistance. The medium was now spread onto selection plates and incubated overnight at 37°C to allow plaque formation.

2.6.2 Plasmid-DNA Extraction from Bacteria

Small amounts of up to 20 µg of plasmid DNA from a 5 ml overnight culture were purified according to manufactures instructions using Plasmid-DNA-Mini-Kit.

2.6.3 Transformation of Yeast Cells (Yeast two Hybrid)

Plasmid DNA was introduced into yeast by a modified lithium acetate method (121). To produce competent cells, several fresh colonies (2 – 3 mm in diameter) were inoculated in 1 ml YPDA, vortexed vigorously for 5 min to disperse clumps and transferred into a flask containing 50 ml YPDA. The cells were incubated at 30ºC with shaking at 250 rpm to stationary phase (OD_{600}>1.5; 14 – 18 hours). 30 ml of the overnight culture

then were diluted in a flask containing 300 ml YPDA to an OD_{600} of 0.2 – 0.3. After shaking the cells for another 3 h, the cell-suspension with an OD_{600} of 0.4 – 0.6 was centrifuged at 1000 x g for 5 min, washed with sterile H_20 and resuspended in 1.5 ml freshly prepared 1x TE/LiAc.
For the transformation, 0.1 ml of the competent cells were mixed with 0.1 mg herring test carrier DNA and 0.1 mg plasmid DNA followed by vortexing with 0.6 ml PEG/LiAc solution. The mixture was incubated at 30ºC for 30 min with shaking, 70 µl DMSO were added and the heat shock was done for 15 min in a 42ºC water bath. Cells were chilled on ice, pelleted (5 sec; 14000 rpm), resuspended in 0.5 ml TE buffer and spread on SD agar plates that selected for desired transformants.

2.6.4 Agarose Gel Electrophoresis

To analyze and isolate DNA according to its mass, agarose gel electrophoresis was carried out. DNA was applied to a gel of 1% agarose/TAE and separated at 100 V. The DNA was visualized in the gel by addition of ethidium bromide under UV light.

2.6.5 Isolation of DNA from Agarose Gels

DNA bands from PCR or restriction reactions were purified from agarose gels using Wizard SV Gel and PCR Clean-Up System according to manufacturer's instructions.

2.6.6 Digestion of DNA with Restriction Enzymes

1 ug of purified DNA was incubated with 1 U of restriction enzyme and a corresponding buffer for 2 – 4 hours at 37°C. To assess complete digestion, the fragments were separated by agarose gel electrophoresis.

2.6.7 Ligation of DNA fragments

Purified DNA fragments were mixed in a molar ratio of 1:3 vector/insert with 40 U of T4-DNA ligase and T4-ligase Buffer in a 20 µl reaction. The reaction was incubated at 16°C over night or at room temperature for 3 hours.

2.6.8 Determination of DNA Concentration

The concentration and purity of DNA/RNA was determined by photometric analysis. Nucleic acids absorb light with an absorption maximum at 260 nm wavelength with an average extinction coefficient of 0.020 $(\mu g/ml)^{-1}\,cm^{-1}$ for double stranded DNA. Thus an optical density of 1 corresponds to a concentration of 50 µg/ml.

The ratio between OD_{260} vs. OD_{280} assesses the purity of the sample with respect to protein contamination. A quotient of 1.8 to 2.0 indicates an optimal sample.

2.6.9 PCR

Template DNA was amplified by Polymerase chain reaction. The PCR program and the concentrations of the components of a typical PCR reaction are listed in the table below.

Component	***Concentration***	***PCR-program***			
		Step	**T (°C)**	**t (s)**	**repeats**
DNA-template	20 ng -1 µg	Denaturation	95	5	
Primer-forward	1 µM	Denaturation	95	1	
Primer-reverse	1 µM	Annealing	55-65	1	35
Polymerase-Buffer	1x	Polymerisation	72	2	
dNTP-mix	0.3 mM	Cooldown	4	10	
Polymerase	0.05 U/µl				
ddH_2O	ad 50 µl				

2.7 Methods of Protein Biochemistry

2.7.1 Protein Expression

Cloned DNA constructs were transformed into the *E.coli* strain Bl21(DE3) or M15(pREP4), respectively. *E.coli* cells containing the expression vector were grown overnight at 37°C in Luria Broth supplemented with appropriate antibiotics. The next morning, fresh media was inoculated with the preculture (1:20) and cells were grown to an OD_{600} of 0.6 to 0.8, induced with 1mM IPTG and harvested 4 hours later.

For the production of selenomethionated protein, cells from the preculture were harvested and washed with PBS. The cells then were used to inoculate Minimal media lacking Gly, Ala, Pro, Asn, Cys and Met and grown to an OD_{600} of 0.5 to 0.6. Per liter of culture, 100 mg of Thr, Lys, and Phe; 50 mg of Leu, Ile, and Val; and 60 mg of L-SeMet was added as solid powder. The temperature then was changed to 30°C, the protein expression was induced with 1 mM IPTG and the cells were harvested the next morning.

2.7.2 Purification of Proteins

2.7.2.1 Purification of Native Sequence LmMIF

Recombinant, native sequence LmMIF protein was produced by expression from the pCRT7/CT-TOPO *E. coli* plasmid, with the inserted sequence engineered with a 3' stop codon to prevent expression of the V5-His carboxy terminal tag in *E.coli* (DE3) cells.

Cells were harvested by centrifugation, washed two times in lysis buffer (30 mM Bis-Tris (pH6.8), 20 mM NaCl) and resuspended at 2.5% of the original volume of growth medium. Cells were lysed in the presence of protease inhibitor cocktail using a French Press. Soluble proteins were collected by centrifugation at 16 rpm for 25 min. The filtered supernatant was applied to a Q-Sepharose Fast Flow column previously equilibrated with lysis buffer. Unbound proteins were washed out of the column using

lysis buffer. LmMIF was eluted in a salt gradient (elution buffer A: 30 mM Bis-Tris (pH 6.8), 400 mM NaCl). LmMIF-containing fractions than were pooled and dialyzed against lysis buffer. For the second purification step, the sample was re-loaded on the Q-Sepharose column equilibrated with lysis buffer and eluted by applying a pH gradient towards 20 mM citric buffer (pH 5.5), 20 mM NaCl. The residual impurities were removed in a third step by gel filtration over a Superdex 75 column (HiLoad 16/60) with 30 mM Bis-Tris (pH 6.8), 20 mM NaCl.

2.7.2.2 Purification of Native Sequence PfMIF

PfMIF was expressed and purified from pCRT7/CT-TOPO *E. coli* plasmid in a similar fashion than LmMIF with the following differences. The harvested cells were resuspended and lysed in 20 mM Tris (pH 8.5), 10 mM NaCl. The soluble protein fraction than was loaded on a Q-Sepharose Fast Flow column and eluted with a linear pH gradient to 20 mM Bis-Tris (pH 6.3), 10 mM NaCl. After rebuffering the PfMIF-containing fractions to 20 mM Tris (pH 8.0), 10 mM NaCl and reloading on the Q-Sepharose column the protein was eluted with a liner salt gradient towards 20 mM Tris (pH 8), 500 mM NaCl.

2.7.2.2.1 Endotoxin Removal from LmMIF and PfMIF

MIF has an unusually high affinity for endotoxin that must be removed to ensure that lipopolysaccharide (LPS) does not interfere with the results of the biological assays. To ensure a low endotoxin content, all buffers used for purification were prepared using endotoxin-free HyPure Cell Culture Grade Water (<0.005 EU/ml; HyClone). Columns were treated in 3 cycles with 2 column volumes of 1 M NaOH followed by 2 column volumes of pyrogen-free water. The resulting MIF preparations contained <20 pg LPS/µg protein as determined by the PyroGene Recombinant Factor C assay (Cambrex BioScience).

2.7.2.3 Purification of Human MIF

Human MIF was produced by expression from the pET11b *E.coli* plasmid. Cells were harvested, lysed by French press in 20 mM Tris (pH 7.4)/20 mM NaCl. Soluble proteins were collected by centrifugation. The filtered lysate then was applied to a DEAE-Sepharose anion exchange column serially connected to a SP-Sepharose cation exchange column equilibrated with 20 mM Tris (pH 7.4), 20 mM NaCl. Under these buffer conditions, most contaminating proteins bind one of the chromatographic media, whereas human MIF does not. The MIF-containing fractions were pooled and concentrated. The residual impurities were removed by gel filtration over an S-75 column (HiLoad 16/60 Superdex 75)

2.7.2.3.1 Endotoxin Removal from Human MIF

For removal of LPS from huMIF, approximately 2 mg of purified protein was applied to reversed phase chromatography on a C8-SepPack column activated with methanol and then washed with low endotoxin water. The bound protein was washed with pure water and 30% acetonitrile and eluted with 60% acetonitrile. The samples were kept at -80 °C until lyophilization. For refolding, lyophilized pellets of MIF were dissolved in 350 µl of 8 M urea and incubated for 1 hour. Four microliters of 1 M DTT was added and the solution was incubated for an additional hour at RT. Three consecutive times, 350 µl of 10 mM DTT were added, the contents were swirled, and the tube was incubated at room temperature for 30 min. The solution was then incubated at 4 °C for 30 min and subsequently centrifuged at 14,000 rpm for 10 min at 4 °C. The protein was dialyzed at 4 °C against 10 mM dithiothreitol in Tris-buffered saline, pH 7.4 using a dialysis Slidealyzer cassette (Pierce) MWCO 7,000 overnight followed by dialysis against Tris-buffered saline over the next several days.

2.7.2.4 Purification of Histidine-tagged p115$^{728-962}$ and PfMIF

p115 or PfMIF were produced by expression from the pET22b *E. coli* plasmid, with the inserted sequence engineered to produce a C-terminal histidine fusion protein. Pelleted bacteria were resuspended in binding buffer (50 mM Tris (pH 8.0), 20 mM imidazole, 10 mM ß-mercaptoethanol, 200 mM NaCl, 10% Glycerol) and lysed by French Press. The crude bacterial extract was purified using a HisTrap FF nickel chelating column with a linear gradient of 20 – 400 mM imidazole/ binding buffer. The peak fractions, as determined by SDS-PAGE, were subjected to gel filtration chromatography.

2.7.2.5 Purification of CD74$^{73-232}$

CD74$^{73-232}$ was expressed from a pQE-30uA *E.coli* expression vector engineered to produce a 6xHis-tagged N-terminal fusion-protein. Given the instability of this protein, it is necessary to work quickly and to keep the protein on ice or at 4°C. It also was essential to use 0.1 mM PMSF in all steps. Pelleted cells were resuspended in lysis buffer (20 mM Tris (pH 8.0), 150 mM NaCl, 10 mM imidazole) and lysed using a French press. CD74 inclusion bodies were separated by centrifugation at 18000 X g for 25 min. The pelleted proteins were resuspended in binding buffer (10 mM imidazole (pH 9.0), 8 M Urea, 150 mM NaCL), homogenized using a dounce homogenizer, filtered and loaded on a HisTrap FF nickel chelating column equilibrated with binding buffer. CD74$^{73-232}$ was eluted using a gradient against elution buffer (500 mM imidazole/ binding buffer). The CD74$^{73-232}$-containing peak was then pooled and slowly dialyzed against refolding buffer (10 mM Tris (pH 8.0), 150 mM NaCl). At this step, a breakdown product of CD74$^{73-232}$ might be detectable by SDS-page analysis which can be removed by reversed phase HPLC using a C4 column. The protein is loaded on the column using 0.1% TFA/H_2O and eluted with a linear gradient against 0.1% TFA/Acetonitrile, pooled and refolded.

2.7.3 SDS-Polyacrylamide Gel Electrophoresis (SDS-PAGE)

Proteins were boiled for 10 min in LDS sample loading buffer to produce a linear polypeptide chain coated with negatively charged LDS molecules. Proteins then were separated according to their size in Bis-Tris 12% polyacrylamide gels (Lammli 1970) at 180 V in a NuPAGE/XCell SureLock chamber.

2.7.4 Coomassie Staining

Coomassie Blue staining is based on the binding of the dye Coomassie Brilliant Blue R250, which binds basic amino acids. Polyacrylamide gels were incubated in Coomassie staining solution. To visualize the proteins, the gel was microwaved in dH_2O three to five times for 2 minutes.

2.7.5 Competition Binding Assay

The binding of LmMIF to recombinant, soluble CD74 ectodomain ($sCD74^{73–232}$), the C-terminal region of the Golgi-associated binding protein p115 ($p115^{702-962}$) or the N-terminal region of CXCR4 ($CXCR4^{1-27}$), respectively was studied by coating individual wells of a 96-well plate with these proteins as described by Leng *et al.* (55). Plates were washed 4 times with TBST (pH 7.4) and blocked with Superblock buffer for two hours at room temperature. Human MIF was biotinylated and added at 2 µg/ml in triplicate wells with increasing concentrations of human MIF or controls. Incubation was continued at room temperature for 2 hours followed by washing with TTBS (pH 7.4). The bound, biotinylated hMIF was detected by adding streptavidin-conjugated alkaline phosphatase for 1 h, followed by washing and detection with *p*-nitrophenyl phosphate. The OD_{405} was measured and values plotted as percent OD_{405} relative to wells containing biotinylated human MIF alone. Each plot represents at least three independently performed assays, and each data point depicts a SEM ≤10%.

2.7.6 BIAcore Analysis

The real-time binding interaction of LmMIF or PfMIF with $sCD74^{73–232}$ measured by surface plasmon resonance was carried out by Chen Y, Kwong YK, Xiong H, and Zhang B (Mt. Sinai School of Medicine, NY) using a BIAcore 2000 optical biosensor (BIAcore) as previously described (55). Briefly, $sCD74^{73–232}$ was diluted in 10 mM sodium acetate (pH 5.2) at 1 µmol. Fifty microliters of a *N*-hyrdoxysuccinimide and *N*-ethyl-*N*-(dimethyaminopropyl)carbodiimide mixture was injected at a speed of 2 µl/min for 25 min, followed by injection of 50 µl of 1 µM purified $sCD74^{73–232}$. Once the surface plasmon resonance reached 10,000 U, the injection was stopped, and the active amine sites were blocked with 35 µl of 1 M ethanolamine (pH 8.5). The immobilized CM5 chip was washed overnight with 1x PBS at 20 µl/min. The derived sensor chips were washed and equilibrated in HEPES or PBS (pH 8.0; 20 µl/min) and the ligand (LmMIF or PfMIF) was introduced at five serial dilutions in BIAcore buffer (1 mM DTT, 2.5 mM $MgCl_2$, 20 mM HEPES, 1 mM EDTA, 150 mM NaCl, 0.005% P20) in 60 – 100 µl injection volumes at a flow rate of 20 µl/min. Binding was measured at 25°C for 5 min, followed by 15 min of dissociation. Sensor chip regeneration was performed for 1 min with 1 M NaCl, 50 mM NaOH. The whole process was repeated three times for each dilution sample. Sensorgram response data were analyzed in the BIA evaluation kinetics package and the equilibrium binding constants calculated.

2.7.7 Determination of Protein Concentrations

Protein concentrations were determined by measuring absorbance at 280 nm. Extinction coefficients were estimated using the following equation:

Equation 1:

$$\varepsilon_{280} = \text{Numb(Tyr)}*\varepsilon_{280}\text{(Tyr)} + \text{Numb(Trp)}*\varepsilon_{280}\text{(Trp)} + \text{Numb(Cysteine)}*\varepsilon_{280}\text{(Cystine)}$$

Where: ε_{280} (Tyr) = 1490, ε_{280} (Trp) = 5500, ε_{280} (Cys) = 125

Protein	Extinction Coefficient [M^{-1} cm^{-1}]
huMIF	13688
LmMIF	10095
PfMIF	7700
$CD74^{73-232}$	19480

Protein concentration of $p115^{702-962}$, which does not possess significant absorbance at 280 nm was measured by Bradford according to manufacturer's instructions.

2.7.8 *D*-Dopachrome Tautomerization Assay

The model MIF substrate, *D*-dopachrome methyl ester (2.4 mM), was prepared as described previously. Tautomerase activity was determined at room temperature by adding a final concentration of 0.75 mM dopachrome methyl ester (ε=3700 $M^{-1}cm^{-1}$) to a 96-well plate containing human MIF or LmMIF in 40 mM potassium phosphate buffer (pH 7.4). The inhibitory effect of ISO-1 or 4-IPP was determined by pre-incubating LmMIF or human MIF with inhibitor for 30 mins prior to addition of the substrate. The initial velocity of the MIF-mediated conversion of *D*-dopachrome methyl ester to indole carboxylic acid methyl ester was measured for 30 sec at λ=475 nm and the specific activity expressed as converted dopachrome in mM/min/μM of protein.

2.7.9 Mass Spectrometry

Recombinant proteins were analyzed by electrospray using a C-4 capillary column and a Q-Tof Micro mass spectrometer at the Proteomics and Mass Spectrometry Resource of the Yale Keck Laboratory. Solvent A was 5% acetonitrile, 0.1% formic acid and 0.02% trifluoroacetic acid. Solvent B consisted of 95% acetonitrile, 0.1% formic acid and 0.02% trifluoroacetic acid. The flow rate was 5μL/min. The mass measurement accuracy of this instrumentation was ± 0.01–0.02%.

2.7.1 Steady-State Fluorescence Spectroscopy

In titration experiments, 2.5 µM LmMIF and various concentrations of $CXCR4^{1-27}$ (0-30 µM) were mixed. Fluorescence intensity was monitored at an excitation wavelength of 288 nm and an emission range of 320-360 nm. Non-linear fitting to an equation describing MIF-$CXCR4^{1-27}$ equilibrium was used to determine the dissociation constant.

2.7.2 NMR-Experiments

Samples for NMR spectroscopy contained 300 µM ^{15}N-MIF and 600 µM $CXCR4^{1-27}$ in 8% D_2O/PBS. $^{1}H^{15}N$-HSQC experiments were carried out at 25 °C in a Varian INOVA 600MHz spectrometer with a 5-mm triple resonance probe equipped with a triple-axis (XYZ) pulsed magnetic field gradient. All pulse sequences were taken from the Varian BioPack user library. Spectra were processed and analyzed using the programs nmrPipe (122) and Sparky (123). Assignment of resonance peaks for MIF was based on a previously published resonance assignment (107).

2.8 Methods of Structural Biology

2.8.1 Protein Crystallization

For protein crystallization, the purified proteins were concentrated using Amicon Ultra Centrifugal Filters with a 5 kDa cutoff. All crystals were obtained by the hanging drop vapor diffusion method at 18 °C. Drops were prepared by combining equal volume of protein solution and reservoir solution.

Initial crystallization trials were performed using different protein concentrations on a Mosquito crystallization robot in a 96-well plate format using the standard Hampton and Wizard screens. Refinement screens were done in 24-well plates using the hanging drop vapor diffusion method with a drop composition of 1 µl protein and 1 µl well solution.

2.8.2 Data Collection of LmMIF

For data collection, the crystals were cryoprotected in the reservoir solution with 20% glycerol. Diffraction data were collected at beamline X29A in the Brookhaven National Laboratory (BNL). Multiple wavelength anomalous diffraction (MAD) data with a selenomethionylated crystal were collected at three different wavelengths (0.97912 Å, 0.97928 Å and 0.96389 Å) and a single wavelength data with a native crystal was collected at 0.95 Å to a resolution of 1.03 Å. The data were indexed at the space group R3 (a=b=52.3 Å, c=96.8 Å) and scaled using HKL2000 (124).

2.8.3 Structure Determination of LmMIF

Intensity conversion to structure factor amplitudes was carried out with SCALA in the CCP4 program package. Initial attempts to solve the structure by the Molecular Replacement method were unsuccessful because of low sequence identity with the human MIF search models (21%).

The three-dimensional structure of LmMIF was solved using the Multi-Wavelength Anomalous Dispersion method (MAD). The initial phase was determined using HKL2MAP (125). The MAD dataset was analyzed with SHELXC and the heavy atom substructure was determined with SHELXD. The phase problem was solved with SHELXE and SHELXD found a solution containing 3 selenium sites in the asymmetric unit of the crystal structure. The human MIF structure (101) was used as a template to build an initial LmMIF model using XTALVIEW (126). The model was refined against the native data using REFMAC (127) and CNS (128) followed by SHELX-97 (129). XTALVIEW was used to visualize the structure and to make manual adjustments of the coordinates to improve their agreement with the electron density map. Crystallographic data collection and refinement statistics are listed in Table 4. The coordinates of the LmMIF structure have been deposited with the Protein Data Bank under accession code 3B64.

Because the electron density could not be seen, the sidechain of residue 4 is absent in the final model.

2.8.4 Data Collection of Human MIF◦4-IPP Complex

Data were collected in house using a Rigaku RAXIS-IV imaging plate area detector. The crystal was cryo-protected in the reservoir solution containing 25% glycerol. Diffraction data were collected at –180 °C and integrated and scaled by HKL2000 (15) to 1.8 Å.

2.8.5 Structure Determination of Human MIF Complexed with 4-IPP

The structure was solved by molecular replacement with Phaser (130) using the structure of MIF in complex with Oxim-11 as search model (120). Refinement was performed using CNS and Refmac (127, 128) and manual manipulation of the model was done using MIFit 4.1. The structure is available from the RCSB Protein Data Bank and has been assigned the RCSB ID code RCSB045257 and PDB ID code 3B9S.

3 Specific Aim

The aim of this thesis was the biochemical, biological and structural characterization the MIF orthologs from the protozoan parasitic species *Leishmania major* and *Plasmodium falciparum*. This work addressed whether the parasitic proteins have the potential to mimic or to interfere with the host homologue and thus play a potential role in the diverse immune evasion strategies employed by these parasites.

To achieve this goal, purification procedures for the parasitic MIF proteins had to be established and structural studies were aimed to elucidate whether the sequence similarity of the parasitic proteins extends to its three-dimensional structure.

In order to accomplish immune evasion, the parasitic proteins should at least interact with some of the host MIF binding partners. Therefore, known intracellular and extracellular interaction partners of the human MIF protein were purified and analyzed for direct interaction via ELISA-based competition assays, surface plasmon resonance spectroscopy, steady-state fluorescence spectroscopy and nuclear magnetic resonance spectroscopy.

Cell migration, ERK1/2 MAP kinase activation and inhibition of apoptosis are important immunological functions linked to MIF. To study whether the parasitic proteins can mimic or block some of these biological characteristics could further support their role in immune evasion.

Finally, small molecular inhibitors aimed at the tautomerase active site of MIF were shown to block its biological function. However, therapeutic interest of existing inhibitors is limited due to low binding affinity; more potent inhibitors are desired. Therefore, an additional aim of this thesis was the characterization of a new, prototypic human MIF inhibitor by crystallographic methods. Furthermore, it was of interest to investigate the potency of existing human MIF inhibitors on their parasitic counterparts for a future development of specific, parasitic MIF inhibitors.

4 Results

4.1 Structure Determination of Human MIF in Complex with the Novel Active Site Inhibitor 4-IPP

4.1.1 Crystallization of Human MIF Complexed with 4-IPP

MIF possesses an unusual ability to catalyze the tautomerization of the non-physiological substrates *D,L*-dopachrome methylester into their corresponding indole derivates (111). Numerous studies have shown the importance of this enzymatic active site for the biological activities of MIF (54, 113, 118, 120). Targeting this site with high affinity inhibitors could provide improved biologic inhibitory activities against MIF.

Using a computational virtual screening strategy, 4-iodo-6-phenyl-pyrimidine (4-IPP) was identified as a small molecule inhibitor of human MIF by Bob Mitchell and colleagues (Figure 10). Preliminary studies performed by this group showed that 4-IPP forms a covalent modification of the MIF protein and inhibits the tautomerization activity with a ~ 5 – 10 times higher potency than the current described inhibitors (118-120).

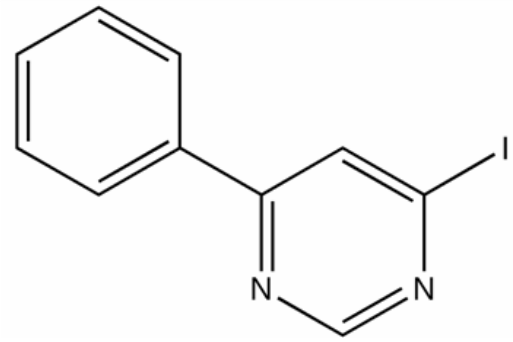

Figure 10. Structure of the small molecule MIF inhibitor 4-iodo-6-phenylpyrimidine.

To determine the site of interaction of 4-IPP with MIF, crystallographic studies were performed. For crystallization trials, a dilution-incubation-concentration strategy was used. MIF diluted to 0.1 mM (in 20 mM Tris (pH 7.4), 20 mM NaCl) was mixed with a 10-fold molar excess of 4-IPP (diluted to 1 mM in DMSO) followed by incubation overnight at room temperature to allow formation of the covalent complex. Using a 3 kDa cut-off filter unit, the mixture was concentrated 10-fold to a final concentration of 1 mM protein. This dilution-concentration step allowed washing out the unbound inhibitor and more importantly, the DMSO concentration was reduced to a concentration acceptable for crystallization trials. Prior to co-crystallization trials, the formation of the complex was confirmed by mass spectroscopy revealing that the co-incubation of MIF with 4-IPP results in a mass increase of 154 kDa. Because 4-iodo-6-phenylpyrimidine has a molecular weight of 282 kDa and the iodine at position 4 of the pyrimidine ring can act as a leaving group, the increased mass of 154 kDa was the expected result of a covalent modification of MIF by de-iodinated 4-IPP.

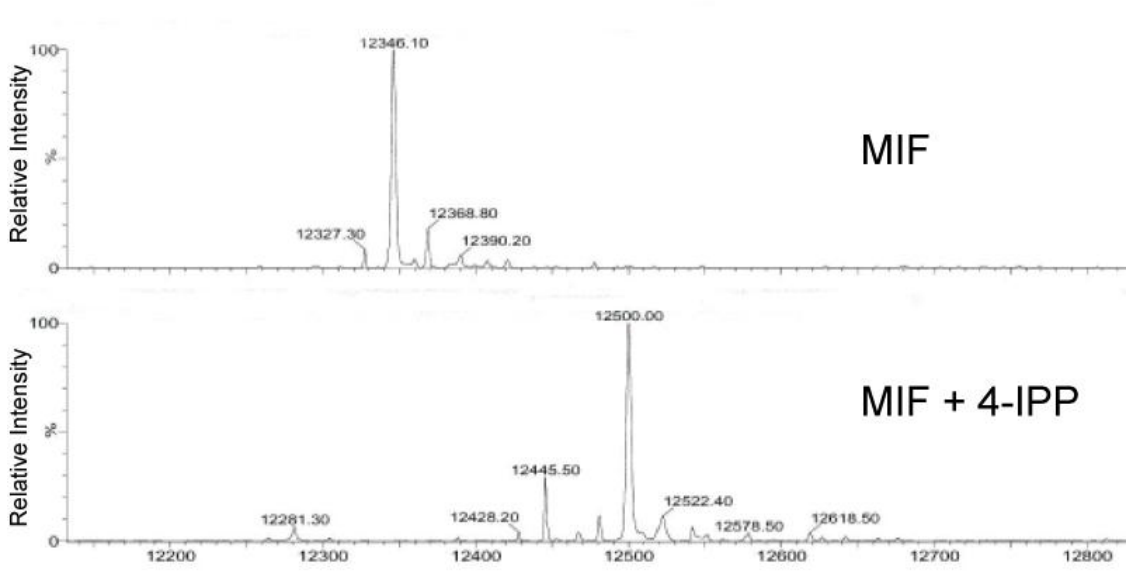

Figure 11. Mass spectroscopy analyses of 4-IPP modification of MIF. MIF was incubated either with DMSO alone (top panel) or 4-IPP (bottom panel).

Crystallization trials performed in 96-well plate formats with available crystallization screens were unsuccessful. However, the complex was crystallized using a crystallization condition established for the co-crystallization of MIF with ISO-1 (2 M ammonium sulfate, 4% isopropanol, 0.1 M Tris (pH 7.5) (112)). Equal volumes of the MIF◦4-IPP complex and reservoir solution were mixed to form 3 µl drops. Out of several trials only one orthorhombic crystal appeared after about 2 weeks with size dimensions of approximately 300 x 250 µm (Figure 12).

The crystal obtained under this condition was used to measure diffraction data leading to structure determination. The data of the crystal were collected in house using a Rigaku RAXIS-IV imaging plate area detector and diffracted to 1.80 Å. The crystal belonged to the space group $P2_12_12_1$ with unit cell parameters of a=67.89 Å, b=67.9 Å, c=88.30 Å and α=β=γ=90°. Data collection and refinement statistics are listed in Table 3.

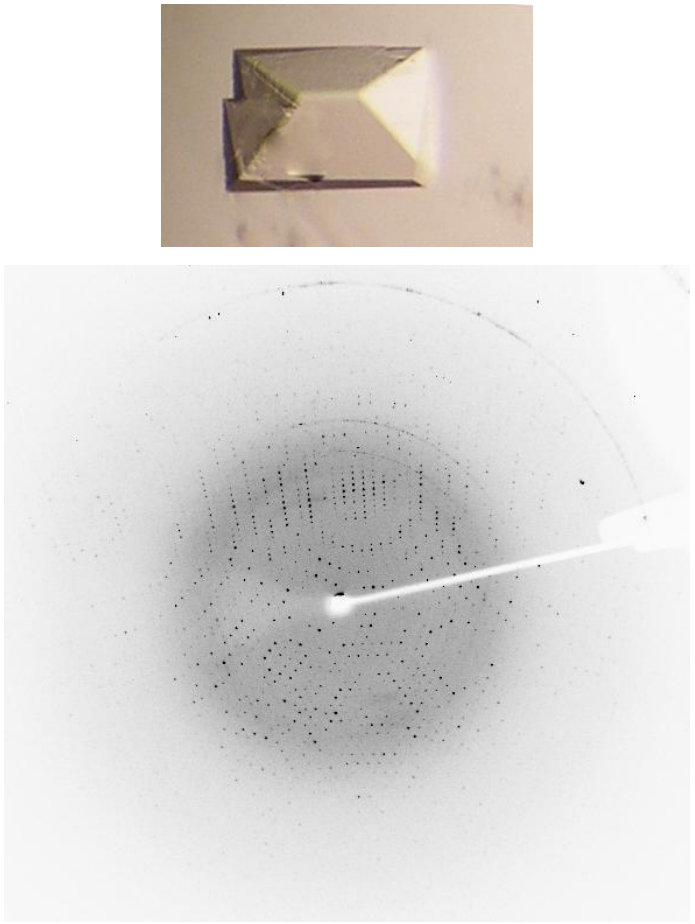

Figure 12. Crystal and diffraction pattern of the MIF◦4-IPP complex. The crystal (top) diffracted to 1.80 Å (bottom).

Table 3. Data collection and refinement statistics.

Data collection	
Space group	$P2_12_12_1$
Cell dimensions	
a, *b*, *c* (Å)	67.89, 67.90, 88.30
α, ß, γ (°)	90, 90, 90
Wavelength (Å)	1.54
Resolution (Å)*	50-1.8 (1.86-1.80)
R_{sym} or R_{merge}	0.062 (0.496)
Average I / σI	21.0 (2.7)
Completeness (%)	97.4 (96.3)
Redundancy	4.5 (4.3)
Refinement	
Resolution (Å)	50-1.8
No. reflections	37563
R_{work} / R_{free}	0.197/ 0.23
Average B factors (No. of atoms)	
Overall	25.67 (2916)
Protein	24.28 (2625)
Inhibitor	34.11 (36)
Water	33.52 (217)
Sulfate	88.41 (20)
Glycerol	47.35 (18)
R.m.s deviations	
Bond lengths (Å)	0.016
Bond angles (°)	1.445
Ramachandran plot (%)**	
most favored	91.0
allowed	9.0

*Highest resolution shell is shown in parenthesis.
**As defined in PROCHECK

4.1.2 The Three-Dimensional Crystal Structure of the MIF◦4-IPP-Complex

The crystal structure of the MIF◦4-IPP complex was solved at 1.8 Å and contained the MIF trimer in the asymmetric unit. As expected from the inhibitory effect on the tautomerization, the small molecular inhibitors were located deep in the tautomerization active site of MIF, where each monomer was complexed with one 4-IPP molecule. As shown in Figure 13,

4-IPP binds covalently to MIF at the nitrogen of the N-terminal proline by substitution of the iodo group at the 4-position of 4-IPP.

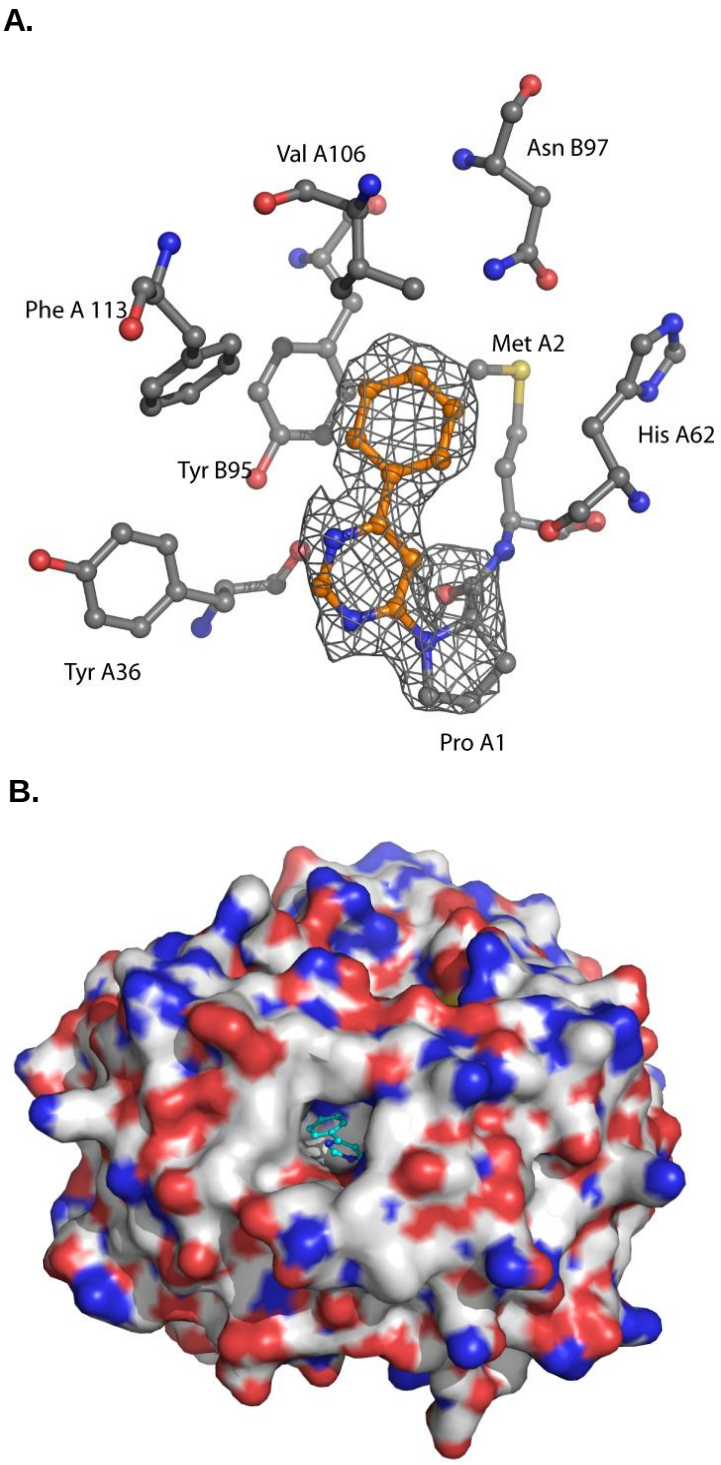

Figure 13. Co-crystallization of MIF and 4-IPP. (***A***) Fo-Fc 'omit' electron density map contoured at 3.0 σ of the MIF◦4-IPP complex (grey wire mesh) calculated with phases from the model in which Pro1 and 6-phenylpyrimidine were omitted. 6-phenylpyrimidine (orange) with its covalent bond to Pro-1, as well as Met A2 and Tyr B95 are represented as sticks. (**B**) Connolly surface of MIF colored by CPK colors with the covalently bound 6-phenylpyrimidine adduct shown in stick representation (PDB entry: 3B9S). Figures were prepared by using PyMOL (104)

In addition to this important covalent bond, structural analysis revealed that there is a hydrophobic interaction that exists between the inhibitor and the side chains of the amino acid residues within 2.5 Ångstroms (with hydrogens): Met A2, Tyr A36, His A62, Val A106, Phe A113, and Tyr B95. The phenyl substituent is oriented deep in the MIF catalytic pocket near Met A2 (Figure 13). This is similar to existing crystal structures of MIF with antagonists 7-hydroxy-2-oxo-chromene-3-carboxylic acid ethyl ester (131) and OXIM6 (120) although the phenyl substituent of bound 4-IPP is located slightly deeper into the binding pocket and in a different orientation. There is some apparent freedom of rotation of the phenyl ring as two different conformations exist in the tri-substituted trimeric MIF crystal structure.

4.2 The Parasitic MIF Orthologs from *Leishmania major* and *Plasmodium falciparum*

In this section, the purification and functional characterization of the MIF orthologs from *L. major* (LmMIF) and *P. falciparum* (PfMIF) are described. Both orthologs were hypothesized to play a role in the immune evasion of the parasites.

4.2.1 Sequence Alignment of LmMIF, PfMIF, and Human MIF

An amino acid sequence alignment of three selected members of the MIF protein family was prepared using the T-Coffee multiple sequence alignment program. The alignment then was subjected to ESPript 2.2 for secondary structure and hydropathic character assignment (Figure 14); for comparing the structures and features of the different proteins, residue numbering for this and the following sections is based on this sequence alignment of the different structures. Altogether, there are 11 invariant residues in MIF (Pro1, Pro12, Leu21, Gly34, Lys35, Pro36, Phe52, Gly54, Gly68, Gly69, Arg96 and Phe116). Human MIF is distinguished by the presence of three conserved cysteines (Cys59, Cys62, and Cys83), Cys59 and Cys62 define a CXXC motif that mediates thiol-protein oxidoreductase activity (114, 117) and Cys83 is suggested to be essential for the *in vivo* association between MIF and p53 (132). These conserved cysteines are absent in the *Leishmania major* and *Plasmodium falciparum* sequences. The MIF N-terminal proline (Pro1) by contrast is universally conserved. Proline-1 functions as a catalytic base in the tautomerization of model substrates, and it has been shown by X-ray crystallography studies of the mammalian proteins to reside within a hydrophobic, substrate-binding pocket (112, 133, 134). Despite the low sequence identity of LmMIF and PfMIF to human MIF (21 and 27 percent, respectively), conservation of residues of the tautomerase active site is obvious as residues implicated in

substrate contact (112) are predominantly found to be highly invariant. Moreover, the overall pattern of hydropathy remains widely conserved (Figure 14).

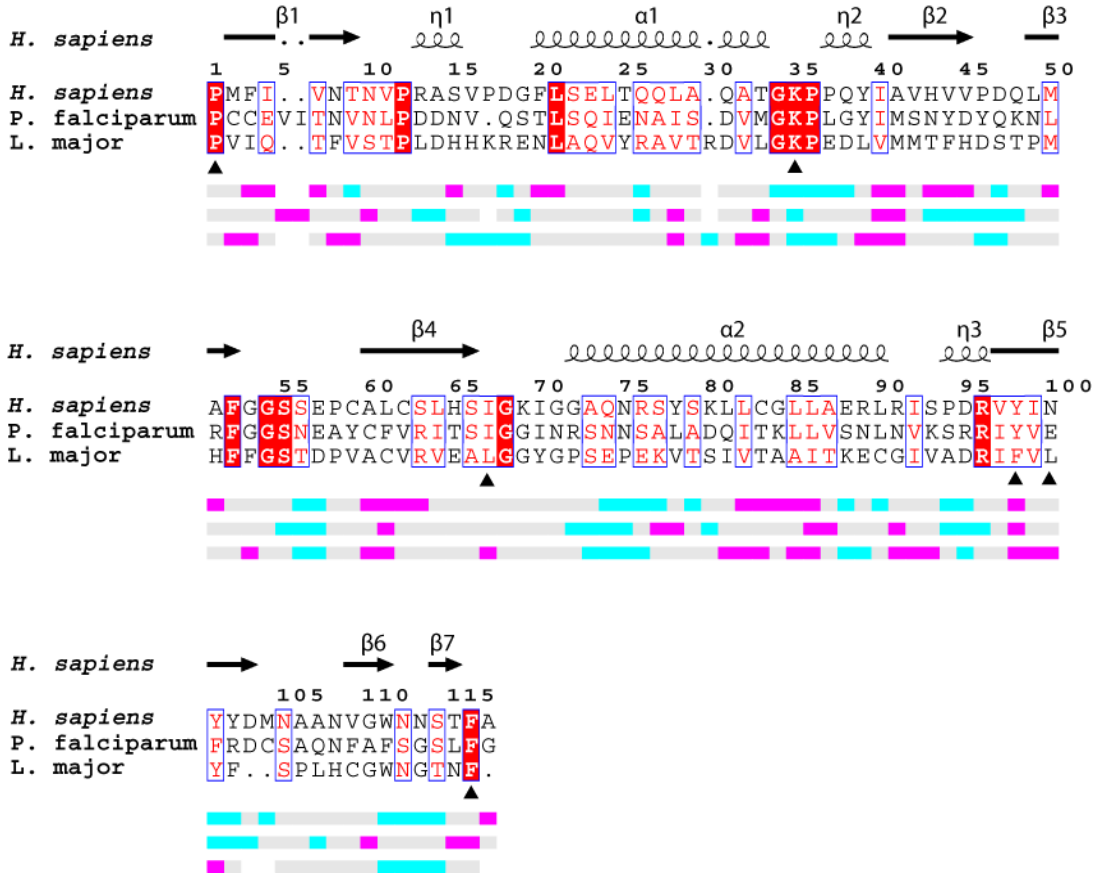

Figure 14. Amino acid sequence alignment. Selected MIF molecules were aligned with the program T-Coffee (135). The figure including secondary structure assignment (PDB-entry 1MIF) and the hydropathic character was generated using the program ESPript 2.2. Residues marked with solid red boxes indicate complete conservation; residues with similarity are labeled in red. Hydropathy for each of the proteins is rendered by the bars bellow the alignment. Pink is hydrophobic, cyan is hydrophilic. The symbol ▲ identifies residues of the tautomerase active site indicated in forming substrate contact (112).

For functional studies of the parasitic MIF orthologs, a native protein sequence was considered important because modification of the N-terminal proline inhibits tautomerase activity (133), and the C-terminus is known to mediate subunit oligomerization in the human MIF protein (101).

4.3 Purification and Characterization of LmMIF

Recombinant, wild-type sequence LmMIF protein was purified by sequential FPLC chromatography in three steps. First, the protein was loaded onto a Q-Sepharose column and eluted with a gradient with increasing salt concentration between 120 and 180 mM NaCl. Protein-containing fractions were pooled, rebuffered and reloaded on the Q-Sepharose column for the second purification step. LmMIF eluted in a pH-gradient at about pH 6. Final purity was obtained from gel chromatography over a Superdex 75 column (Figure 15).

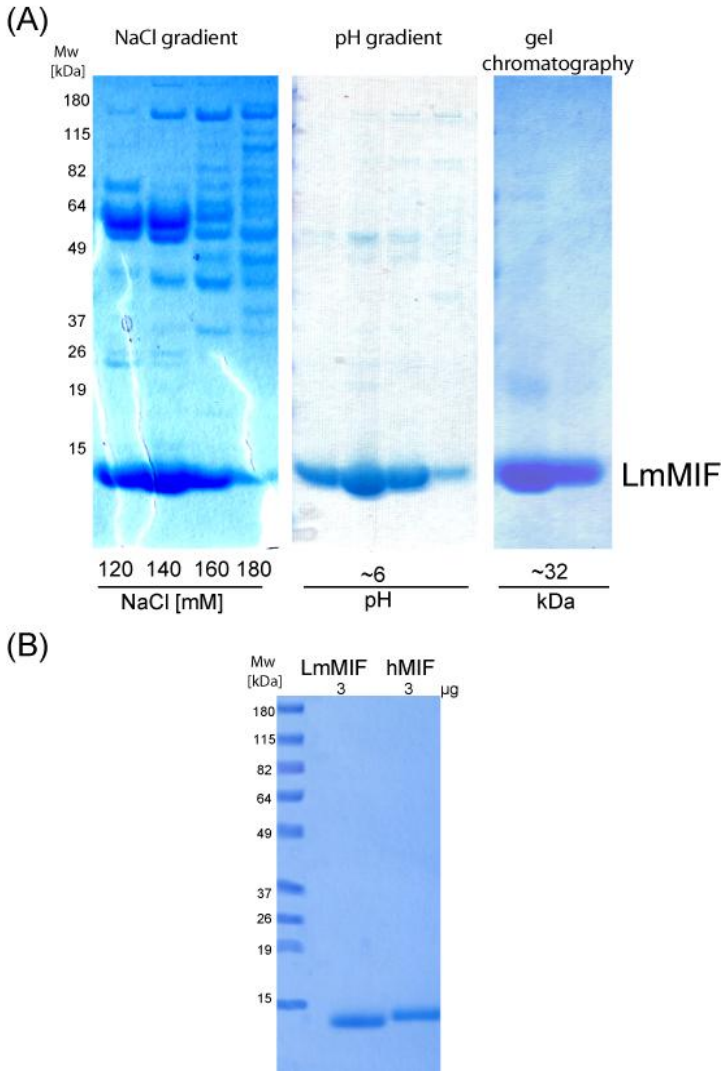

Figure 15. Sequential purification of LmMIF by anion exchange and size exclusion chromatography (***A***) The protein was stepwise purified starting with a salt gradient followed by a pH-gradient over a Q-sepharose column. Final purity was achieved by size exclusion chromatography over a S75 column. (***B***) Purity of LmMIF compared to human MIF.

As estimated from the SDS-PAGE (Figure 16), the final purity of the LmMIF product was >98% and yielded 15 mg of protein per liter of *E. coli* culture.

The major peak of LmMIF eluted at an apparent molecular mass of 32 kDa on a size exclusion column (Figure 16). The observed mass of ~32 kDa is well above the dimer mass of 24.762 kDa, supporting a trimeric state in solution, but the mass is also significantly below the full trimer mass of 37.143 kDa (106, 108). However, the unusual small partial specific volume reported for human MIF strongly supports a trimeric state (108).

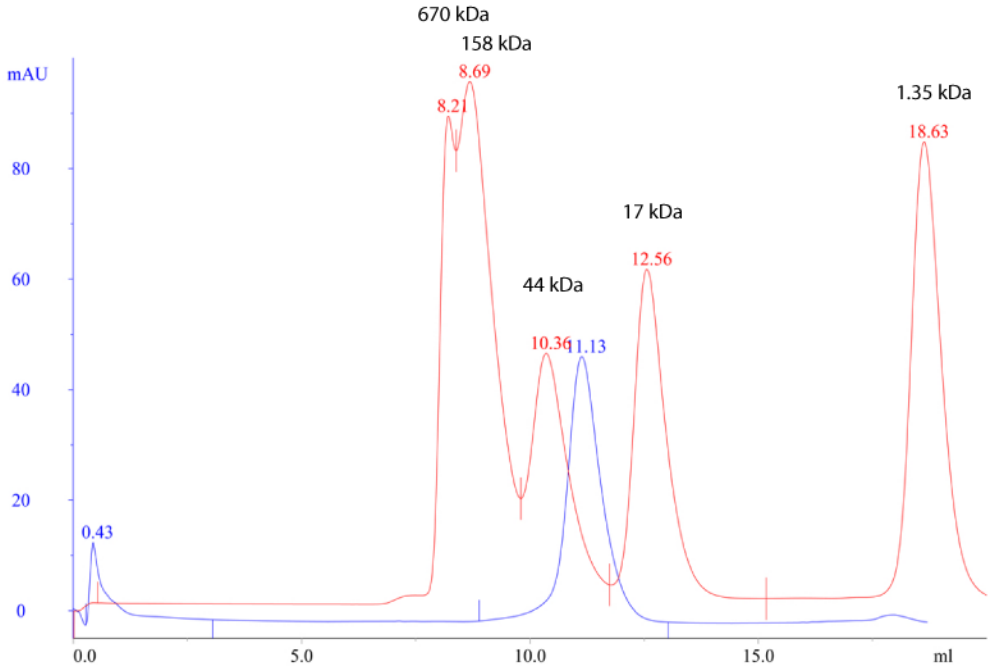

Figure 16. Recombinant LmMIF elutes as a trimer in size exclusion chromatography. thyroglobulin (670 kDa), bovine gamma-globulin (158 kDa), chicken ovalbumin (44 kDa), equine myoglobin (17 kDa), and vitamin B_{12} (1.35) were used as standards.

Electrospray ionization of purified LmMIF protein gave an m/z of 12383.56 (Figure 17), which is within 0.02% of the predicted mass of the translated amino acid sequence (calculated MW: 12381.22 Da) with a correct processing of the initiating methionine.

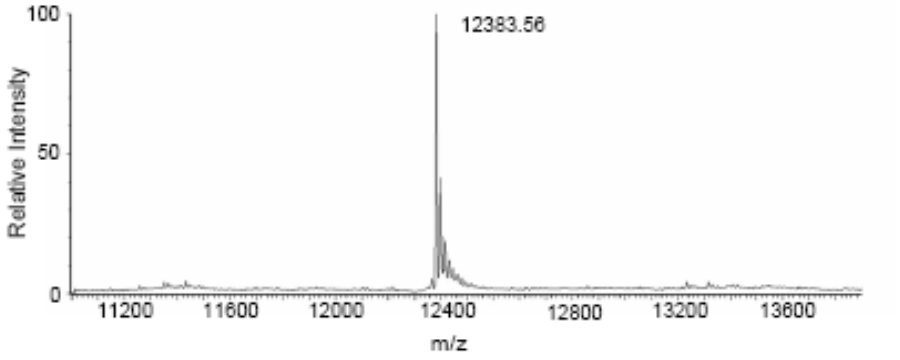

Figure 17. Electrospray ionization mass spectrometry of LmMIF showing a molecular mass (m/z) that lies within 0.02% accuracy of the predicted m/z (12381.22 Da).

4.3.1 LmMIF Activity Studies

In order to investigate the idea that LmMIF mimics or interferes with human MIF function, it was important to determine whether the enzymatic activities are conserved in the ortholog by comparing the tautomerase activity of pure, recombinant LmMIF with human MIF.

As shown in Figure 18, LmMIF tautomerizes *D*-dopachrome, but the specific activity for the reaction is 13-fold lower than that measured for human MIF (LmMIF: 0.25 mM/min/μM, human MIF: 3.35 mM/min/μM). To further study the grade of conservation of the active site, the ability of MIF inhibitors to interact with the *Leishmania* protein was investigated. The tested inhibitors included (*S,R*)-3-(4-hydroxyphenyl)-4,5-dihydro-5-isoxazole acetic acid methyl ester (ISO-1) and 4-iodo-6-phenylpyrimidine (4-IPP). The competitive inhibitor ISO-1 inhibits human MIF but not LmMIF, suggesting a selective interaction of this compound with the human MIF tautomerization site. In contrast, 4-IPP, which forms a covalent modification of the human MIF N-terminal proline (Section 4.1 above), inhibits the tautomerization activity of both MIF proteins with a greater inhibitory effect on LmMIF.

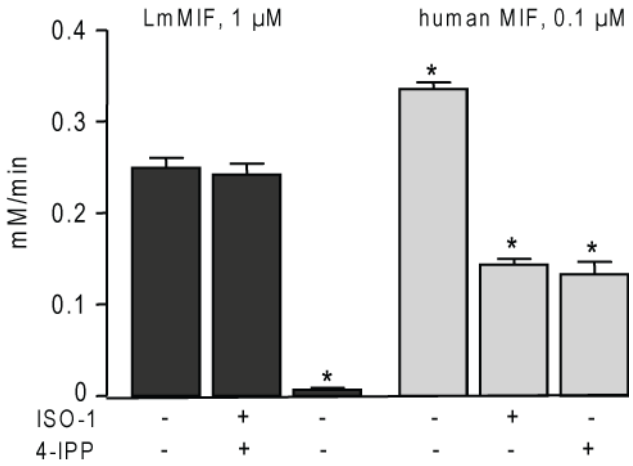

Figure 18. Tautomerization activity of LmMIF and human MIF measured with the substrate *D*-dopachrome. A representative reaction is shown for LmMIF at 1 µM and for human MIF at 0.1 µM. The small-molecule inhibitors ISO-1 or 4-IPP were preincubated with MIF at 1000- or 1-fold molar excess, respectively. The lower tautomerase activity of LmMIF made it necessary to use a higher concentration of this protein for the inhibition studies. Data are means ± SD of triplicate measurements. The p values were calculated by Student's t test. $p < 0.001$ for human MIF vs LmMIF, for 4-IPP treated LmMIF vs untreated LmMIF, for ISO-1- or 4-IPP-treated human MIF vs untreated human MIF, and for 4-IPP-treated LmMIF vs 4-IPP-treated human MIF.

4.3.2 Crystallization of LmMIF

Crystallization conditions for LmMIF were screened by the hanging drop vapor diffusion method; crystals grew in several conditions. However, the best hit was found for condition 41 of the Crystal Screen (Hampton Research). The solution included 0.1 M HEPES-Na (pH 7.5), 20% (v/v) isopropanol and 20% (w/v) polyethylene glycol 4000. The rhombohedral crystals were prepared reproducibly by mixing 1 µl of protein solution (8 mg/ml) and 1 µl reservoir solution and appeared after 3 weeks with size dimensions of approximately 600 x 500 µm (Figure 19). Selenomethionine (Se-Met) LmMIF crystals did not grow under this condition, instead the crystals grew after two days using 0.1 M tri-sodium citrate dihydrate (pH 5.6), 10% (v/v) isopropanol and 20% (w/v) polyethylene glycol 4000 as precipitant solution.

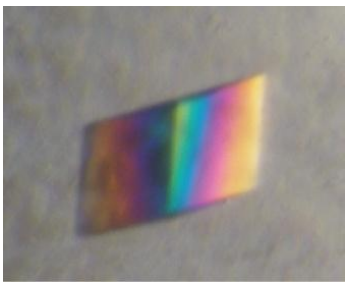

Figure 19. Crystal of native LmMIF.

A native and a seleneomethionine substituted crystal obtained under these conditions were used to collect diffraction data leading to structure determination at beamline X29A in the Brookhaven National Laboratory (BNL) (Figure 20). Crystallographic data collection and refinement statistics are listed in Table 4.

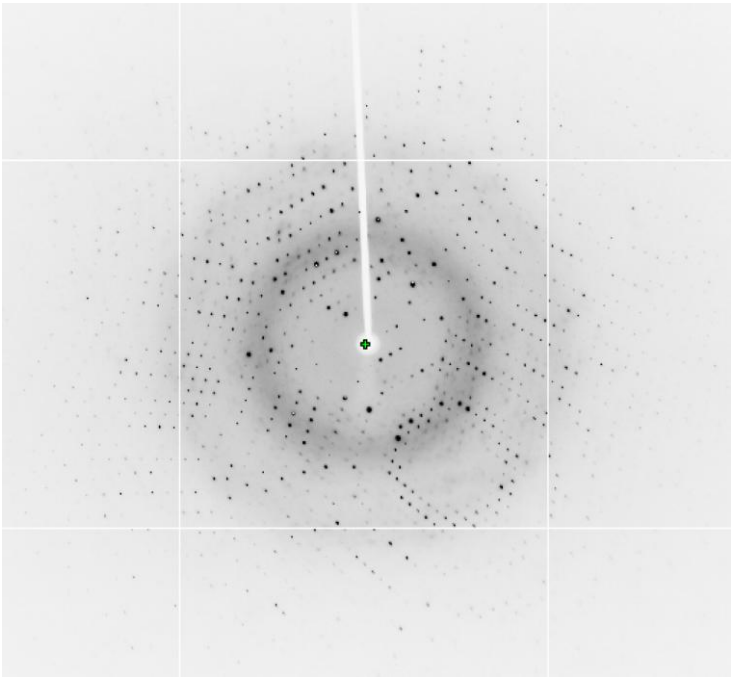

Figure 20. Diffraction pattern of native LmMIF. The crystal diffracted to 1.03 Å resolution and belonged to the space group R3.

Table 4. Data Collection and refinment statsistics of LmMIF.

	Native	Se-Met		
Data collection				
Space group	R3	R3		
Cell dimensions				
a, *b*, *c* (Å)	52.32, 52.32, 96.82	52.11, 52.11, 96.83		
α, ß, γ (°)	90, 90, 120	90, 90, 120		
		Peak	*Inflection*	*Remote*
Wavelength (Å)	0.95	0.97912	0.97928	0.96389
Resolution (Å)*	50-1.03 (1.07-1.03)	1.6	1.6	1.6
R_{sym} or R_{merge}	0.051 (0.228)	0.066	0.051	0.052
I / σI	22 (6.8)	6.4	6.8	6.6
Completeness (%)	95.5 (71.6)	99.7	99.6	99.7
Redundancy	5.2 (3.4)	7.2	7.2	7.3
Refinement				
Resolution (Å)	10-1.03			
No. reflections	44388			
R_{work} / R_{free}	0.139/ 0.157			
No. atoms	1004			
Protein	880			
Ligand/ion	4			
Water	120			
B-factors				
Protein	14.2			
Ligand/ion	40			
Water	28.7			
R.m.s deviations				
Bond lengths (Å)	0.016			
Bond angles (°)	2.1			
Ramachandran plot (%)**				
most favored	94.7			
allowed	5.4			

*Highest resolution shell is shown in parenthesis.

**As defined in PROCHECK

4.3.3 The Three-Dimensional Crystal Structure of LmMIF

The X-ray crystal structure of LmMIF was solved at a resolution of 1.03 Å in spacegroup R3. There is 1 protomer with approximate dimensions of 45*19*18 Å per asymmetric unit that forms a trimer with two protomers from adjacent asymmetric units (Figure 21*A*). As expected, the topology of the LmMIF protomer is very similar to human MIF. As its mammalian countertype, the protozoan protein consists out of 2 alpha-helixes and 6 beta-strands of which four form a ß-sheet and the remaining two help to

stabilize the trimer. The two proteins superimpose very well with a root mean square deviation of the Cα backbone of 1.8 Å (Figure 21*B*).

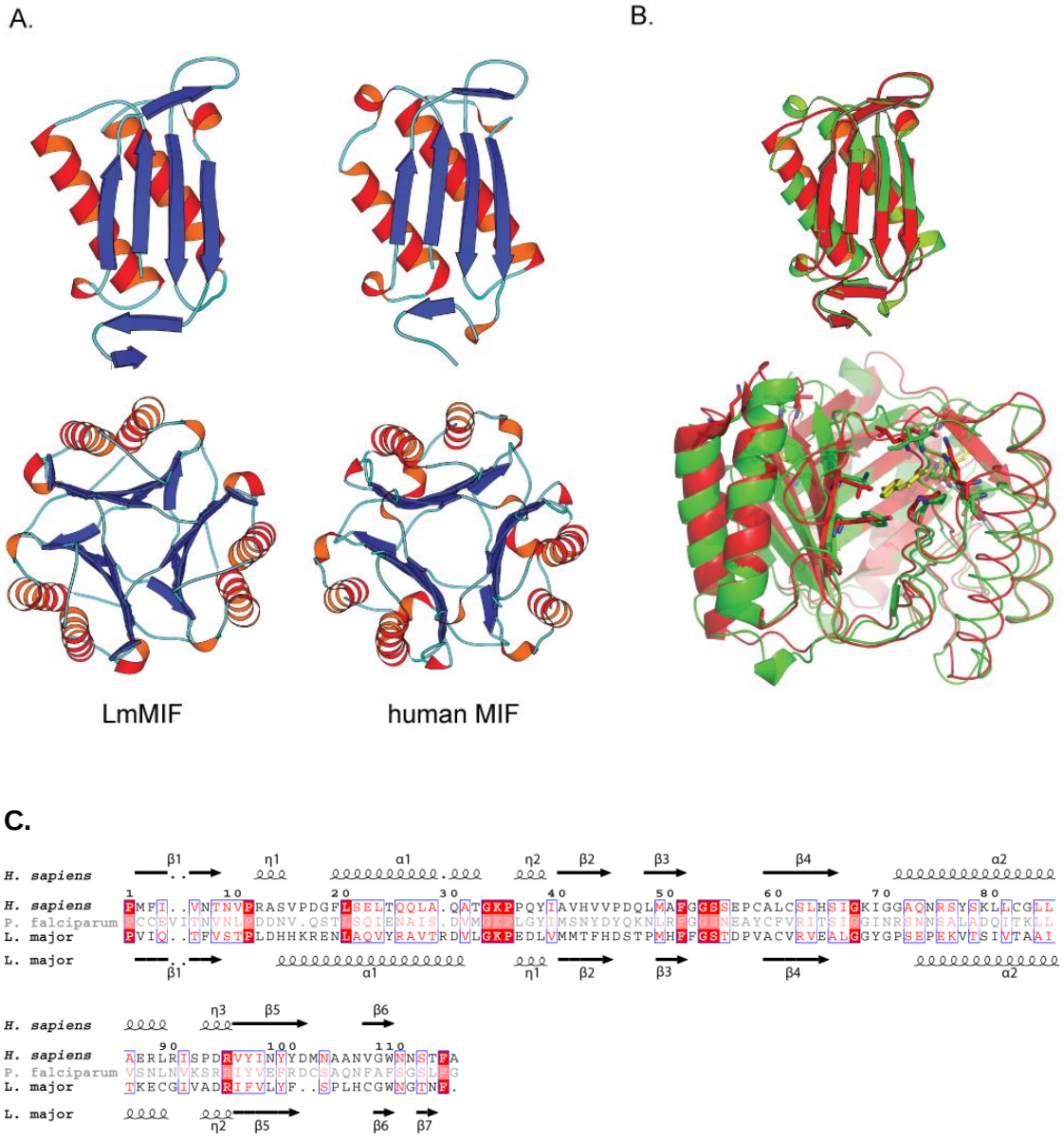

Figure 21. Conserved structure between LmMIF and MIF.
(*A*). Schematic representation of the LmMIF and human MIF protomers (upper panel) and trimers (lower panel) with secondary structure elements shown in blue (ß-sheet), red (α-helix) and cyan (random coil). **(*B*).** Superimposition of the backbone ribbon diagrams of monomeric and trimeric LmMIF (red) and human MIF (green). In the trimeric representation, one of the protomers is displayed as backbone trace. Also shown in the trimer representation are the sidechain residues implicated in substrate recognition. The substrate p-hydroxyphenylpyruvate is displayed in yellow. (***C***) Sequence alignment with secondary structure elements for LmMIF and hMIF. The program Molscript (136) was used to prepare Fig. A, PyMOL (104) was used to prepare Fig B.

The tautomerase active site is structurally conserved, forming a deep pocket around Pro1. The 13-fold lower tautomerase activity of LmMIF compared to human MIF (described in 4.3.1) may be explained by comparing the tautomerization site of the two proteins. In contrast to human MIF, the tautomerase active site of LmMIF shows a negative electrostatic potential which is caused by the proximity of Glu65 on the base inside the catalytic pocket (Figure 22*A*). The low tautomerase activity can further be explained using a theoretical model of substrate docked in the active site of LmMIF (Figure 22*B*). LmMIF shares with human and mouse MIF two out of the five amino acids (Pro1 and Lys35) that have been implicated in substrate contact, however three residues are absent. The replacement of Ile67 by a Leu in LmMIF is probably less significant because the contact involves a backbone hydrogen bond, whereas the substitution of Tyr98 and Asn100 by the hydrophobic residues Phe and Leu, respectively, eliminates two side chain hydrogen bonds to the substrate. While tautomerase activity is reduced in LmMIF, it is notable that the overall structure of the N-terminal region and hydrophic pocket remain similar as they are conserved in all other MIF or *D*-dopachrome tautomerases that have been characterized.

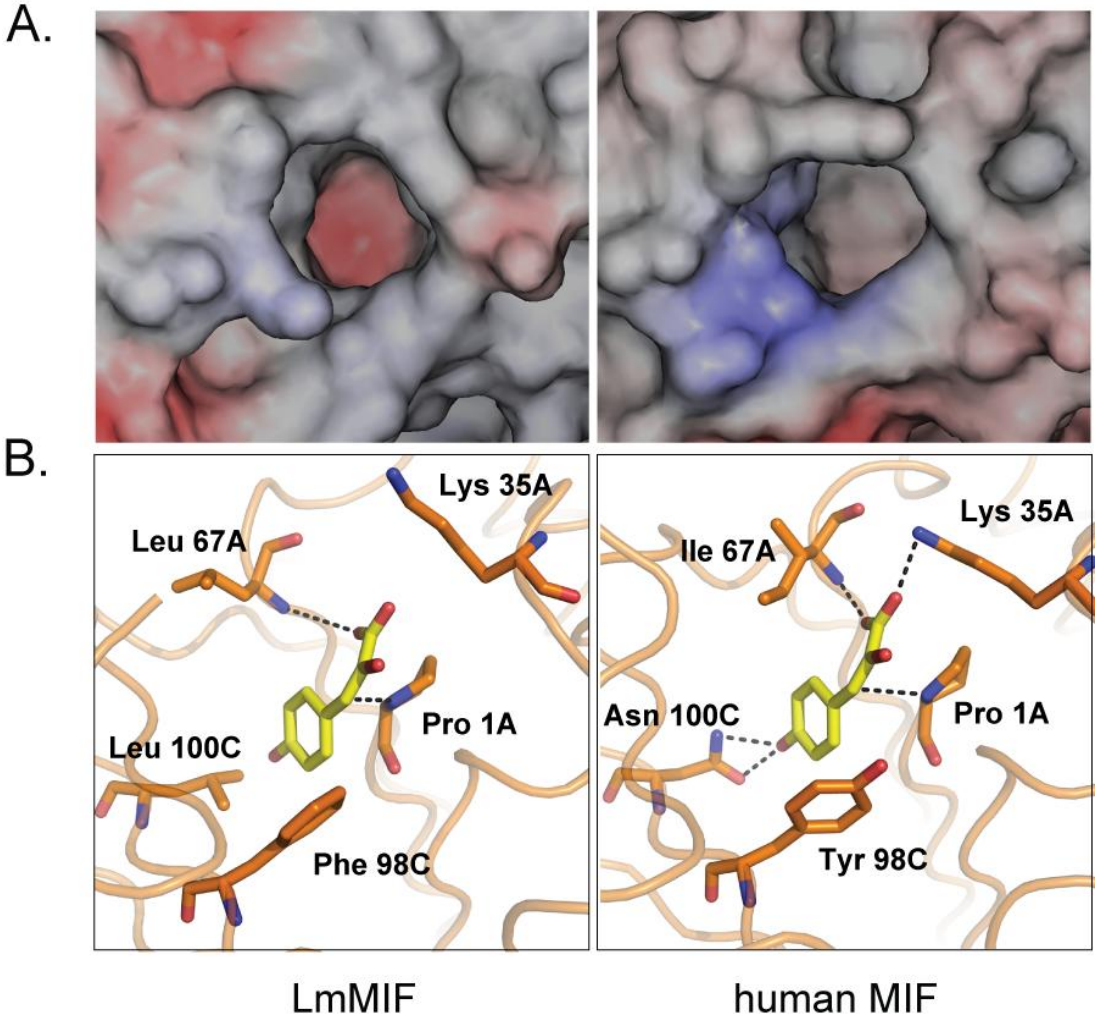

Figure 22. Active site comparison of LmMIF and human MIF.
(*A*). Electrostatic surface potential of the tautomerase site of LmMIF and human MIF. The negatively charged surface potential is colored in red and the positive potential in blue. (***B***) Molecular model of active site residues implicated in substrate contact for LmMIF based on a crystal structure of MIF complexed with *p*-hydroxyphenylpyruvate (112). Residue numbering refers to sequence alignment of Figure 22. The program Spock (137) was used to generate Fig. A, PyMOL (104) was used to prepare Fig B.

4.3.4 Human and *Leishmania* MIF Interaction Studies

Analyzing the crystal structure of LmMIF and comparing to human MIF lead to the hypothesis that the parasitic MIF protein might interfere with human MIF function by forming mixed oligomers with the later protein. This speculation resulted from the overlay of the trimer of human MIF and LmMIF; it was evident that a human MIF protomer can theoretically be replaced with a LmMIF molecule without causing any clashes in the mixed trimer (Figure 23*A*). This observation was supported by a

computational docking program in which one PDB-file with the coordinates of a LmMIF dimer and one PDB-file with the coordinates of a human MIF monomer were submitted to the ClusProServer. ClusPro Server uses ZDOCKs fast Fourier transform to search all possible binding modes for the proteins, evaluating based on shape complementarily, desolation energy, and electrostatics. The human MIF protein was docked in correct orientation to form a complete trimeric molecule (Figure 23*B*). To examine this possible interaction, yeast-two-hybrid studies were performed.

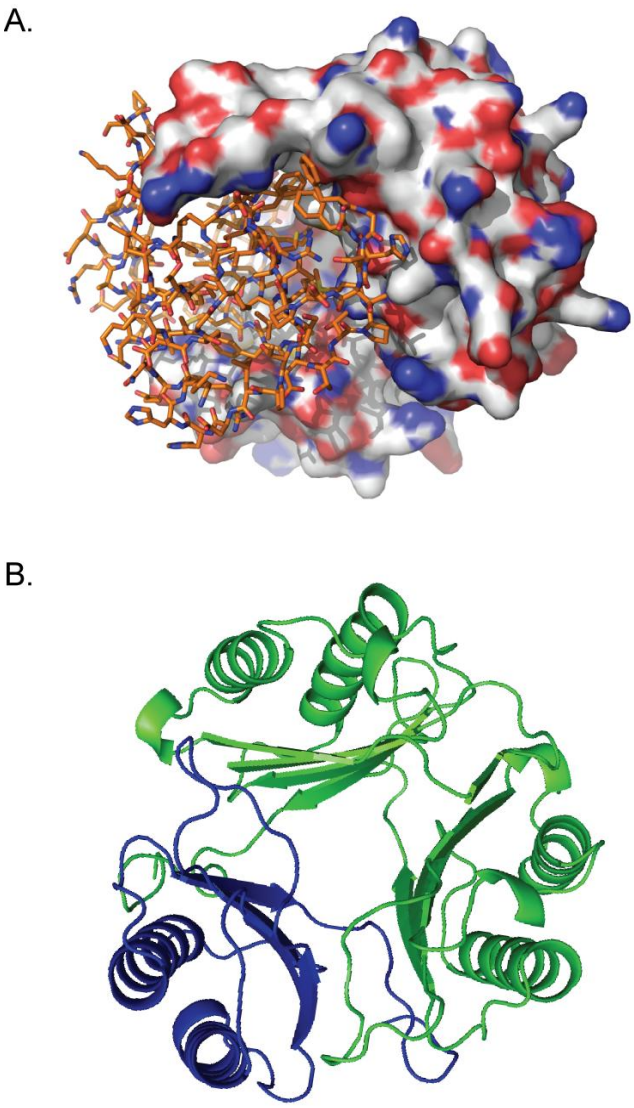

Figure 23. Theoretical mixed trimer formation of human and Leishmania MIF. (***A***) One monomer of human MIF (Connolly surface, colored by CPK) is replaced with a LmMIF ortholog (stick representation). (***B***) Docking of human MIF (blue) into 2 molecules of LmMIF (green) performed by using ClusPro Server. Figures were prepared by using PyMOL (104).

4.3.4.1Yeast Two Hybrid

In a recent study a yeast two hybrid system where the MIF cDNA served as “bait” and a human pituitary cDNA library was used as “prey’; several positive colonies encoded the MIF cDNA in the prey-vector (138) showing the oligomer formation of MIF can be observed in this system. Thus, a similar approach was used to identify whether human MIF can interact directly with LmMIF.

In the Matchmaker GAL4 Two-Hybrid system used for the present study, a bait gene was expressed as a fusion of the GAL4 DNA-binding domain (DNA-BD) and the prey gene was expressed as a fusion of the GAL4 activation domain (DNA-AD). When the DNA-binding and the DNA-activation domain are brought in proximity by interaction of the bait and prey proteins, the transcription of four reporter genes is activated.

Human and *Leishmania* MIF were cloned in both the bait or prey vector allowing four possible combinations of co-transformation into the AH109 cell line:

- hMIF-BD and hMIF-AD
- LmMIF-BD and LmMIF-AD
- hMIF-BD and LmMIF-AD
- LmMIF-BD and hMIF-AD

The co-transformation of the hMIF/hMIF or LmMIF/LmMIF bait-prey pair served as positive control, respectively.

While the positive yeast controls expressing hMIF/hMIF or LmMIF/LmMIF grew on medium- (SD/-His/-Leu/-Trp) and high- (SD/-Ade/-His/-Leu/-Trp/X-α-gal) stringency selection plates, the mixed trans-formations did not (Figure 24). The results indicate that a potential inter-ference of LmMIF with the human immune system is not mediated by mixed trimer formation and disruption of the host MIF cytokine function.

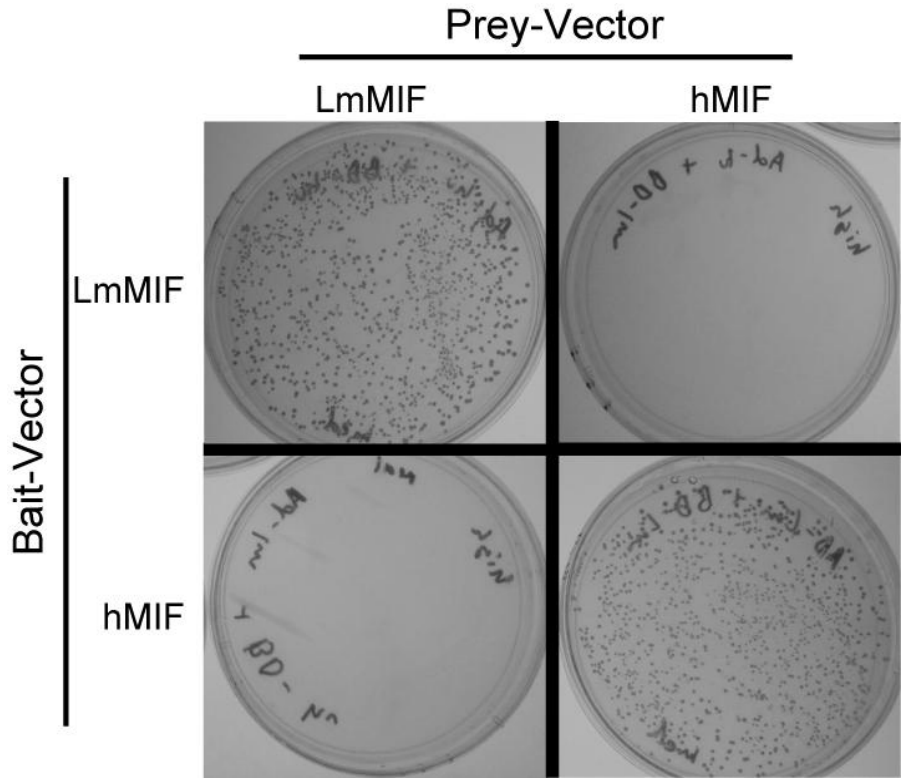

Figure 24. No mixed trimer formation of human and *Leishmania* MIF as assayed by a yeast two hybrid system. Bait and prey vector were co-transformed as indicated and spread on high-stringency selection plates (SD/-Ade/-His/-Leu/-Trp/X-α-gal). Interaction of proteins was analyzed 3 days later.

4.3.5 *In vitro* Binding of LmMIF to the Human MIF Receptor CD74 and to the Human MIF-tethering Protein p115

4.3.5.1 The MIF-CD74 Interaction

The cytokine MIF was shown to activate cells by engaging its cell surface binding receptor, CD74, and a high-affinity binding interaction between MIF and the CD74 ectodomain ($CD74^{73-232}$, sCD74) has been demonstrated (55).

To examine the binding of LmMIF to the human MIF receptor, a competition-binding assay was utilized to test whether recombinant LmMIF competes with biotinylated human MIF for binding to immobilized sCD74 (Figure 25*A*). LmMIF inhibited the interaction

between human MIF and sCD74, but inhibition was not as complete as achieved with human MIF as a competitor.

The results of the competition assay were confirmed by measuring the equilibrium dissociation constant for the binding of LmMIF to sCD74 by surface plasmon resonance spectroscopy (BIAcore analysis). The real-time binding interactions measured by this method revealed a high affinity of LmMIF to the human MIF receptor CD74 with a K_d of 2.9 x 10^{-8} M (Figure 25*B*). This contrasts with the previously determined K_d of 9.0 x 10^{-9} M for the binding of human MIF to sCD74 (55). These results indicate that LmMIF binds to the human MIF receptor with high affinity, albeit with a 3-fold lower K_d than recombinant human MIF.

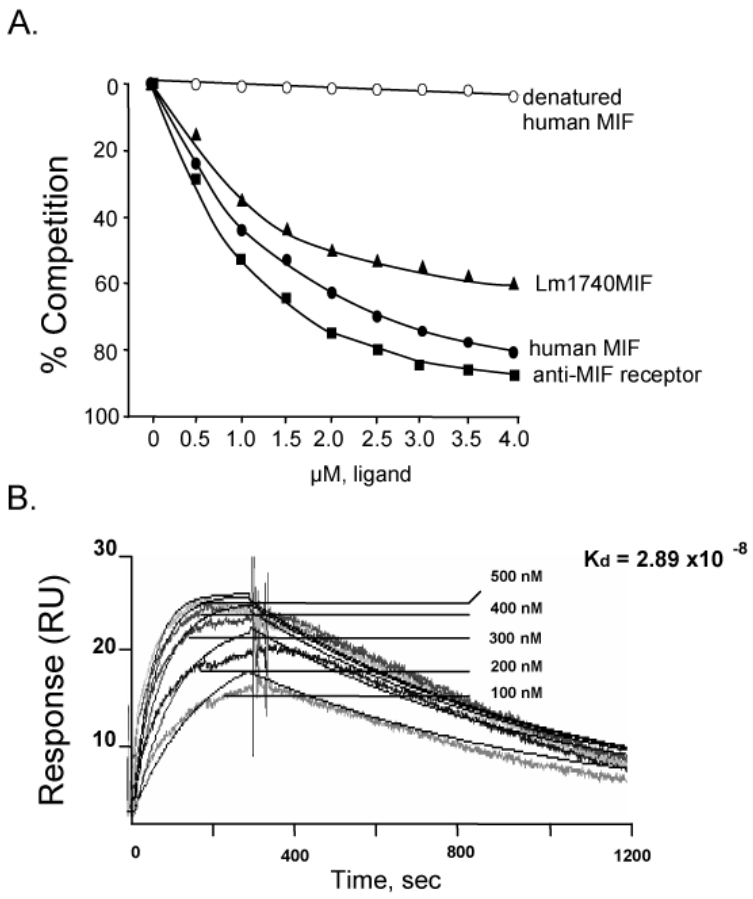

Figure 25. LmMIF binds to the MIF receptor CD74. (***A***) Concentration dependent binding of LmMIF and human MIF to the immobilized, human MIF receptor CD74 ectodomain (sCD74) using biotinylated human MIF as a competitor. A neutralizing anti-MIF receptor mAb (LN2) and heat-denatured, recombinant human MIF served as positive and negative controls for this assay. Values are the means of quadruplicate measurements. (***B***) Realtime surface plasmon resonance analysis (BIAcore) of the interaction between recombinant LmMIF and sCD74.

4.3.5.2 The LmMIF-p115 Interaction

In a recent study on the secretion of the leaderless cytokine MIF, the Golgi-associated protein p115 was identified as an intracellular binding partner and critical component for the regulated secretion of MIF from monocytes/macrophages (138). As macrophages are the primary hosts of the *Leishmania* parasite it was of interest to elucidate whether p115 interacts with LmMIF and possibly uses the host's secretion pathway to release LmMIF from infected cells for immune evasion strategies.

In order to biochemically analyze the interaction between LmMIF and p115, the carboxy-terminal region of p115 ($p115^{702-962}$) described to interact with human MIF was expressed and purified from *E.coli* as a histidine-tag fusion protein *(*Figure 26*).*

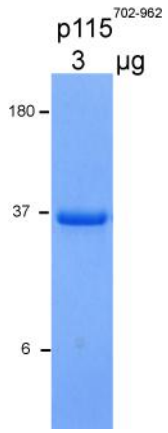

Figure 26. SDS-PAGE of $p115^{702-962}$. Following cell disruption the soluble proteins were loaded onto a Ni-NTA column. In the second purification step (Superdex S75), all impurities contained in the Ni-NTA pool were eliminated.

Utilizing the competition binding assay, an inhibition of the interaction of biotinylated hMIF with $p115^{702-962}$ was observed with increasing concentrations of LmMIF (Figure 27).

Moreover, the competition of LmMIF for $p115^{702-962}$ binding is significantly stronger than the binding observed for hMIF with the strongest difference at low protein concentration (0.25 – 1µM). This finding is in contrast to the binding of LmMIF to the human MIF receptor CD74 where a stronger binding of the mammalian protein to the receptor was detected (Figure 25).

The binding of LmMIF to p115$^{702-962}$ suggests the possible secretion of the parasitic protein from infected cells is mediated by the same pathway than proposed for the host protein.

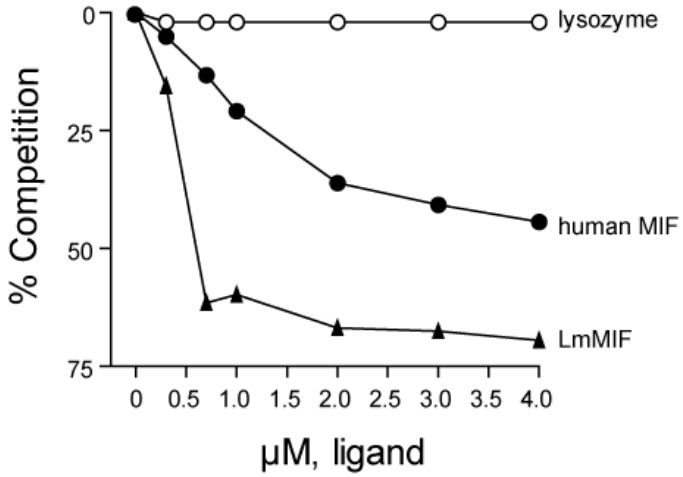

Figure 27. LmMIF binds to p115$^{702-962}$. Concentration dependent binding of LmMIF and human MIF to the immobilized carboxy-terminal region of p115$^{702-962}$ using biotinylated human MIF as a competitor. Lysozyme served as negative control for this assay. Values are the means of triplicate measurements.

4.3.6 Cellular Uptake of LmMIF

Although MIF is a cytokine and thus modulates immune activity by receptor-mediated pathways intracellular actions by direct interaction with the Jun activating binding protein (Jab1) (139), p53 (132) and p115 (138) have been described. These studies suggest that cytokine activities of MIF are mediated by p53 and Jab1-dependent pathways after uptake into target cells. The amino acid residues 57-63 of human MIF, which include the CXXC motif are important for Jab1 binding and modulation. This motif is absent in LmMIF. Similarly, Cys83, critical for p53 interaction is absent in the ortholog. In light of these studies, it was of interest to address whether LmMIF is internalized into target cells giving the potential of modulating intracellular pathways of non-infected cells. Figure 28 shows, exogenous, fluorescein-labeled, recombinant LmMIF (and human MIF) enters the macrophage cell line RAW264.7 and is

targeted into the cytosolic compartment with no observed difference relative to human MIF.

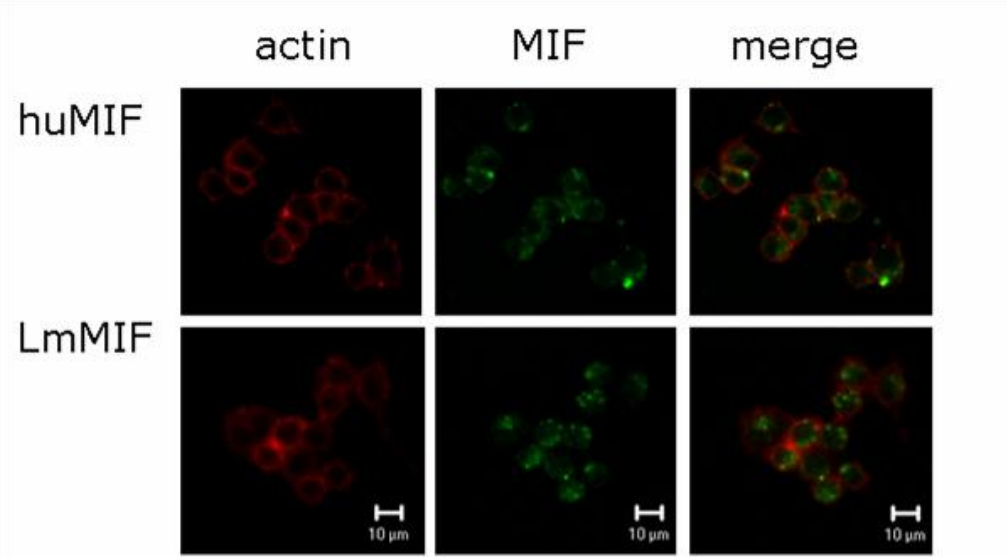

Figure 28. LmMIF is internalized by macrophages.
Exogenously added LmMIF is internalized by RAW 264.7 macrophages. 1.5 µM fluorescein-labelled LmMIF or human MIF (green) was added to the cells and staining for ß-actin (red) was performed 30 min later as described in Materials and Methods.

4.3.7 Chemotaxis Activity of LmMIF for Human Monocytes

A major target of human MIF is the macrophage, a key cell in immune and inflammatory response. Once produced, MIF inhibits their movement (42, 49), however, MIF also exerts a chemoattractant effect on mononuclear cells. Given the fact that macrophages are the final host of the *Leishmania* parasite, a crucial step for establishment of disease may be the attraction and accumulation of their target cells. As shown in Figure 29, human peripheral blood monocytes migrated to a concentration gradient of LPS-free recombinant LmMIF and human MIF across a transwell membrane. These results demonstrate that LmMIF can chemotactically mobilize macrophages in a manner quantitatively similar to human MIF. As with the tautomerase assay, the small molecule MIF antagonist, ISO-1, binds to the human MIF tautomerization site (118) and

inhibits MIF-induced chemoattraction (140) whereas LmMIF function is not influenced by the small molecular inhibitor. In contrast, the covalent inhibitor, 4-IPP, inhibited migration induced by MIF and LmMIF.

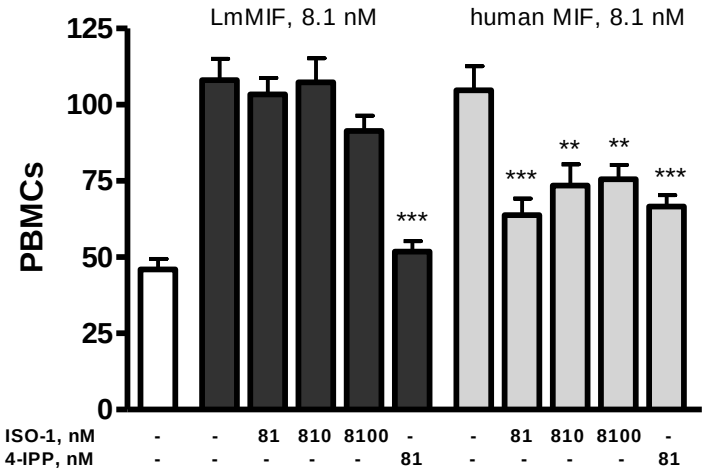

Figure 29. LmMIF induces mononuclear cell migration.
Human peripheral blood mononuclear cells (PBMCs) were subject to migration analysis with or without 8.1 nM (100 ng/ml) recombinant LmMIF in the lower chamber. Human MIF served as positive control. The MIF inhibitor ISO-1 was added in 10, 100 and 1000 fold-molar excess to the recombinant protein, and the inhibitor 4-IPP was added in 10 fold-molar excess. Results are representative of two independent experiments and are expressed as the mean number of 12 counted fields ±SEM. The p values were calculated by the Student's t test. **p<0.01, ***p<0.001 for LmMIF or human MIF versus protein with inhibitors.

4.4 Purification and Characterization of PfMIF

Plasmodium falciparum MIF (PfMIF) was purified by sequential anion exchange chromatography comparable to the methodology employed for LmMIF purification. The protein lysate first was loaded on a Q-Sepharose column equilibrated with Tris (pH 8.0), 10 mM NaCl, 20 mM (Buffer A) and eluted with a pH-gradient from pH 8 towards pH 6.3. The protein containing fractions were pooled, re-buffered (Buffer A) and re-loaded on the Q-Sepharose column equilibrated with Buffer A and eluted via salt gradient. Final impurities were eliminated by size exclusion chromatography over a Superdex S75 column equilibrated with PBS. The final product is shown in Figure 30 with an estimated purity of >98%.

Similar to LmMIF, PfMIF elutes in a S75 size exclusion column at an approximate molecular mass of 32 KDa which is consistent with a dimer or trimer of the 12.713 KDa protein (Figure 30).

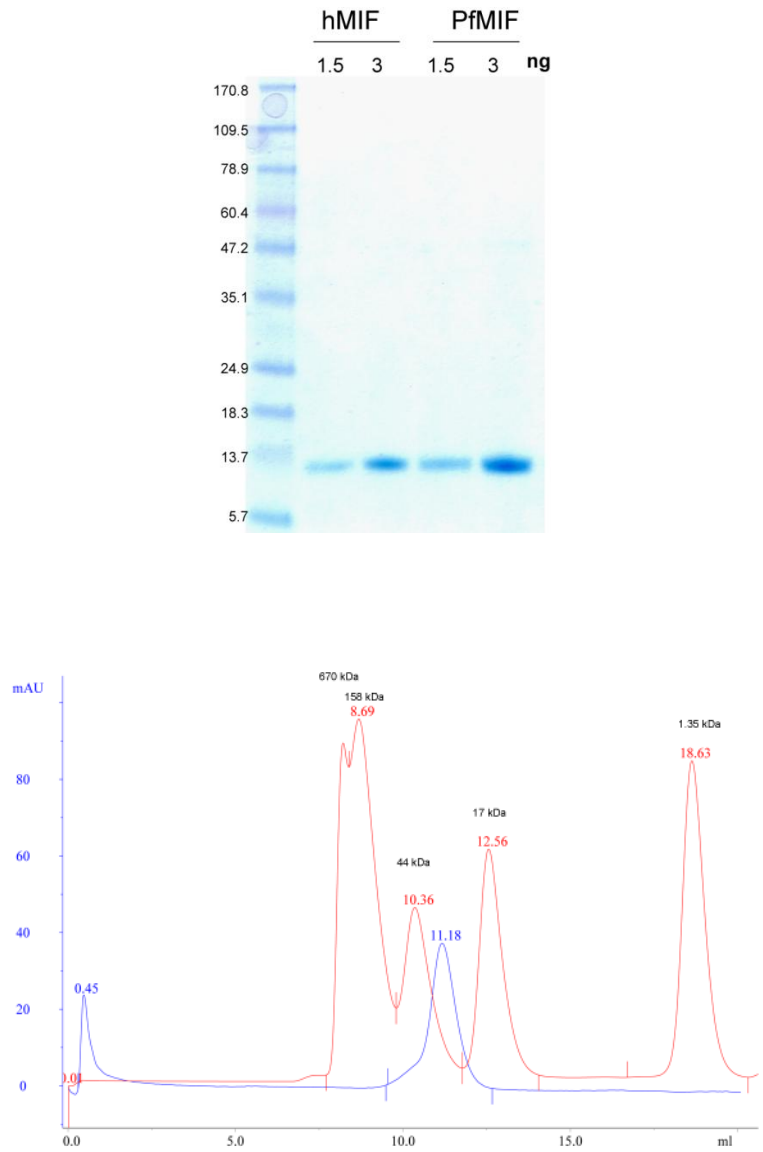

Figure 30. Purified recombinant PfMIF. (*A*) Purity of PfMIF compared to human MIF is analyzed by SDS-PAGE followed by Coomassie staining. **(*B*)** PfMIF elutes at an apparent molecular weight of 32 kDa in size exclusion chromatography (blue). Standards (red) included thyroglobulin (670 kDa), bovine gamma-globulin (158 kDa), chicken ovalbumin (44 kDa), equine myoglobin (17 kDa), and vitamin B12 (1.35kDa).

Figure 31*A* displays the grade of conserved residues of PfMIF in a three-dimensional model based on the sequence alignment from 4.2.1. The residues surrounding the tautomerase active site are highly conserved, however, no tautomerase activity of PfMIF was observed when tested with

the substrate *D*-Dopachrome (data not shown). An enzymatic activity was observed using the substrate HPP (Figure 31*B*), but the measured activity at standard assay conditions was more than 100-fold lower compared to human MIF. These findings contrast with the data obtained for LmMIF, which showed high enzymatic activity for the substrate *D*-Dopachrome and very little for HPP.

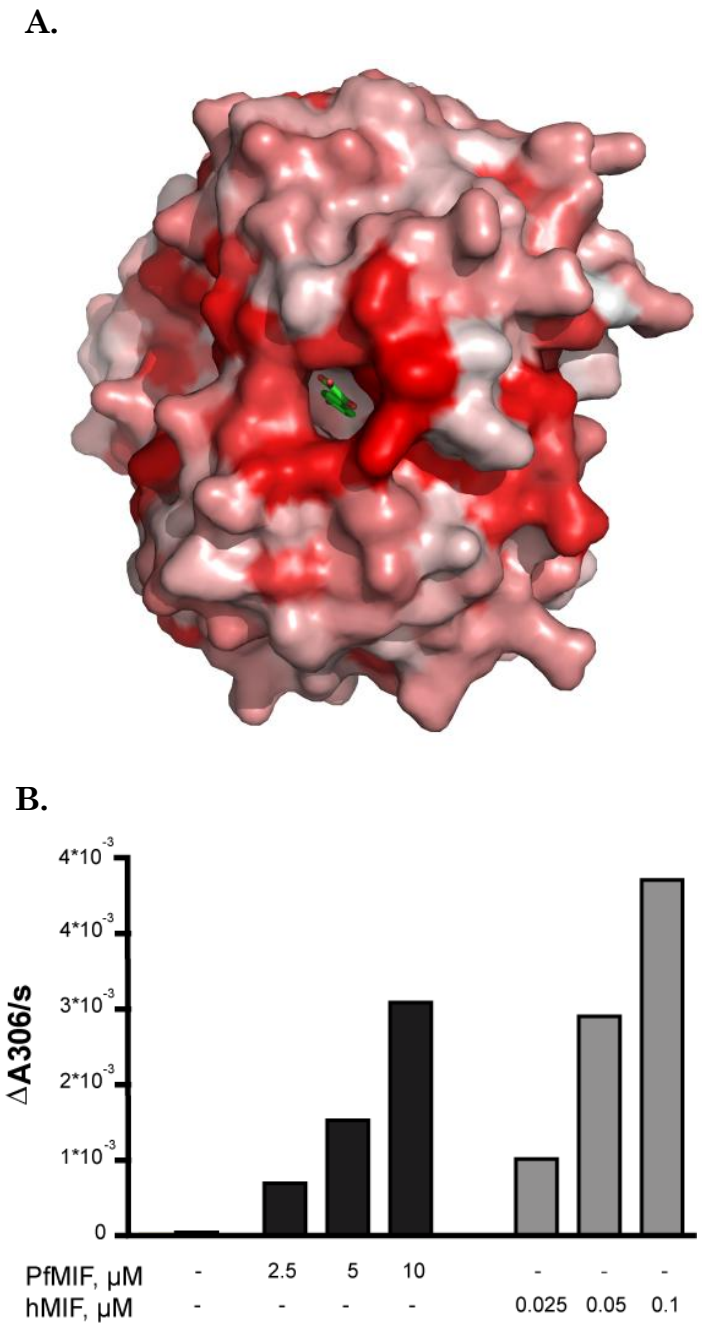

Figure 31. The active site of PfMIF is conserved. (*A)* Three-dimensional model of PfMIF based on the sequence similarity of to human MIF displayed on the structure of human MIF where dark red shows identical residues and white shows no similarity. HPP is displayed in the active site. This figure was prepared with Pymol (104) and ProtSkin (141). ***(B)*** Tautomerase activity of PfMIF with the substrate p-hydroxyphenylpyruvate.

4.4.1 *In vitro* Binding of PfMIF to the human MIF Receptor CD74

Real-time surface plasmon resonance analysis (BIAcore) revealed PfMIF to bind the human MIF receptor CD74 with a similar binding constant as measured for LmMIF (K_d = 2.67 x 10^{-8} M) but ~3 fold lower than human MIF itself.

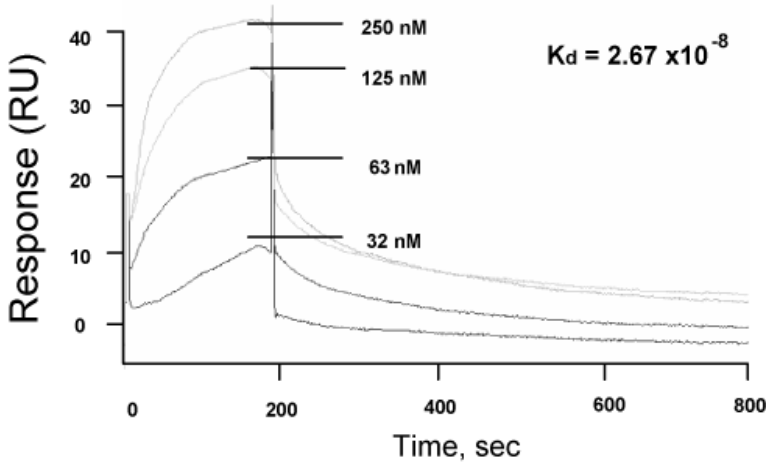

Figure 32. PfMIF binds to the MIF receptor CD74. Real-time surface plasmon resonance analysis (BIAcore) of the interaction between recombinant LmMIF and sCD74.

4.4.2 Crystallization of PfMIF

Prior to screening for crystallization conditions, PfMIF was concentrated to 11 mg/ml. The best crystallization hit was obtained from condition 17 of the Hampton Crystal Screen (0.1 M Tris (pH 8.5), 2 M LiSO4, 30% PEG 4000). This condition was optimized in a 24-well plate format by performing a pH gradient from pH 7.5 to pH 9.0 and a precipitant gradient from 25% to 35% PEG 4000. Several crystals grew over 5 – 8 days. However, these crystals had an irregular shape which could not be improved by additives. Nevertheless, X-ray diffraction data were collected on an R-axis IV detector (Rigaku) at the macromolecular crystallography facility at the Yale University School of Medicine. The crystal diffracted to

3.1 Å in spacegroup I222. However, molecular replacement against human MIF using the collect dataset was not successful.

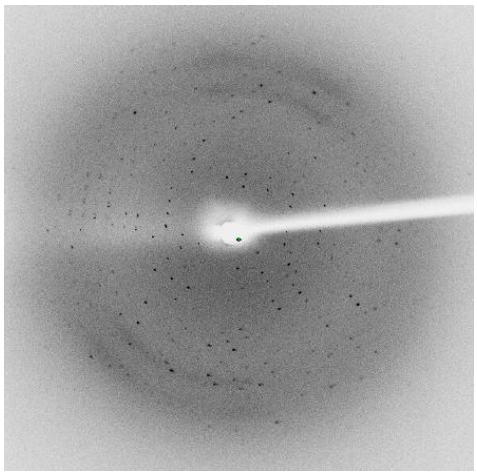

Figure 33. Diffraction pattern of PfMIF

It is attempted to further optimize the initially successful crystallization condition, and to produce Se-Met derivates for solving the structure of PfMIF by multiwavelength anomalous diffraction (MAD) phasing.

4.5 Mapping the Binding of MIF to the Chemokine Receptor CXCR4

MIF acts as a major regulator of inflammatory cell recruitment and atherogenesis. A recent study describes these chemokine-like functions of MIF to be mediated by interaction with the chemokine receptors CXCR4 and CXCR2. Moreover, MIF was shown to compete with CXCL12 for binding of the CXCR4 receptor (56). However, the molecular details of this interaction have not yet been determined.

To investigate whether the N-terminal region of CXCR4, which is the determinant for the binding of CXCL12 (142) is also involved in binding to MIF, cell-transmigration studies were performed. As shown in Figure 34*A*, human and LmMIF-induced chemoattraction of PBMCs is efficiently blocked by the addition of $CXCR4^{1-27}$. In order to analyze whether the inhibitory effect observed in cell-transmigration is caused by direct binding of MIF to $CXCR4^{1-27}$, protein-protein interactions were probed by steady state fluorescence spectroscopy. LmMIF showed significant increase in fluorescence intensity in a $CXCR4^{1-27}$ concentration-dependent-manner with a high affinity interaction (K_d = 3.1±0.8 µM) (Figure 34*B*). The measured dissociation constant is in range with the previously reported K_d of 1.3±0.5 µM for the interaction between CXCL12 and $CXCR4^{1-38}$ as determined by NMR-spectroscopy (143). Similar results were obtained for human MIF, however, due to low intrinsic fluorescence the K_d was not calculated. The direct interaction between the N-terminal tail of CXCR4 was also confirmed by the competitive binding assay with the peptide bound to the surface and competition of biotinylated MIF with increasing concentration of human MIF (Figure 34*C*).

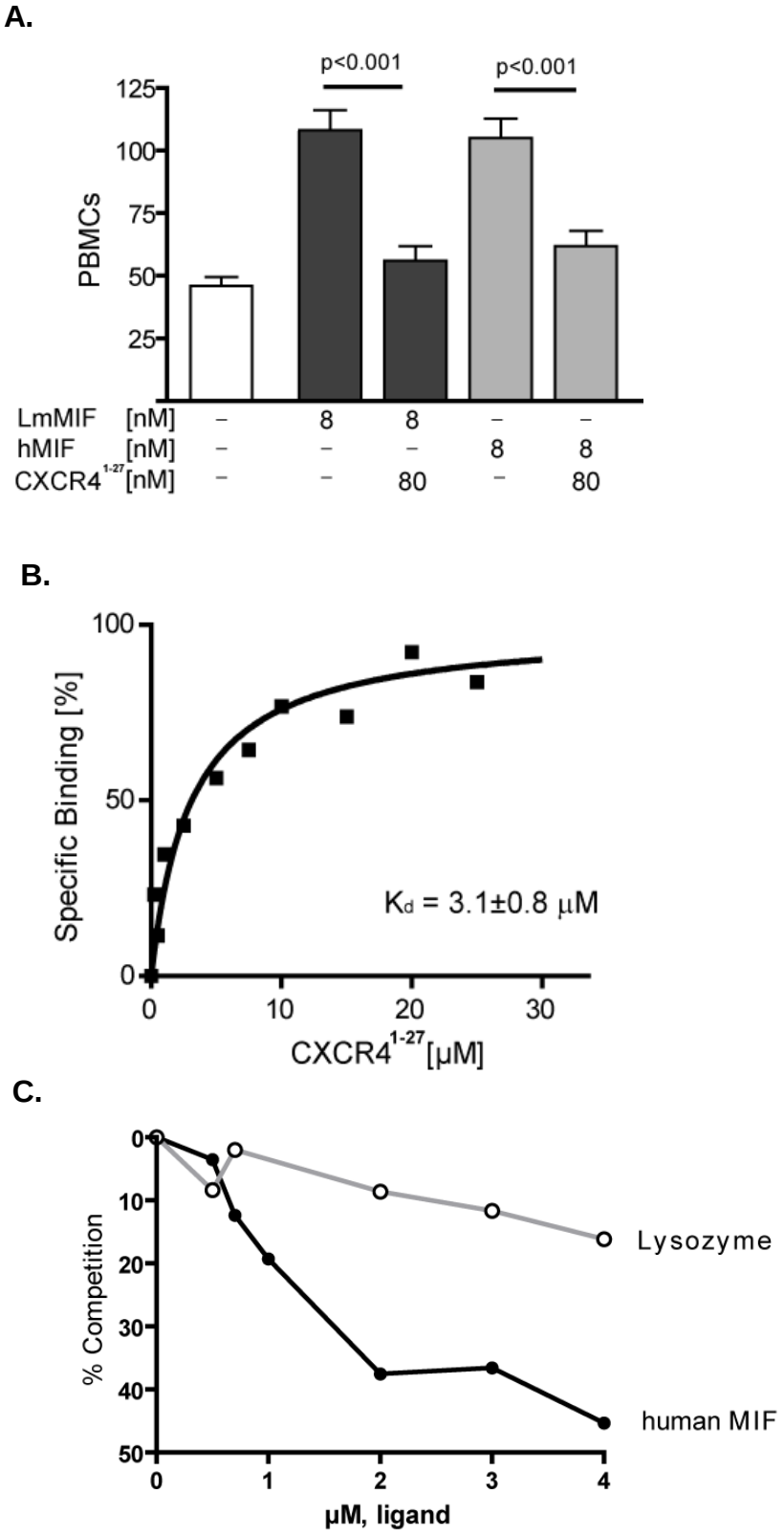

Figure 34. CXCR4$^{1-27}$ efficiently blocks MIF induced mononuclear cell migration by direct interaction. (***A***) Human PBMCs were subjected to migration analysis in the presence of human MIF or LmMIF. CXCR4$^{1-27}$ was added in 10-fold molar excess. Results are expressed as mean±S.D (n = 12). (***B***) Binding of CXCR4$^{1-27}$ to LmMIF observed by steady-state tryptophan fluorescence spectroscopy reveals an apparent dissociation constant of 3.1 (±0.8) µM. (***C***) Competition binding assay.

To map the MIF binding site for CXCR4, initial NMR studies were performed. ^{15}N-MIF in the presence or absence of CXCR4$^{1-27}$ was subjected to NMR spectroscopy. The resulting ^{1}H^{15}N-HSQC spectra indicate differences between human MIF and the complex between human MIF and CXCR4$^{1-27}$ (Figure 35*A*). Individual residues that might be involved in the interaction are indicated in Figure 35*B*.

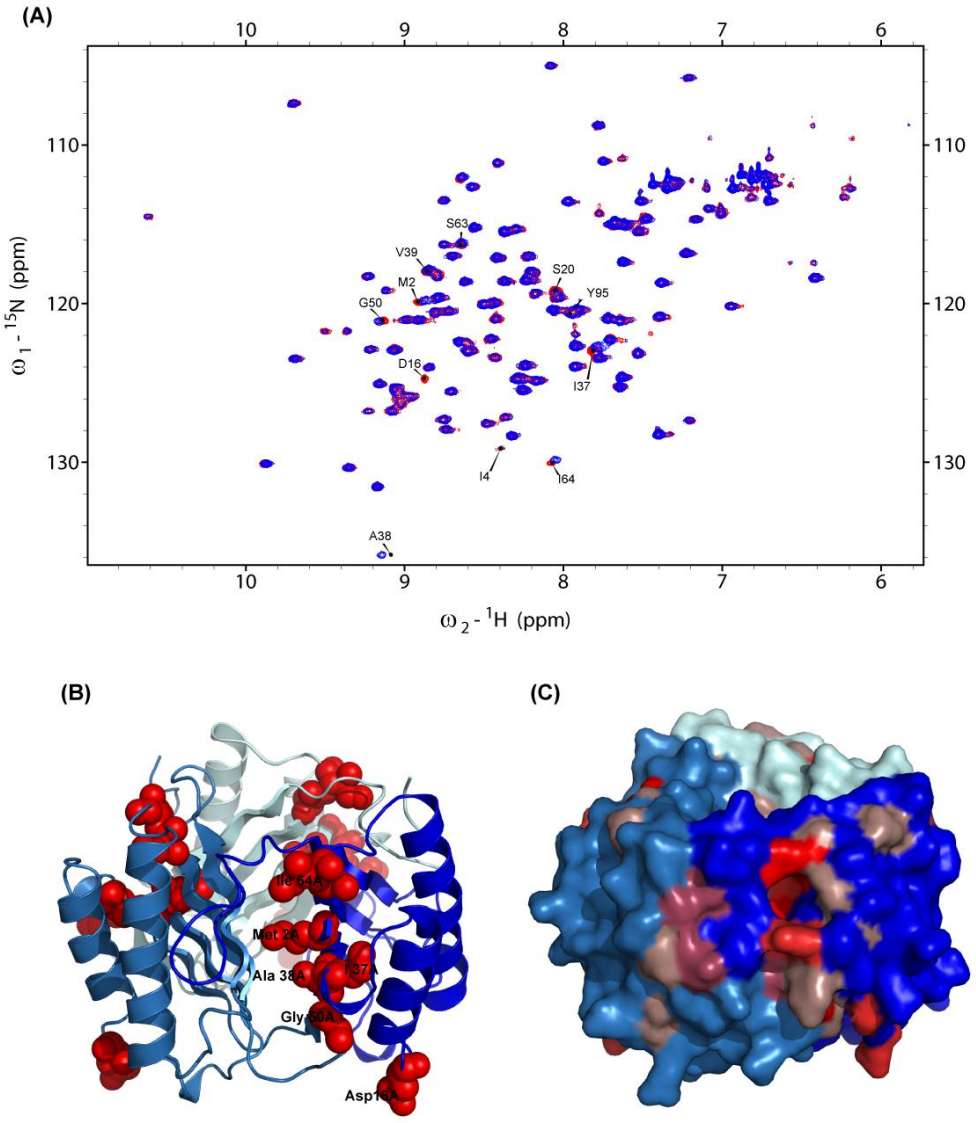

Figure 35. NMR spectroscopic studies of human MIF and CXCR4$^{1-27}$ interaction. (***A***) Overlay of ^{15}N-^{1}H-HSQC spectra of 300 µM ^{15}N-hMIF (blue) and 300 µM ^{15}N-hMIF with 900 µM CXCR4$^{1-27}$ peptide (red). Spectra were collected at 25˚C at pH 6.8. Resonance peaks with the largest chemical shift changes are indicated for the human MIF ^{15}N-^{1}H-HSQC spectra. (***B***) Trimer of human MIF with residues undergoing the greatest chemical shift changes upon peptide binding (red spheres). (***C***) Surface rendering of the trimer of human MIF. Greater chemical shift changes upon peptide binding are displayed in increasing intensity of red. Each subunit is colored in a different shade of blue.

5 Discussion

5.1 The Prototypic Covalent MIF Inhibitor 4-IPP

The cytokine macrophage migration inhibitory is an important regulator of the innate and adaptive immunity and plays a pivotal role in the pathogenesis of chronic and acute inflammatory diseases such as septic shock (47), cancer (73), and rheumatoid arthritis (70). Serum MIF levels positively correlate with the severity of Gram-negative and -positive sepsis in humans (144). MIF levels are also markedly elevated in most tumor types (73) and correlate with rheumatoid arthritis severity (145).

Several biological treatment options such as anti-MIF antibodies or soluble receptors might be an option to counteract MIF related diseases. In fact, studies investigating neutralizing antibodies have proven the potential of targeting MIF as a treatment option for inflammatory disease (68, 146, 147). Although biological antagonists, such as etanercept and infliximab are successfully used as anti TNF-α therapies in treatment of rheumatoid arthritis (148), the production of such biological agents is difficult, time consuming and expensive; the dose necessary for an effective anti-MIF treatment would cause high costs and thus a development of medication from this direction seems unlikely. A much more affordable option is the use of non-protein based inhibitors. While in general the identification or design of small molecule cytokine inhibitors is problematic due to the complex interactions between cytokines and their receptors, MIF's unique enzymatic activity allows for fast screening of potential inhibitors.

Existing inhibitors have been shown to suppress MIF's cytokine function and promising effects on MIF related diseases have been described in mouse models investigating septic shock (54, 120) and West Nile virus infection (149). These positive effects are even more impressive when considering the relatively low affinity of the existing MIF inhibitors for MIF's *D*-dopachrome tautomerase active site (micromolar range); this

supports the potential therapeutic benefits for an inhibitor with even higher binding affinity.

The co-crystal structure of the MIF◦4-IPP-complex shows that 4-IPP is de-halogenated upon contact with enzymatically active MIF and subsequently forms a covalent bond between position 4 of the pyrimidine and the N-terminal nitrogen of proline 1. This inhibitor not only has a ~10-fold higher potency in blocking the catalytic reaction of MIF, but the covalent modification also makes this inhibitor to a suicide substrate for MIF. Electrophilic compounds that produce covalent modification are generally of negligible interest for pharmaceutical development due to the potential for side effects, such as non-specific irreversible modification of non-targeted proteins and the formation of neo-antigens. Nevertheless, such compounds may be a viable option for terminal conditions such as metastatic cancer. Non-covalent inhibitors provided proof-of-concept for the therapeutic utility of blocking MIF (54, 118, 120). However, for these non-covalent inhibitors the homotrimeric structure of MIF and the assembly of the hydrophobic pocket are required for binding; as soon as the trimer dissociates, the inhibitory effect is lost. This is of particular interest because the oligomeric state of MIF in physiological conditions is still debated in the MIF community (106, 108). Whether the trimeric form of MIF alone is responsible for MIF's biological functions or if the dimeric or monomeric forms also contribute to certain biologic functions remains under active investigation. Once bound, a covalent inhibitor has the potential to overcome the limitations of blocking only the trimeric form of MIF.

Based on the MIF◦4-IPP crystal structure, our collaborators Mitchell and colleagues were able to identify four analogues of 4-IPP that are ~10 – 20x more potent than parental 4-IPP in blocking MIF-dependent catalysis (IC_{50} ~200 – 400 nM). Of note, the group has investigated a potential toxicity of 4-IPP in a mouse model by intraperitoneal injections of 1 – 4 mg daily over a course of 7 days and observed no acute toxicity.

5.2 The MIF Ortholog from *Leishmania major*

Leishmaniasis is a vector-borne parasitic disease that is transmitted during the bloodmeal of an infected sandfly. Depending on the *Leishmania* species and the host's immune response, the disease presents a spectrum from self-healing cutaneous lesions to severe visceral disease and death. The early inflammatory response is suggested to be critical for the outcome of the *Leishmania* infection. It was demonstrated that the local control of infection and the development of subsequent immunity is mediated by the host's innate, antimicrobial immune response and by an adaptive Th1 cell response (150-152). However, *Leishmania* parasites have acquired highly sophisticated immune evasion mechanisms to escape the host's immune response. Some of the known strategies include a "silent entry" in host phagocytes by receptor-mediated-phagocytosis, thus avoiding the initial activation and the oxidative burst of the infected macrophages (153, 154), the inhibition of host defense mechanisms such as protein kinase C (PKC) activation (155) and upregulation of iNOS (156); and most importantly, the inhibition of the initial IL-12 production of infected macrophages, thus preventing T-cell priming towards a Th1 response (157). The exact mechanisms by which *Leishmania* spp. influences the host's immune response nevertheless remain poorly understood and the mediators regulating the immune evasion of the parasite are just beginning to emerge.

Host MIF was previously shown to play a critical role in mediating the hosts' resistance to *Leishmania* infections. Purified, recombinant MIF was reported to activate murine macrophages to kill *L. major* more efficiently (98). Correspondingly, MIF deficient mice were described as more susceptible to *L. major* infections (99). In addition, a recent clinical study reported an increased MIF level in $CD2^{+}$ T-cells of *L. donovani* infected patients after anti-leishmanicidal treatment (158).

The recent discovery of two MIF orthologs in the *L. major* genome has raised the question of whether these protein products influence the host's immune system. This hypothesis is supported by the finding of MIF-

orthologs in several primitive eukaryotic parasites (*Brugia malayi* (87), *Ancylostoma ceylanicum* (88), *Eimeria spp.* (159) *Trichinella spp* (160), *Plasmodium spp.* (89, 90)) that show remarkable similarity to the mammalian counterpart.

In my thesis, a potential mediator of immune evasion mechanisms from *Leishmania major*, the human MIF ortholog Lm1740MIF (LmMIF) has been characterized and the results clearly support its hypothesized role in immune evasion strategies.

Recombinant LmMIF was produced from a high yield bacterial expression system and purified by fast protein liquid chromatography, resulting in a pure product with negligible concentrations of endotoxin for functional studies. Native LmMIF was cloned in a native sequence and not fusion protein form because of evidence that modifications of both the C- and N-terminus of the protein interfere with the correct fold and function of the protein (101, 113).

The solution of the high resolution x-ray crystal structure of LmMIF revealed the primary structure identity of 21% between LmMIF and human MIF is extended to the three-dimensional-fold of the two proteins (RMSD =1.8 Å). In particular, the hydrophobic pocket of the tautomerase/ isomerase active site displays a remarkable conservation and not surprisingly, allows the parasitic protein to catalyze the tautomerization reaction of the non-physiological substrate *D*-Dopachrome. However, a difference in the electrostatic potential due to the presence of Glu65 and three additional significant amino acid substitutions of residues that have been implicated in forming substrate contacts (112) distinguish the active sites sufficiently to be selective for different small molecules. While all parasitic MIF orthologs that have been studied to date have been shown to posses at least some tautomerase or isomerase activity for one of the substrates *D*-dopachrome or HPP (86-90), no inhibitor for an active site of parasitic MIF proteins has been reported previously. Herein, the human MIF inhibitor 4-IPP is revealed to interfere with the tautomerase activity of LmMIF and moreover, was shown to efficiently block the LmMIF-

induced chemotaxis of monocytes whereas the reversible MIF inhibitor ISO-1 did not influence LmMIFs function. Small molecule inhibitors of human MIF that are designed to bind the tautomerase site and interfere with biological function are presently in preclinical development. Given the structural and functional differences in the tautomerase sites of human and *Leishmania* MIF, it is possible that inhibitors may be designed to interfere selectively with *Leishmania* MIF.

MIF has been shown previously to bind to the CD74 extracellular domain on macrophages, thus activating the ERK1/2 MAP-kinase signaling pathway (55) and induction of cell survival (60). LmMIF bound with high affinity to the extracellular domain of the human MIF receptor CD74, as assessed both by an *in vitro* competition binding assay and by surface plasmon resonance spectroscopy. Although the residues involved in forming surface contacts between MIF and the extracellular domain of the MIF receptor CD74 are not known, MIF's N-terminal region appears to play an important role in these interactions (119). The structural homology between *Leishmania* MIF and human MIF is sufficiently conserved to allow for high affinity binding of LmMIF with the human receptor.

In addition to the described functional activity of LmMIF to attract monocytes, it is important to mention that Daniela Kamir was able to show that recombinant LmMIF protects macrophages from apoptosis and activates ERK1/2 signal transduction in a CD74- dependent manner (53). Consistent with the 3-fold lower K_d of LmMIF for the CD74 receptor, the activity in these functional assays was in general reduced compared to mammalian MIF.

The present results indicate that the *Leishmania* ortholog of the cytokine MIF activates the human MIF receptor CD74 to influence the functional responses of monocytes/macrophages. Because *Leishmania* is an intracellular parasite of the monocyte/macrophage, it may be hypothesized that one function of *Leishmania*-encoded MIF is to sustain monocyte/ macrophage survival and contribute to the persistence of the parasite so

that it may complete its infectious life cycle. The precise molecular mechanism underlying LmMIF's activation of CD74 remains to be investigated; for instance, the protein may be secreted from infected cells (161) and bind to the cell surface receptor CD74, or it may engage CD74 intracellularly.

Of note, a recent study examining the unconventional secretion of MIF revealed p115 as an intracellular binding partner and critical component for the regulated secretion of MIF from monocytes/macrophages (138). A competition binding assay performed in the present work suggests that LmMIF binds the Golgi-associated protein p115 with high affinity and more efficiently than human MIF. This finding allows us to hypothesize that LmMIF expressed from the *L. major* amastigote stage in infected macrophages makes use of the human MIF secretion pathway to activate the CD74-dependent ERK1/2 survival-signaling pathway (60) of the hosts cell in an autocrine manner. It is also notable that preliminary experiments suggest that LmMIF also actives AKT-signaling (data not shown), a survival pathway that was previously reported to enhance cell survival by autocrine action of MIF in a CD74-dependent manner (64).

With Lm1740MIF (LmMIF), this study addressed only one of the two MIF orthologs expressed by *L. major*. The second ortholog Lm1750MIF, which has a sequence identity of 21% to the human protein and 58% to Lm1740MIF, was shown to protect RAW264.7 macrophages from apoptosis. Whether Lm1750MIF also is active in enzymatical and functional assays has to be determined and might be essential for a successful development of anti-leishmanicidal treatment options based on MIF orthologs.

Although the data obtained are consistent with a role for *Leishmania* MIF in modulating the host immune response, they do not exclude the possibility of an intrinsic function for LmMIF in the growth or replication of the parasite. A physiological role for LmMIF in the parasite life cycle and a closer examination of whether these proteins function as virulence factors may be attained by creating strains of Leishmania lacking MIF

orthologs. Such studies also may provide support for the selective, pharmacological targeting of Leishmania MIF for therapeutic benefit.

An additional question posed by the findings of this thesis was whether there exist further functional roles for *Leishmania* MIF with respect to host-parasite interaction. The chemokine receptors CXCR2 and CXCR4 have recently been shown to be integral components by which MIF triggers leukocyte chemotaxis (56). Studies in regards to the interaction between CXCR2/4 and MIF are ongoing, and the inclusion of LmMIF in these analyses is crucial to further elucidate the functional mechanisms of the parasitic MIF protein. LmMIF also might use the p115-mediated secretion pathway to enable it to act as a chemoattractant for the recruitment of new host cells (20, 30) via the chemokine receptors CXCR2 and CXCR4 (56).

5.3 Interaction of Human and *Leishmania* MIF with the Chemokine Receptor CXCR4

Activation of the guanine nucleotide-binding protein (G protein)-coupled receptor CXCR4 by its cognate ligand CXCL12 is hypothesized to occur through a two site mechanism. According to this model, CXCL12 makes the initial contact with the N-terminus of the receptor. Subsequently, the chemokine interacts with a secondary site on the receptor, which leads to high affinity binding and receptor activation (162) (Figure 36). The N-terminal 17 residues of CXCR4 were described as the principal determinants of binding of CXCL12 to CXCR4, with a major contribution from the first six residues (142).

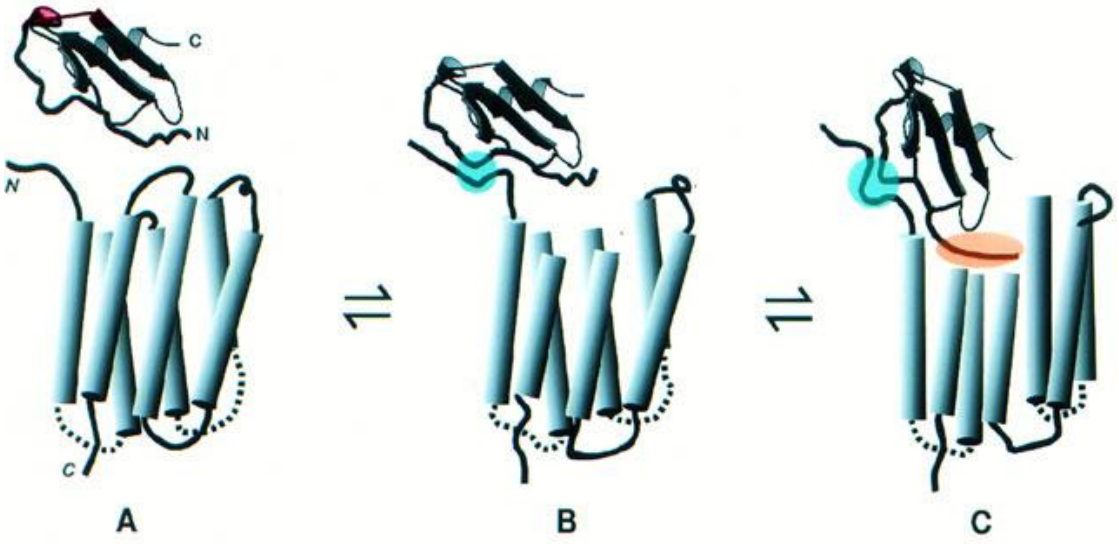

Figure 36. Model of the interaction between CXCL12 and its receptor CXCR4. The scheme indicates that chemokines interact first with their docking and then with their triggering site. The extracellular loops connecting helical segments are omitted in the middle and right-hand schemes for clarity (162).

Although the structure of MIF is unique with no significant sequence homology to chemokines, it possesses many functional properties of a chemokine: MIF induces integrin-dependent arrest and transmigration of monocytes and T-cells and competes with the cognate ligand CXCL12 for the binding to the chemokine receptor CXCR4 (56). In the present study, the molecular mechanism by which MIF interacts with the chemokine

receptor CXCR4 was addressed. The four assays used in this study, NMR spectroscopy, steady-state fluorescence spectroscopy, competition binding assay, and cell transmigration, confirmed independently, that MIF, like CXCL12, interacts with the N-terminal 27 residues of CXCR4. Notably, the binding affinity (K_d + 3.1±0.8 µM) was similar to the previously reported binding constant for the interaction between CXCL12 and $CXCR4^{1-38}$ (143). Whether MIF binding occurs in a similar manner as described for CXCL12 (in a two step binding process, Figure 36) has not been addressed, neither can it be excluded that a different length nor posttranslational modifications of the N-terminal peptide, in particular sulfation, improves the binding affinity for MIF. The described interaction of MIF/LmMIF with CXCR4 not only provides new molecular details and insights into MIF-related autoimmune and inflammatory diseases, but also unfolds a possible new pathway of parasitic MIF-orthologs to interfere with the host immune system. Further study of the molecular mode of interaction might provide a new opportunity to block the (parasitic)-MIF◦CXCR4 interactions specifically and thus may aid in the design of new drugs targeting both MIF-related diseases and immune evasive strategies of parasites. To accomplish this aim, the co-crystallizations of the MIF◦$CXCR4^{1-27}$ complex as well as more extensive NMR studies are intended.

Further studies also should be aimed to elucidate whether active site inhibitors of MIF can interfere with the binding of MIF to CXCR2 and CXCR4. Addition of the N-terminal CXCR4 peptide in a MIF tautomerase activity assay did not result in inhibition of this enzymatic activity (data not shown). These results indicate that $CXCR4^{1-27}$ does not bind the enzymatically active N-terminus of MIF and thus inhibitors of the active site might not influence MIF◦$CXCR4^{1-27}$ binding directly. However, monocyte migration assays clearly showed that the tested inhibitors abolish MIF induced cell migration. Because CXCR2 and CXCR4 are suggested as mediators of MIF's ability to induce cell migration (56), these results suggest that the tested inhibitors block the MIF◦CXCR2/4

interaction and/or activation, perhaps by interfering with the binding of additional regions of the chemokine receptors that have not been addressed in this study. The MIF◦CXCR2 interaction has not been investigated in this thesis, the methods used for the examination of the MIF◦CXCR4$^{1-27}$ interaction however, can be transferred to assess whether the N-terminal region of CXCR2 plays a similarly important role in the interaction with MIF.

5.4 The MIF Ortholog from *Plasmodium falciparum*

The role of host MIF in malaria infection previously has been addressed and a correlation between disease development and MIF-level has been described (92, 94, 95, 163, 164). Furthermore, the parasitic homolog of *Plasmodium falciparum* (PfMIF) was initially characterized by two groups in the year 2007 (89, 90). However, in both studies the PfMIF sequence was cloned and expressed with either an amino- (90) or a carboxy-terminal tag (89) for affinity purification. As discussed earlier, both the N-terminus and the C-terminus of MIF are crucial for MIF's function and oligomerization, thus the purification and characterization of the native sequence PfMIF is considered critical for a decisive study.

In accordance to the previously reported elution of histidine-tagged PfMIF at a calculated mass of 30 kDa (90), the purified native sequence PfMIF protein elutes at ~32 kDa as determined by size exclusion chromatography. Based on a report revealing the human MIF-trimer to have an unusual small partial specific volume (108) and observations from our lab obtained from dynamic light scattering experiments, we conclude that PfMIF (like LmMIF) is a trimer in solution. However, further studies are required to determine the oligomeric status with certainty at physiological concentrations.

The data obtained in this work concerning the direct interaction of PfMIF with the human MIF-receptor CD74 with high affinity match well with the previously reported findings of PfMIF's ability to mimic the function of the host's protein. These results strongly support the presumed role of PfMIF in immune evasion mechanisms. To further examine the relevance of the *Plasmodium* MIF protein in the course of disease, it is inevitable to carefully investigate the pathogenicity of *Plasmodium* parasites lacking the MIF gene. Although it was reported previously that *MIF* gene-deficient *P. berghei* parasites exhibit no significant change in growth characteristics or virulence features during blood stage infection in rodents, the number of circulating reticulocytes was reported to be higher

in hosts infected with the knockout parasites (90). Recent data also indicate that mice infected with MIF-knockout parasites display a marked difference in the cytokine expression profile compared to mice infected with wild type parasites (personal communication; Tiffany Sun and Richard Bucala).

6 Summary

The cytokine macrophage migration inhibitory factor (MIF) is a key mediator of the innate and adaptive immune system and plays a critical role in many inflammatory diseases. MIF is required to combat serious infections; however, high-level production of MIF has been linked to a severe outcome of many diseases including adult respiratory distress syndrome, septic shock, rheumatoid arthritis, atherosclerosis and cancer. Over the last years, MIF has also been ascribed important functions in the host defense against several parasitic infections. Consequently, anti-MIF therapies have been suggested as a potential therapeutic approach for treating MIF-related diseases.

Unique among cytokines, MIF possesses an enzymatic activity that is evolutionarily conserved. Herein, 4-iodo-6-phenylpyrimidine (4-IPP), a MIF inhibitor which is ~ 5 – 10 times more potent in blocking MIF-dependent catalysis than other prototypical MIF inhibitors is described. Crystallographic studies reveal 4-IPP to serve as a suicide substrate for MIF, resulting in the covalent modification of the catalytically active N-terminal proline and loss of function of MIF-induced monocyte migration.

Additionally, two parasitic orthologs of MIF, which are produced by the obligate intracellular parasites, *Leishmania major* (LmMIF) and *Plasmodium falciparum* (PfMIF) were studied. An interest in the structure and function of MIF orthologs from parasites has emerged recently as they might have relevant functions in corrupting the host MIF's induced immune defense mechanisms. By co-evolving with the immune system, parasitic organisms have evolved specialized strategies to circumvent the host's immune defense mechanisms to increase their own chances of survival. To assess whether LmMIF and PfMIF have the potential to disrupt immunological pathways of the host's immune system, the parasitic proteins were recombinantly produced and purified. LmMIF and PfMIF show significant binding interaction with the human MIF receptor, CD74 (K_d ~ 2.8 x 10^{-8} M), and like its mammalian counterpart,

the recombinant LmMIF protein is internalized by macrophages, induces monocyte cell migration, ERK1/2 MAP kinase activation, inhibits the activation-induced apoptosis of macrophages and binds the Golgi-associated tethering protein p115. The *Leishmania* MIF protein shows significant structural homology with human MIF as revealed by a high-resolution x-ray crystal structure (1.03 Å). Significant differences between the two proteins in the N-terminal tautomerization site are evident, and evidence for the selective, species-specific inhibition of MIF by small-molecule antagonists that target this site is provided.

Finally, this thesis was aimed to further elucidate the molecular basis of MIF's chemokine-like functions which were recently shown to be mediated through interaction to the chemokine receptors CXCR4 and CXCR2. However, the molecular details of this interaction have not yet been determined. Herein, a peptide derived from the N-terminal extracellular region of the CXCR4 receptor as a site of interaction with human MIF and *Leishmania major* MIF is described. From a competitive binding assay and $^{1}H^{15}N$ chemical shift perturbation studies, a direct binding interaction between MIF and the N-terminal 27 residues of CXCR4 is shown. Titration studies using steady-state fluorescence spectroscopy resulted in a dissociation constant of 3.1×10^{-6} M. Notably, LmMIF/MIF-triggered monocyte chemotaxis activity is ablated by this N-terminal CXCR4 peptide.

The present study not only provides a crystallographic characterization of the prototypic MIF inhibitor 4-IPP for a potential treatment of MIF-related autoimmune and inflammatory diseases, but also unfolds possible new pathways of parasitic MIF-orthologs to interfere with the host immune system. The study of the molecular mode of interaction of MIF and its binding partners will provide new opportunities to block these interactions specifically, and thus may aid in the design of new drugs targeting MIF-related diseases and immune evasive strategies of parasites.

7 References

1. Bogdan, C., and Rollinghoff, M. (1998) The immune response to Leishmania: mechanisms of parasite control and evasion. *Int J Parasitol* 28, 121-134
2. Sacks, D., and Sher, A. (2002) Evasion of innate immunity by parasitic protozoa. *Nat Immunol* 3, 1041-1047
3. Manoury, B., Gregory, W. F., Maizels, R. M., and Watts, C. (2001) Bm-CPI-2, a cystatin homolog secreted by the filarial parasite Brugia malayi, inhibits class II MHC-restricted antigen processing. *Curr Biol* 11, 447-451
4. Borst, P., Rudenko, G., Taylor, M. C., Blundell, P. A., Van Leeuwen, F., Bitter, W., Cross, M., and McCulloch, R. (1996) Antigenic variation in trypanosomes. *Arch Med Res* 27, 379-388
5. Kyes, S., Horrocks, P., and Newbold, C. (2001) Antigenic variation at the infected red cell surface in malaria. *Annu Rev Microbiol* 55, 673-707
6. Belkaid, Y., Hoffmann, K. F., Mendez, S., Kamhawi, S., Udey, M. C., Wynn, T. A., and Sacks, D. L. (2001) The role of interleukin (IL)-10 in the persistence of Leishmania major in the skin after healing and the therapeutic potential of anti-IL-10 receptor antibody for sterile cure. *J Exp Med* 194, 1497-1506
7. Trinchieri, G. (2007) Interleukin-10 production by effector T cells: Th1 cells show self control. *J Exp Med* 204, 239-243
8. Couper, K. N., Blount, D. G., and Riley, E. M. (2008) IL-10: the master regulator of immunity to infection. *J Immunol* 180, 5771-5777
9. Vouldoukis, I., Becherel, P. A., Riveros-Moreno, V., Arock, M., da Silva, O., Debre, P., Mazier, D., and Mossalayi, M. D. (1997) Interleukin-10 and interleukin-4 inhibit intracellular killing of Leishmania infantum and Leishmania major by human macrophages by decreasing nitric oxide generation. *Eur J Immunol* 27, 860-865
10. Moore, K. W., de Waal Malefyt, R., Coffman, R. L., and O'Garra, A. (2001) Interleukin-10 and the interleukin-10 receptor. *Annu Rev Immunol* 19, 683-765
11. Schmid-Hempel, P. (2008) Parasite immune evasion: a momentous molecular war. *Trends Ecol Evol*
12. Melby, P. C. (2002) Recent developments in leishmaniasis. *Curr Opin Infect Dis* 15, 485-490
13. WHO The worlds health Report 2004. In
14. Reithinger, R., Dujardin, J. C., Louzir, H., Pirmez, C., Alexander, B., and Brooker, S. (2007) Cutaneous leishmaniasis. *Lancet Infect Dis* 7, 581-596
15. Chappuis, F., Sundar, S., Hailu, A., Ghalib, H., Rijal, S., Peeling, R. W., Alvar, J., and Boelaert, M. (2007) Visceral leishmaniasis: what are the needs for diagnosis, treatment and control? *Nat Rev Microbiol* 5, 873-882
16. Stojkovic, M., Junghanss, T., Krause, E., and Davidson, R. N. (2007) First case of typical Old World cutaneous leishmaniasis treated with miltefosine. *Int J Dermatol* 46, 385-387
17. Lainson&Shaw (1987) *Evolution, classification and geographical distribution.* Vol. 1
18. Killick-Kendrick, R. (1999) The biology and control of phlebotomine sand flies. *Clin Dermatol* 17, 279-289
19. Sunderkotter, C., Kunz, M., Steinbrink, K., Meinardus-Hager, G., Goebeler, M., Bildau, H., and Sorg, C. (1993) Resistance of mice to experimental

leishmaniasis is associated with more rapid appearance of mature macrophages in vitro and in vivo. *J Immunol* 151, 4891-4901

20. van Zandbergen, G., Klinger, M., Mueller, A., Dannenberg, S., Gebert, A., Solbach, W., and Laskay, T. (2004) Cutting edge: neutrophil granulocyte serves as a vector for Leishmania entry into macrophages. *J Immunol* 173, 6521-6525
21. Laufs, H., Muller, K., Fleischer, J., Reiling, N., Jahnke, N., Jensenius, J. C., Solbach, W., and Laskay, T. (2002) Intracellular survival of Leishmania major in neutrophil granulocytes after uptake in the absence of heat-labile serum factors. *Infect Immun* 70, 826-835
22. Muller, K., van Zandbergen, G., Hansen, B., Laufs, H., Jahnke, N., Solbach, W., and Laskay, T. (2001) Chemokines, natural killer cells and granulocytes in the early course of Leishmania major infection in mice. *Med Microbiol Immunol* 190, 73-76
23. Teixeira, M. J., Teixeira, C. R., Andrade, B. B., Barral-Netto, M., and Barral, A. (2006) Chemokines in host-parasite interactions in leishmaniasis. *Trends Parasitol* 22, 32-40
24. Sacks, D., and Noben-Trauth, N. (2002) The immunology of susceptibility and resistance to Leishmania major in mice. *Nat Rev Immunol* 2, 845-858
25. Tripathi, P., Singh, V., and Naik, S. (2007) Immune response to leishmania: paradox rather than paradigm. *FEMS Immunol Med Microbiol* 51, 229-242
26. Scott, P. (1998) Differentiation, regulation, and death of T helper cell subsets during infection with Leishmania major. *Immunol Res* 17, 229-238
27. Dey, R., Majumder, N., Bhattacharyya Majumdar, S., Bhattacharjee, S., Banerjee, S., Roy, S., and Majumdar, S. (2007) Induction of host protective Th1 immune response by chemokines in Leishmania donovani-infected BALB/c mice. *Scand J Immunol* 66, 671-683
28. Mehlhorn, H., and Armstrong, P. M. (2001) *Encyclopedic reference of parasitology : diseases, treatment, therapy*, Springer, Berlin ; New York
29. Frankenburg, S., Leibovici, V., Mansbach, N., Turco, S. J., and Rosen, G. (1990) Effect of glycolipids of Leishmania parasites on human monocyte activity. Inhibition by lipophosphoglycan. *J Immunol* 145, 4284-4289
30. van Zandbergen, G., Hermann, N., Laufs, H., Solbach, W., and Laskay, T. (2002) Leishmania promastigotes release a granulocyte chemotactic factor and induce interleukin-8 release but inhibit gamma interferon-inducible protein 10 production by neutrophil granulocytes. *Infect Immun* 70, 4177-4184
31. Reiner, N. E., and Malemud, C. J. (1985) Arachidonic acid metabolism by murine peritoneal macrophages infected with Leishmania donovani: in vitro evidence for parasite-induced alterations in cyclooxygenase and lipoxygenase pathways. *J Immunol* 134, 556-563
32. Moore, K. J., and Matlashewski, G. (1994) Intracellular infection by Leishmania donovani inhibits macrophage apoptosis. *J Immunol* 152, 2930-2937
33. Croft, S. L., Sundar, S., and Fairlamb, A. H. (2006) Drug resistance in leishmaniasis. *Clin Microbiol Rev* 19, 111-126
34. Molina, R., Gradoni, L., and Alvar, J. (2003) HIV and the transmission of Leishmania. *Ann Trop Med Parasitol* 97 Suppl 1, 29-45
35. Snow, R. W., Guerra, C. A., Noor, A. M., Myint, H. Y., and Hay, S. I. (2005) The global distribution of clinical episodes of Plasmodium falciparum malaria. *Nature* 434, 214-217

36. Pouniotis, D. S., Proudfoot, O., Minigo, G., Hanley, J. L., and Plebanski, M. (2004) Malaria parasite interactions with the human host. *J Postgrad Med* 50, 30-34
37. Miller, L. H., Baruch, D. I., Marsh, K., and Doumbo, O. K. (2002) The pathogenic basis of malaria. *Nature* 415, 673-679
38. Langreth, S. G., and Peterson, E. (1985) Pathogenicity, stability, and immunogenicity of a knobless clone of Plasmodium falciparum in Colombian owl monkeys. *Infect Immun* 47, 760-766
39. Chen, Q., Schlichtherle, M., and Wahlgren, M. (2000) Molecular aspects of severe malaria. *Clin Microbiol Rev* 13, 439-450
40. Toure-Balde, A., Sarthou, J. L., Aribot, G., Michel, P., Trape, J. F., Rogier, C., and Roussilhon, C. (1996) Plasmodium falciparum induces apoptosis in human mononuclear cells. *Infect Immun* 64, 744-750
41. Bloom, B. R., and Bennett, B. (1966) Mechanism of a reaction in vitro associated with delayed-type hypersensitivity. *Science* 153, 80-82
42. David, J. R. (1966) Delayed hypersensitivity in vitro: its mediation by cell-free substances formed by lymphoid cell-antigen interaction. *Proc Natl Acad Sci U S A* 56, 72-77
43. Churchill, W. H., Jr., Piessens, W. F., Sulis, C. A., and David, J. R. (1975) Macrophages activated as suspension cultures with lymphocyte mediators devoid of antigen become cytotoxic for tumor cells. *J Immunol* 115, 781-786
44. Nathan, C. F., Karnovsky, M. L., and David, J. R. (1971) Alterations of macrophage functions by mediators from lymphocytes. *J Exp Med* 133, 1356-1376
45. Nathan, C. F., Remold, H. G., and David, J. R. (1973) Characterization of a lymphocyte factor which alters macrophage functions. *J Exp Med* 137, 275-290
46. Weiser, W. Y., Temple, P. A., Witek-Giannotti, J. S., Remold, H. G., Clark, S. C., and David, J. R. (1989) Molecular cloning of a cDNA encoding a human macrophage migration inhibitory factor. *Proc Natl Acad Sci U S A* 86, 7522-7526
47. Bernhagen, J., Calandra, T., Mitchell, R. A., Martin, S. B., Tracey, K. J., Voelter, W., Manogue, K. R., Cerami, A., and Bucala, R. (1993) MIF is a pituitary-derived cytokine that potentiates lethal endotoxaemia. *Nature* 365, 756-759
48. Calandra, T., Bernhagen, J., Mitchell, R. A., and Bucala, R. (1994) The macrophage is an important and previously unrecognized source of macrophage migration inhibitory factor. *J Exp Med* 179, 1895-1902
49. Bernhagen, J., Mitchell, R. A., Calandra, T., Voelter, W., Cerami, A., and Bucala, R. (1994) Purification, bioactivity, and secondary structure analysis of mouse and human macrophage migration inhibitory factor (MIF). *Biochemistry* 33, 14144-14155
50. Bozza, M., Satoskar, A. R., Lin, G., Lu, B., Humbles, A. A., Gerard, C., and David, J. R. (1999) Targeted disruption of migration inhibitory factor gene reveals its critical role in sepsis. *J Exp Med* 189, 341-346
51. Flaster, H., Bernhagen, J., Calandra, T., and Bucala, R. (2007) The macrophage migration inhibitory factor-glucocorticoid dyad: regulation of inflammation and immunity. *Mol Endocrinol* 21, 1267-1280
52. Lue, H., Kleemann, R., Calandra, T., Roger, T., and Bernhagen, J. (2002) Macrophage migration inhibitory factor (MIF): mechanisms of action and role in disease. *Microbes Infect* 4, 449-460

53. Kamir, D., Zierow, S., Leng, L., Cho, Y., Diaz, Y., Griffith, J., McDonald, C., Merk, M., Mitchell, R. A., Trent, J., Chen, Y., Kwong, Y. K., Xiong, H., Vermeire, J., Cappello, M., McMahon-Pratt, D., Walker, J., Bernhagen, J., Lolis, E., and Bucala, R. (2008) A leishmania ortholog of macrophage migration inhibitory factor modulates host macrophage responses. *J Immunol* 180, 8250-8261
54. Al-Abed, Y., Dabideen, D., Aljabari, B., Valster, A., Messmer, D., Ochani, M., Tanovic, M., Ochani, K., Bacher, M., Nicoletti, F., Metz, C., Pavlov, V. A., Miller, E. J., and Tracey, K. J. (2005) ISO-1 binding to the tautomerase active site of MIF inhibits its pro-inflammatory activity and increases survival in severe sepsis. *J Biol Chem* 280, 36541-36544
55. Leng, L., Metz, C. N., Fang, Y., Xu, J., Donnelly, S., Baugh, J., Delohery, T., Chen, Y., Mitchell, R. A., and Bucala, R. (2003) MIF signal transduction initiated by binding to CD74. *J Exp Med* 197, 1467-1476
56. Bernhagen, J., Krohn, R., Lue, H., Gregory, J. L., Zernecke, A., Koenen, R. R., Dewor, M., Georgiev, I., Schober, A., Leng, L., Kooistra, T., Fingerle-Rowson, G., Ghezzi, P., Kleemann, R., McColl, S. R., Bucala, R., Hickey, M. J., and Weber, C. (2007) MIF is a noncognate ligand of CXC chemokine receptors in inflammatory and atherogenic cell recruitment. *Nat Med* 13, 587-596
57. Becker-Herman, S., Arie, G., Medvedovsky, H., Kerem, A., and Shachar, I. (2005) CD74 is a member of the regulated intramembrane proteolysis-processed protein family. *Mol Biol Cell* 16, 5061-5069
58. Binsky, I., Haran, M., Starlets, D., Gore, Y., Lantner, F., Harpaz, N., Leng, L., Goldenberg, D. M., Shvidel, L., Berrebi, A., Bucala, R., and Shachar, I. (2007) IL-8 secreted in a macrophage migration-inhibitory factor- and CD74-dependent manner regulates B cell chronic lymphocytic leukemia survival. *Proc Natl Acad Sci U S A* 104, 13408-13413
59. Shi, X., Leng, L., Wang, T., Wang, W., Du, X., Li, J., McDonald, C., Chen, Z., Murphy, J. W., Lolis, E., Noble, P., Knudson, W., and Bucala, R. (2006) CD44 is the signaling component of the macrophage migration inhibitory factor-CD74 receptor complex. *Immunity* 25, 595-606
60. Gore, Y., Starlets, D., Maharshak, N., Becker-Herman, S., Kaneyuki, U., Leng, L., Bucala, R., and Shachar, I. (2008) Macrophage migration inhibitory factor induces B cell survival by activation of a CD74-CD44 receptor complex. *J Biol Chem* 283, 2784-2792
61. Mitchell, R. A., Metz, C. N., Peng, T., and Bucala, R. (1999) Sustained mitogen-activated protein kinase (MAPK) and cytoplasmic phospholipase A2 activation by macrophage migration inhibitory factor (MIF). Regulatory role in cell proliferation and glucocorticoid action. *J Biol Chem* 274, 18100-18106
62. Fruman, D. A. (2004) Phosphoinositide 3-kinase and its targets in B-cell and T-cell signaling. *Curr Opin Immunol* 16, 314-320
63. Amin, M. A., Haas, C. S., Zhu, K., Mansfield, P. J., Kim, M. J., Lackowski, N. P., and Koch, A. E. (2006) Migration inhibitory factor up-regulates vascular cell adhesion molecule-1 and intercellular adhesion molecule-1 via Src, PI3 kinase, and NFkappaB. *Blood* 107, 2252-2261
64. Lue, H., Thiele, M., Franz, J., Dahl, E., Speckgens, S., Leng, L., Fingerle-Rowson, G., Bucala, R., Luscher, B., and Bernhagen, J. (2007) Macrophage migration inhibitory factor (MIF) promotes cell survival by activation of the Akt pathway and role for CSN5/JAB1 in the control of autocrine MIF activity. *Oncogene* 26, 5046-5059

65. Hudson, J. D., Shoaibi, M. A., Maestro, R., Carnero, A., Hannon, G. J., and Beach, D. H. (1999) A proinflammatory cytokine inhibits p53 tumor suppressor activity. *J Exp Med* 190, 1375-1382
66. Calandra, T., Bernhagen, J., Metz, C. N., Spiegel, L. A., Bacher, M., Donnelly, T., Cerami, A., and Bucala, R. (1995) MIF as a glucocorticoid-induced modulator of cytokine production. *Nature* 377, 68-71
67. Bacher, M., Metz, C. N., Calandra, T., Mayer, K., Chesney, J., Lohoff, M., Gemsa, D., Donnelly, T., and Bucala, R. (1996) An essential regulatory role for macrophage migration inhibitory factor in T-cell activation. *Proc Natl Acad Sci U S A* 93, 7849-7854
68. Calandra, T., Echtenacher, B., Roy, D. L., Pugin, J., Metz, C. N., Hultner, L., Heumann, D., Mannel, D., Bucala, R., and Glauser, M. P. (2000) Protection from septic shock by neutralization of macrophage migration inhibitory factor. *Nat Med* 6, 164-170
69. Donnelly, S. C., Haslett, C., Reid, P. T., Grant, I. S., Wallace, W. A., Metz, C. N., Bruce, L. J., and Bucala, R. (1997) Regulatory role for macrophage migration inhibitory factor in acute respiratory distress syndrome. *Nat Med* 3, 320-323
70. Leech, M., Metz, C., Hall, P., Hutchinson, P., Gianis, K., Smith, M., Weedon, H., Holdsworth, S. R., Bucala, R., and Morand, E. F. (1999) Macrophage migration inhibitory factor in rheumatoid arthritis: evidence of proinflammatory function and regulation by glucocorticoids. *Arthritis Rheum* 42, 1601-1608
71. Burger-Kentischer, A., Goebel, H., Seiler, R., Fraedrich, G., Schaefer, H. E., Dimmeler, S., Kleemann, R., Bernhagen, J., and Ihling, C. (2002) Expression of macrophage migration inhibitory factor in different stages of human atherosclerosis. *Circulation* 105, 1561-1566
72. Yang, N., Nikolic-Paterson, D. J., Ng, Y. Y., Mu, W., Metz, C., Bacher, M., Meinhardt, A., Bucala, R., Atkins, R. C., and Lan, H. Y. (1998) Reversal of established rat crescentic glomerulonephritis by blockade of macrophage migration inhibitory factor (MIF): potential role of MIF in regulating glucocorticoid production. *Mol Med* 4, 413-424
73. Mitchell, R. A. (2004) Mechanisms and effectors of MIF-dependent promotion of tumourigenesis. *Cell Signal* 16, 13-19
74. Lai, K. N., Leung, J. C., Metz, C. N., Lai, F. M., Bucala, R., and Lan, H. Y. (2003) Role for macrophage migration inhibitory factor in acute respiratory distress syndrome. *J Pathol* 199, 496-508
75. Pan, J. H., Sukhova, G. K., Yang, J. T., Wang, B., Xie, T., Fu, H., Zhang, Y., Satoskar, A. R., David, J. R., Metz, C. N., Bucala, R., Fang, K., Simon, D. I., Chapman, H. A., Libby, P., and Shi, G. P. (2004) Macrophage migration inhibitory factor deficiency impairs atherosclerosis in low-density lipoprotein receptor-deficient mice. *Circulation* 109, 3149-3153
76. Burger-Kentischer, A., Gobel, H., Kleemann, R., Zernecke, A., Bucala, R., Leng, L., Finkelmeier, D., Geiger, G., Schaefer, H. E., Schober, A., Weber, C., Brunner, H., Rutten, H., Ihling, C., and Bernhagen, J. (2006) Reduction of the aortic inflammatory response in spontaneous atherosclerosis by blockade of macrophage migration inhibitory factor (MIF). *Atherosclerosis* 184, 28-38
77. Meyer-Siegler, K. L., Bellino, M. A., and Tannenbaum, M. (2002) Macrophage migration inhibitory factor evaluation compared with prostate specific antigen as a biomarker in patients with prostate carcinoma. *Cancer* 94, 1449-1456

78. Lee, H., Rhee, H., Kang, H. J., Kim, H. S., Min, B. S., Kim, N. K., and Kim, H. (2008) Macrophage migration inhibitory factor may be used as an early diagnostic marker in colorectal carcinomas. *Am J Clin Pathol* 129, 772-779
79. Pyle, M. E., Korbonits, M., Gueorguiev, M., Jordan, S., Kola, B., Morris, D. G., Meinhardt, A., Powell, M. P., Claret, F. X., Zhang, Q., Metz, C., Bucala, R., and Grossman, A. B. (2003) Macrophage migration inhibitory factor expression is increased in pituitary adenoma cell nuclei. *J Endocrinol* 176, 103-110
80. Shimizu, T., Abe, R., Nakamura, H., Ohkawara, A., Suzuki, M., and Nishihira, J. (1999) High expression of macrophage migration inhibitory factor in human melanoma cells and its role in tumor cell growth and angiogenesis. *Biochem Biophys Res Commun* 264, 751-758
81. Bando, H., Matsumoto, G., Bando, M., Muta, M., Ogawa, T., Funata, N., Nishihira, J., Koike, M., and Toi, M. (2002) Expression of macrophage migration inhibitory factor in human breast cancer: association with nodal spread. *Jpn J Cancer Res* 93, 389-396
82. Munaut, C., Boniver, J., Foidart, J. M., and Deprez, M. (2002) Macrophage migration inhibitory factor (MIF) expression in human glioblastomas correlates with vascular endothelial growth factor (VEGF) expression. *Neuropathol Appl Neurobiol* 28, 452-460
83. Akbar, S. M., Abe, M., Murakami, H., Tanimoto, K., Kumagi, T., Yamashita, Y., Michitaka, K., Horiike, N., and Onji, M. (2001) Macrophage migration inhibitory factor in hepatocellular carcinoma and liver cirrhosis; relevance to pathogenesis. *Cancer Lett* 171, 125-132
84. Krockenberger, M., Dombrowski, Y., Weidler, C., Ossadnik, M., Honig, A., Hausler, S., Voigt, H., Becker, J. C., Leng, L., Steinle, A., Weller, M., Bucala, R., Dietl, J., and Wischhusen, J. (2008) Macrophage Migration Inhibitory Factor Contributes to the Immune Escape of Ovarian Cancer by Down-Regulating NKG2D. *J Immunol* 180, 7338-7348
85. Calandra, T., and Roger, T. (2003) Macrophage migration inhibitory factor: a regulator of innate immunity. *Nat Rev Immunol* 3, 791-800
86. Pastrana, D. V., Raghavan, N., FitzGerald, P., Eisinger, S. W., Metz, C., Bucala, R., Schleimer, R. P., Bickel, C., and Scott, A. L. (1998) Filarial nematode parasites secrete a homologue of the human cytokine macrophage migration inhibitory factor. *Infect Immun* 66, 5955-5963
87. Zang, X., Taylor, P., Wang, J. M., Meyer, D. J., Scott, A. L., Walkinshaw, M. D., and Maizels, R. M. (2002) Homologues of human macrophage migration inhibitory factor from a parasitic nematode. Gene cloning, protein activity, and crystal structure. *J Biol Chem* 277, 44261-44267
88. Cho, Y., Jones, B. F., Vermeire, J. J., Leng, L., DiFedele, L., Harrison, L. M., Xiong, H., Kwong, Y. K., Chen, Y., Bucala, R., Lolis, E., and Cappello, M. (2007) Structural and functional characterization of a secreted hookworm Macrophage Migration Inhibitory Factor (MIF) that interacts with the human MIF receptor CD74. *J Biol Chem* 282, 23447-23456
89. Cordery, D. V., Kishore, U., Kyes, S., Shafi, M. J., Watkins, K. R., Williams, T. N., Marsh, K., and Urban, B. C. (2007) Characterization of a Plasmodium falciparum macrophage-migration inhibitory factor homologue. *J Infect Dis* 195, 905-912
90. Augustijn, K. D., Kleemann, R., Thompson, J., Kooistra, T., Crawford, C. E., Reece, S. E., Pain, A., Siebum, A. H., Janse, C. J., and Waters, A. P. (2007) Functional characterization of the Plasmodium falciparum and P. berghei

homologues of macrophage migration inhibitory factor. *Infect Immun* 75, 1116-1128

91. Jaworski, D. C., Jasinskas, A., Metz, C. N., Bucala, R., and Barbour, A. G. (2001) Identification and characterization of a homologue of the pro-inflammatory cytokine Macrophage Migration Inhibitory Factor in the tick, Amblyomma americanum. *Insect Mol Biol* 10, 323-331
92. Martiney, J. A., Sherry, B., Metz, C. N., Espinoza, M., Ferrer, A. S., Calandra, T., Broxmeyer, H. E., and Bucala, R. (2000) Macrophage migration inhibitory factor release by macrophages after ingestion of Plasmodium chabaudi-infected erythrocytes: possible role in the pathogenesis of malarial anemia. *Infect Immun* 68, 2259-2267
93. Chaiyaroj, S. C., Rutta, A. S., Muenthaisong, K., Watkins, P., Na Ubol, M., and Looareesuwan, S. (2004) Reduced levels of transforming growth factor-beta1, interleukin-12 and increased migration inhibitory factor are associated with severe malaria. *Acta Trop* 89, 319-327
94. McDevitt, M. A., Xie, J., Shanmugasundaram, G., Griffith, J., Liu, A., McDonald, C., Thuma, P., Gordeuk, V. R., Metz, C. N., Mitchell, R., Keefer, J., David, J., Leng, L., and Bucala, R. (2006) A critical role for the host mediator macrophage migration inhibitory factor in the pathogenesis of malarial anemia. *J Exp Med* 203, 1185-1196
95. Awandare, G. A., Hittner, J. B., Kremsner, P. G., Ochiel, D. O., Keller, C. C., Weinberg, J. B., Clark, I. A., and Perkins, D. J. (2006) Decreased circulating macrophage migration inhibitory factor (MIF) protein and blood mononuclear cell MIF transcripts in children with Plasmodium falciparum malaria. *Clin Immunol* 119, 219-225
96. Awandare, G. A., Kremsner, P. G., Hittner, J. B., Keller, C. C., Clark, I. A., Weinberg, J. B., and Perkins, D. J. (2007) Higher production of peripheral blood macrophage migration inhibitory factor in healthy children with a history of mild malaria relative to children with a history of severe malaria. *Am J Trop Med Hyg* 76, 1033-1036
97. Xu, D., McSorley, S. J., Tetley, L., Chatfield, S., Dougan, G., Chan, W. L., Satoskar, A., David, J. R., and Liew, F. Y. (1998) Protective effect on Leishmania major infection of migration inhibitory factor, TNF-alpha, and IFN-gamma administered orally via attenuated Salmonella typhimurium. *J Immunol* 160, 1285-1289
98. Juttner, S., Bernhagen, J., Metz, C. N., Rollinghoff, M., Bucala, R., and Gessner, A. (1998) Migration inhibitory factor induces killing of Leishmania major by macrophages: dependence on reactive nitrogen intermediates and endogenous TNF-alpha. *J Immunol* 161, 2383-2390
99. Satoskar, A. R., Bozza, M., Rodriguez Sosa, M., Lin, G., and David, J. R. (2001) Migration-inhibitory factor gene-deficient mice are susceptible to cutaneous Leishmania major infection. *Infect Immun* 69, 906-911
100. Peacock, C. S., Seeger, K., Harris, D., Murphy, L., Ruiz, J. C., Quail, M. A., Peters, N., Adlem, E., Tivey, A., Aslett, M., Kerhornou, A., Ivens, A., Fraser, A., Rajandream, M. A., Carver, T., Norbertczak, H., Chillingworth, T., Hance, Z., Jagels, K., Moule, S., Ormond, D., Rutter, S., Squares, R., Whitehead, S., Rabbinowitsch, E., Arrowsmith, C., White, B., Thurston, S., Bringaud, F., Baldauf, S. L., Faulconbridge, A., Jeffares, D., Depledge, D. P., Oyola, S. O., Hilley, J. D., Brito, L. O., Tosi, L. R., Barrell, B., Cruz, A. K., Mottram, J. C., Smith, D. F., and Berriman, M. (2007) Comparative genomic analysis of three Leishmania species that cause diverse human disease. *Nat Genet* 39, 839-847

101. Sun, H. W., Bernhagen, J., Bucala, R., and Lolis, E. (1996) Crystal structure at 2.6-A resolution of human macrophage migration inhibitory factor. *Proc Natl Acad Sci U S A* 93, 5191-5196
102. Kato, Y., Muto, T., Tomura, T., Tsumura, H., Watarai, H., Mikayama, T., Ishizaka, K., and Kuroki, R. (1996) The crystal structure of human glycosylation-inhibiting factor is a trimeric barrel with three 6-stranded beta-sheets. *Proc Natl Acad Sci U S A* 93, 3007-3010
103. Suzuki, M., Sugimoto, H., Nakagawa, A., Tanaka, I., Nishihira, J., and Sakai, M. (1996) Crystal structure of the macrophage migration inhibitory factor from rat liver. *Nat Struct Biol* 3, 259-266
104. Delano, W. (2002) The PyMOL Molecular Graphics System.
105. Nishihira, J., Kuriyama, T., Sakai, M., Nishi, S., Ohki, S., and Hikichi, K. (1995) The structure and physicochemical properties of rat liver macrophage migration inhibitory factor. *Biochim Biophys Acta* 1247, 159-162
106. Mischke, R., Kleemann, R., Brunner, H., and Bernhagen, J. (1998) Cross-linking and mutational analysis of the oligomerization state of the cytokine macrophage migration inhibitory factor (MIF). *FEBS Lett* 427, 85-90
107. Muhlhahn, P., Bernhagen, J., Czisch, M., Georgescu, J., Renner, C., Ross, A., Bucala, R., and Holak, T. A. (1996) NMR characterization of structure, backbone dynamics, and glutathione binding of the human macrophage migration inhibitory factor (MIF). *Protein Sci* 5, 2095-2103
108. Philo, J. S., Yang, T. H., and LaBarre, M. (2004) Re-examining the oligomerization state of macrophage migration inhibitory factor (MIF) in solution. *Biophys Chem* 108, 77-87
109. Ren, Y., Lin, C. L., Li, Z., Chen, X. Y., Huang, X., Lui, V., Nicholls, J., Lan, H. Y., and Tam, P. K. (2005) Up-regulation of macrophage migration inhibitory factor in infants with acute neonatal necrotizing enterocolitis. *Histopathology* 46, 659-667
110. Rosengren, E., Aman, P., Thelin, S., Hansson, C., Ahlfors, S., Bjork, P., Jacobsson, L., and Rorsman, H. (1997) The macrophage migration inhibitory factor MIF is a phenylpyruvate tautomerase. *FEBS Lett* 417, 85-88
111. Rosengren, E., Bucala, R., Aman, P., Jacobsson, L., Odh, G., Metz, C. N., and Rorsman, H. (1996) The immunoregulatory mediator macrophage migration inhibitory factor (MIF) catalyzes a tautomerization reaction. *Mol Med* 2, 143-149
112. Lubetsky, J. B., Swope, M., Dealwis, C., Blake, P., and Lolis, E. (1999) Pro-1 of macrophage migration inhibitory factor functions as a catalytic base in the phenylpyruvate tautomerase activity. *Biochemistry* 38, 7346-7354
113. Swope, M., Sun, H. W., Blake, P. R., and Lolis, E. (1998) Direct link between cytokine activity and a catalytic site for macrophage migration inhibitory factor. *Embo J* 17, 3534-3541
114. Kleemann, R., Mischke, R., Kapurniotu, A., Brunner, H., and Bernhagen, J. (1998) Specific reduction of insulin disulfides by macrophage migration inhibitory factor (MIF) with glutathione and dihydrolipoamide: potential role in cellular redox processes. *FEBS Lett* 430, 191-196
115. Thiele, M., and Bernhagen, J. (2005) Link between macrophage migration inhibitory factor and cellular redox regulation. *Antioxid Redox Signal* 7, 1234-1248
116. Kleemann, R., Hausser, A., Geiger, G., Mischke, R., Burger-Kentischer, A., Flieger, O., Johannes, F. J., Roger, T., Calandra, T., Kapurniotu, A., Grell, M., Finkelmeier, D., Brunner, H., and Bernhagen, J. (2000) Intracellular action of

the cytokine MIF to modulate AP-1 activity and the cell cycle through Jab1. *Nature* 408, 211-216

117. Nguyen, M. T., Beck, J., Lue, H., Funfzig, H., Kleemann, R., Koolwijk, P., Kapurniotu, A., and Bernhagen, J. (2003) A 16-residue peptide fragment of macrophage migration inhibitory factor, MIF-(50-65), exhibits redox activity and has MIF-like biological functions. *J Biol Chem* 278, 33654-33671
118. Lubetsky, J. B., Dios, A., Han, J., Aljabari, B., Ruzsicska, B., Mitchell, R., Lolis, E., and Al-Abed, Y. (2002) The tautomerase active site of macrophage migration inhibitory factor is a potential target for discovery of novel anti-inflammatory agents. *J Biol Chem* 277, 24976-24982
119. Senter, P. D., Al-Abed, Y., Metz, C. N., Benigni, F., Mitchell, R. A., Chesney, J., Han, J., Gartner, C. G., Nelson, S. D., Todaro, G. J., and Bucala, R. (2002) Inhibition of macrophage migration inhibitory factor (MIF) tautomerase and biological activities by acetaminophen metabolites. *Proc Natl Acad Sci U S A* 99, 144-149
120. Crichlow, G. V., Cheng, K. F., Dabideen, D., Ochani, M., Aljabari, B., Pavlov, V. A., Miller, E. J., Lolis, E., and Al-Abed, Y. (2007) Alternative chemical modifications reverse the binding orientation of a pharmacophore scaffold in the active site of macrophage migration inhibitory factor. *J Biol Chem* 282, 23089-23095
121. Gietz, D., St Jean, A., Woods, R. A., and Schiestl, R. H. (1992) Improved method for high efficiency transformation of intact yeast cells. *Nucleic Acids Res* 20, 1425
122. Delaglio, F., Grzesiek, S., Vuister, G. W., Zhu, G., Pfeifer, J., and Bax, A. (1995) NMRPipe: a multidimensional spectral processing system based on UNIX pipes. *J Biomol NMR* 6, 277-293
123. Dealwis, C., Fernandez, E. J., Thompson, D. A., Simon, R. J., Siani, M. A., and Lolis, E. (1998) Crystal structure of chemically synthesized [N33A] stromal cell-derived factor 1alpha, a potent ligand for the HIV-1 "fusin" coreceptor. *Proc Natl Acad Sci U S A* 95, 6941-6946
124. Otwinowski, Z., and Minor, W. (1997) Processing of X-ray Diffraction Data Collected in Oscillation Mode. *Methods in Enzymology* 276 Macromolecular Crystallography, part A, p.307-326, 1997,C.W. Carter, Jr. & R. M. Sweet, Eds., Academic Press (New York).
125. Pape, T., and Schneider, T. R. (2004) HKL2MAP: a graphical user interface for phasing with SHELX programs. *Journal of Applied Crystallography* 37, 843-844
126. McRee, D. E. (1992) A visual protein crystallographic software system for X11/XView. *J. Molecular Graphics* 10, 44-46
127. Murshudov, G. N., Vagin, A. A., and Dodson, E. J. (1997) Refinement of macromolecular structures by the maximum-likelihood method. *Acta Crystallogr D Biol Crystallogr* 53, 240-255
128. Brunger, A. T., Adams, P. D., Clore, G. M., DeLano, W. L., Gros, P., Grosse-Kunstleve, R. W., Jiang, J. S., Kuszewski, J., Nilges, M., Pannu, N. S., Read, R. J., Rice, L. M., Simonson, T., and Warren, G. L. (1998) Crystallography & NMR system: A new software suite for macromolecular structure determination. *Acta Crystallogr D Biol Crystallogr* 54, 905-921
129. Sheldrick, G. M., and Schneider, T. R. (1997) SHELXL: high-resolution refinement. *Methods Enzymol* 277, 319-343
130. Storoni, L. C., McCoy, A. J., and Read, R. J. (2004) Likelihood-enhanced fast rotation functions. *Acta Crystallogr D Biol Crystallogr* 60, 432-438

131. Orita, M., Yamamoto, S., Katayama, N., Aoki, M., Takayama, K., Yamagiwa, Y., Seki, N., Suzuki, H., Kurihara, H., Sakashita, H., Takeuchi, M., Fujita, S., Yamada, T., and Tanaka, A. (2001) Coumarin and chromen-4-one analogues as tautomerase inhibitors of macrophage migration inhibitory factor: discovery and X-ray crystallography. *J Med Chem* 44, 540-547
132. Jung, H., Seong, H. A., and Ha, H. (2008) Critical role of cysteine residue 81 of macrophage migration inhibitory factor (MIF) in MIF-induced inhibition of p53 activity. *J Biol Chem*
133. Bendrat, K., Al-Abed, Y., Callaway, D. J., Peng, T., Calandra, T., Metz, C. N., and Bucala, R. (1997) Biochemical and mutational investigations of the enzymatic activity of macrophage migration inhibitory factor. *Biochemistry* 36, 15356-15362
134. Stamps, S. L., Fitzgerald, M. C., and Whitman, C. P. (1998) Characterization of the role of the amino-terminal proline in the enzymatic activity catalyzed by macrophage migration inhibitory factor. *Biochemistry* 37, 10195-10202
135. Poirot, O., O'Toole, E., and Notredame, C. (2003) Tcoffee@igs: A web server for computing, evaluating and combining multiple sequence alignments. *Nucleic Acids Res* 31, 3503-3506
136. Kraulis, P. J. (1991) Molscript: a program to produce both detailed and schematic plots of protein structures *J. Appl. Crystallogr.* 24, 946-950
137. Cristpher, J. A. (1998) SPOCK: The Structural Properties Observation and Calculation Kit Program Manual.
138. Merk, M., Baugh, J., Zierow, S., Leng, L., Pal, U., Lee, S., Ebert, A., Mizue, Y., Trent, J., Mitchell, R. A., Nickel, W., Kavathas, P., Bernhagen, J., and Bucala, R. (2008) The Golgi-associated Protein p115 Mediates the Secretion of Macrophage Migration Inhibitory Factor (MIF). *Mol Biol Cell*, re-submitted
139. Kleemann, R., Rorsman, H., Rosengren, E., Mischke, R., Mai, N. T., and Bernhagen, J. (2000) Dissection of the enzymatic and immunologic functions of macrophage migration inhibitory factor. Full immunologic activity of N-terminally truncated mutants. *Eur J Biochem* 267, 7183-7193
140. Cho, Y. S., Jones, B. F., Vermeire, J. J., Leng, L., DiFedele, L., Harrison, L. M., Xiong, H. B., Kwong, Y. K. A., Chen, Y., Bucala, R., Lolis, E., and Cappello, M. (2007) Structural and functional characterization of a secreted hookworm macrophage migration inhibitory factor (MIF) that interacts with the human MIF receptor CD74. *Journal of Biological Chemistry* 282, 23447-23456
141. Deprez, C., Lloubes, R., Gavioli, M., Marion, D., Guerlesquin, F., and Blanchard, L. (2005) Solution structure of the E.coli TolA C-terminal domain reveals conformational changes upon binding to the phage g3p N-terminal domain. *J Mol Biol* 346, 1047-1057
142. Gozansky, E. K., Louis, J. M., Caffrey, M., and Clore, G. M. (2005) Mapping the binding of the N-terminal extracellular tail of the CXCR4 receptor to stromal cell-derived factor-1alpha. *J Mol Biol* 345, 651-658
143. Veldkamp, C. T., Seibert, C., Peterson, F. C., Sakmar, T. P., and Volkman, B. F. (2006) Recognition of a CXCR4 sulfotyrosine by the chemokine stromal cell-derived factor-1alpha (SDF-1alpha/CXCL12). *J Mol Biol* 359, 1400-1409
144. Calandra, T. (2001) Pathogenesis of septic shock: implications for prevention and treatment. *J Chemother* 13 Spec No 1, 173-180
145. Radstake, T. R., Sweep, F. C., Welsing, P., Franke, B., Vermeulen, S. H., Geurts-Moespot, A., Calandra, T., Donn, R., and van Riel, P. L. (2005) Correlation of rheumatoid arthritis severity with the genetic functional variants

and circulating levels of macrophage migration inhibitory factor. *Arthritis Rheum* 52, 3020-3029

146. Leech, M., Metz, C., Bucala, R., and Morand, E. F. (2000) Regulation of macrophage migration inhibitory factor by endogenous glucocorticoids in rat adjuvant-induced arthritis. *Arthritis Rheum* 43, 827-833
147. Santos, L., Hall, P., Metz, C., Bucala, R., and Morand, E. F. (2001) Role of macrophage migration inhibitory factor (MIF) in murine antigen-induced arthritis: interaction with glucocorticoids. *Clin Exp Immunol* 123, 309-314
148. Tracey, D., Klareskog, L., Sasso, E. H., Salfeld, J. G., and Tak, P. P. (2008) Tumor necrosis factor antagonist mechanisms of action: a comprehensive review. *Pharmacol Ther* 117, 244-279
149. Arjona, A., Foellmer, H. G., Town, T., Leng, L., McDonald, C., Wang, T., Wong, S. J., Montgomery, R. R., Fikrig, E., and Bucala, R. (2007) Abrogation of macrophage migration inhibitory factor decreases West Nile virus lethality by limiting viral neuroinvasion. *J Clin Invest* 117, 3059-3066
150. Laskay, T., Diefenbach, A., Rollinghoff, M., and Solbach, W. (1995) Early parasite containment is decisive for resistance to Leishmania major infection. *Eur J Immunol* 25, 2220-2227
151. Scharton-Kersten, T., and Scott, P. (1995) The role of the innate immune response in Th1 cell development following Leishmania major infection. *J Leukoc Biol* 57, 515-522
152. Leiby, D. A., Schreiber, R. D., and Nacy, C. A. (1993) IFN-gamma produced in vivo during the first two days is critical for resolution of murine Leishmania major infections. *Microb Pathog* 14, 495-500
153. Underhill, D. M., and Ozinsky, A. (2002) Phagocytosis of microbes: complexity in action. *Annu Rev Immunol* 20, 825-852
154. Buchmuller-Rouiller, Y., and Mauel, J. (1987) Impairment of the oxidative metabolism of mouse peritoneal macrophages by intracellular Leishmania spp. *Infect Immun* 55, 587-593
155. Descoteaux, A., Matlashewski, G., and Turco, S. J. (1992) Inhibition of macrophage protein kinase C-mediated protein phosphorylation by Leishmania donovani lipophosphoglycan. *J Immunol* 149, 3008-3015
156. Balestieri, F. M., Queiroz, A. R., Scavone, C., Costa, V. M., Barral-Netto, M., and Abrahamsohn Ide, A. (2002) Leishmania (L.) amazonensis-induced inhibition of nitric oxide synthesis in host macrophages. *Microbes Infect* 4, 23-29
157. Jayakumar, A., Widenmaier, R., Ma, X., and McDowell, M. A. (2008) Transcriptional inhibition of interleukin-12 promoter activity in Leishmania spp.-infected macrophages. *J Parasitol* 94, 84-93
158. Bimal, S., Singh, S. K., Das, V. N., Sinha, P. K., Gupta, A. K., Bhattacharya, S. K., and Das, P. (2005) Leishmania donovani: effect of therapy on expression of CD2 antigen and secretion of macrophage migration inhibition factor by T-cells in patients with visceral leishmaniasis. *Exp Parasitol* 111, 130-132
159. Miska, K. B., Fetterer, R. H., Lillehoj, H. S., Jenkins, M. C., Allen, P. C., and Harper, S. B. (2007) Characterisation of macrophage migration inhibitory factor from Eimeria species infectious to chickens. *Mol Biochem Parasitol* 151, 173-183
160. Tan, T. H., Edgerton, S. A., Kumari, R., McAlister, M. S., Roe, S. M., Nagl, S., Pearl, L. H., Selkirk, M. E., Bianco, A. E., Totty, N. F., Engwerda, C.,

Gray, C. A., and Meyer, D. J. (2001) Macrophage migration inhibitory factor of the parasitic nematode Trichinella spiralis. *Biochem J* 357, 373-383

161. Flieger, O., Engling, A., Bucala, R., Lue, H., Nickel, W., and Bernhagen, J. (2003) Regulated secretion of macrophage migration inhibitory factor is mediated by a non-classical pathway involving an ABC transporter. *FEBS Lett* 551, 78-86
162. Crump, M. P., Gong, J. H., Loetscher, P., Rajarathnam, K., Amara, A., Arenzana-Seisdedos, F., Virelizier, J. L., Baggiolini, M., Sykes, B. D., and Clark-Lewis, I. (1997) Solution structure and basis for functional activity of stromal cell-derived factor-1; dissociation of CXCR4 activation from binding and inhibition of HIV-1. *Embo J* 16, 6996-7007
163. Coleman, R. M., Bruce, A., and Rencricca, N. J. (1976) Malaria: macrophage migration inhibition factor (MIF). *J Parasitol* 62, 137-138
164. De Mast, Q., Sweep, F. C., McCall, M., Geurts-Moespot, A., Hermsen, C., Calandra, T., Netea, M. G., Sauerwein, R. W., and van der Ven, A. J. (2008) A decrease of plasma macrophage migration inhibitory factor concentration is associated with lower numbers of circulating lymphocytes in experimental Plasmodium falciparum malaria. *Parasite Immunol* 30, 133-138

Curriculum Vitae

Name		Swen Zierow
Geburtsdatum		29.05.78
Geburtsort		Furtwangen
Staatsangehörigkeit		deutsch
Schulbildung	08/85 - 07/89	Friedrich-Hepting-Grundschule, Vöhrenbach
	08/89 - 06/98	Otto-Hahn-Gymnasium, Furtwangen
Zivildienst	07/98 - 08/99	Paritätischer Wohlfahrtsverband, Freiburg
Hochschulstudium	10/99 - 09/01	**Grundstudium Biologie,** Albert-Ludwigs-Universität, Freiburg
	04/02 – 08/05	**Hauptstudium Biologie**, RWTH Aachen, Aachen
	02/06 - 12/08	**Promotion**, An der RWTH-Aachen in Kooperation mit der *Yale University School of Medicine*, USA unter Betreuung von Universitätsprofessor Dr. Jürgen Bernhagen (RWTH Aachen) und Professor Elias Lolis (*Yale University*)
Auszeichnungen	10/01 – 03/02	Praktikumsförderung des DAAD
	01/06 – 01/08	Doktorandenstipendium des DAAD
	09/08	Auszeichnung für "*Excellence in Inflammation Research*" der 15. *C. Gordon Van Arman Scholarship Competition*.
Publikationen und Abstracts	Publikationen	Kamir D*, **Zierow S* (equal contribution)**, *et al*. (2008). "A leishmania ortholog of macrophage migration inhibitory factor modulates host macrophage responses." *J. Immunology* 180(12): 8250-61.
		Winner M, Meier J, **Zierow S**, *et al*. (2008). "A novel, macrophage migration inhibitory factor suicide substrate inhibits motility and growth of lung cancer cells."*Cancer Research.* 68(18): 7253-7257.
		Merk M, Baugh J, **Zierow S**, *et al* (2008). "The Golgi-associated Protein p115 mediates the secretion on Macrophage Migration Inhibitory Factor (MIF)". In Revision bei *Mol. Biol. Cell*
	Poster und Vorträge	**Zierow S**, *et al.* (2006) "CSN5 and MIF enhance TGF-β signaling in transdifferentiating hepatic stellate cells." *The Fourth International Symposium on COP9 Signalosome, Proteasom*e, *and eIF3*. New Haven, CT, USA.
		Zierow S, *et al.* (2008) "Mapping of the Binding of Macrophage Migration Inhibitory Factor (MIF) to the Chemokine Receptor CXCR4" *The 15th International Conference of the Inflammation Research Association.* Chantilly, VA, USA.